Stony Brook University

Synthesis of oxynitride materials for solar water splitting: investigations with ambient pressure and high pressure synthesis techniques

A Dissertation Presented

by

Hingure Arachchilage Naveen Dharmagunawardhane

to

The Graduate School

in Partial Fulfillment of the

Requirements

for the Degree of

Doctor of Philosophy

in

Materials Science & Engineering

Stony Brook University

January 2017

Stony Brook University
The Graduate School

Hingure Arachchilage Naveen Dharmagunawardhane

We, the dissertation committee for the above candidate for the
Doctor of Philosophy degree, hereby recommend
acceptance of this dissertation.

John B. Parise– Dissertation Advisor
Distinguished Professor, Department of Geosciences

Dilip Gersappe - Chairperson of Defense
Professor, Department of Materials Science and Engineering

Tadanori Koga – Committee Member
Associate Professor, Department of Materials Science and Engineering

Matthew L. Whitaker – Committee Member
Mineral Physics Institute.

This dissertation is accepted by the Graduate School

Charles Taber

Dean of the Graduate School

Abstract of the Dissertation

Synthesis of oxynitride materials for solar water splitting: investigations with ambient pressure and high pressure synthesis techniques

by

Hingure Arachchilage Naveen Dharmagunawardhane
Doctor of Philosophy

in

Materials Science & Engineering

Stony Brook University

2016

Solar water splitting, a photocatalytic process where water is directly split into hydrogen and oxygen using sunlight absorbing semiconductor materials, is one of the most sought after methods to make hydrogen economy a reality. Oxynitrides containing d^0 and d^{10} cations tend to have the appropriate band structure required for solar water splitting. So far, reported efficiencies are not high enough for practical use and synthesizing an oxynitride showing high enough efficiency remains necessary. In this dissertation, we discuss the synthesis of oxynitrides and studying their optical and photocatalytic properties with a particular emphasis on utilizing exploratory high pressure synthesis.

High pressure synthesis is an interesting route to synthesize oxynitrides as this can stabilize reactants that tend to decompose at ambient pressure, helping to achieve the intended stoichiometry. For synthesis, we selected candidate compositions from published theoretical studies. Reactions were carried out at pressures around 1-3 GPa and at temperatures up to

1300^0C in a multi-anvil large volume press. Phase changes were observed with *in situ* X-ray scattering. In these experiments, we found that most d^0 and d^{10} cations tend to reduce in the high pressure reaction environment as temperature increases, but Zr^{4+}, Hf^{4+}, and Ta^{5+} tend to retain their oxidation state. This information will be helpful in future theoretical studies to accurately predict stable oxynitrides synthesizable at high pressure.

We synthesized $(GaN)_{1-x}(ZnO)_x$ solid solution in the entire composition range at 1 GPa, 1150^0C. The material showed photocatalytic H_2 evolution activity even without surface modification with co catalysts, first such observed for this system. The minimum band gap of 2.65 eV and the highest H_2 evolution activity of 2.31 μmol/h were observed at $x = 0.51$.

On our initial investigation on the synthesis of gallium oxynitride spinel ($Ga_3O_3N_3$) at high pressure, we found that the material could be formed by direct ammonolysis of gallium nitrate hydrate at ambient pressure. The formed product was nanocrystalline and exhibited an indirect band gap of 2.5 eV. The material photocatalytically evolved H_2 at an initial rate 8 μmol/ h, but the activity diminished after five hours due to degradation forming gallium oxide hydroxide.

Dedication

To my dear wife, Uthpala

Table of Contents

Abstract…… iii

Dedication…… v

Table of contents……... vi

List of Figures……ix

List of Tables…….xiii

Acknowledgements ……..xiv

Chapter 1: Introduction 1

1.1 Overview ……. 1

1.2 The process of water splitting……... 2

1.3 Research Objectives…….. 4

References 6

Chapter 2: Exploratory synthesis for novel oxynitrides with *in situ* high pressure Techniques…….7

2.1 Introduction……7

2.2 Theoretical studies …… 8

2.2.1 First Principle high throughput screening of oxynitrides by Wu et al 8

2.2.2 Formability of perovskite oxynitrides predicted from tolerance and octahedral factors by Li et al……9

2.2.3 Estimating band gap……..11

2.3 Choosing compositions ……...13

2.4 Experimental……14

2.4.1 High Pressure Synthesis……14

2.4.2 Synthesis of Zr_2ON_2 and Hf_2ON_2…….17

2.4.3 Synthesis of TaON……17

2.5 Results and Discussion…… 17

2.5.1 $Zr_3O_3N_2$…… 18

2.5.2 Zr_2ON_2-Y_2O_3 and Hf_2ON_2 –Y_2O_3…….. 20

2.5.3 Zr_2ON_2-Sc_2O_3 and Hf_2ON_2 –Sc_2O_3……... 24

2.5.4 InN-Nb_2O_5…… 26

2.5.5 InN-TaON …… 27

2.5.6 Zr_2ON_2-Ba_3N_2……..... 29

2.5.7 Zr_2ON_2-GaN……. 29

2.5.6 Identified issues and suggestions for future research…….. 32

2.6 Summery and conclusions…… 33

2.7 Acknowledgements……. 34

References…….. 35

Chapter 3: Photocatalytic hydrogen evolution using nanocrystalline gallium oxynitride spinel……38

3.1 Introduction……. 38

3.2 Experimental……39

3.2.1 Synthesis of Gallium Oxynitride Spinel…….. 39

3.2.2 Characterization……39

3.3 Results and Discussion…… 40

3.3.1 Synthesis……... 40

3.3.2 Optical Properties……..45

3.3.3 Photocatalytic H2 production and stability in water…… 50

3.4 Conclusions…… 56

3.5 Acknowledgements…….. 56

References…… 57

Chapter 4: Optical properties and photocatalytic activity of $(GaN)_{1-x}(ZnO)_x$ solid solution synthesized at high pressure in the entire composition range…… 60

4.1 Introduction…….. 60

4.2 Experimental ……. 61

4.2.1 GaN synthesis…….. 61

4.2.2 High Pressure synthesis…… 61

4.2.3 Optical properties and photocatalytic activity…….. 62

4.3 Results and Discussion…….63

4.3.1 Compositional analysis …… 63

4.3.2 Optical properties……. 69

4.3.3 Photocatalytic Activity……. 75

4.4 Conclusions…… 79

4.5 Acknowledgements…… 80

References……..81

Complete Bibliography …….. 84

List of Figures

Chapter 1

Figure 1.1(a) …… 3

The basic principles of water splitting

Figure 1.1(b)…… 3

The process of overall water splitting by a particulate photo catalyst

Chapter 2

Figure 2.1…….. 10

Structure of perovskite $SrTiO_3$ with Sr at A sites (green) and Ti at octahedral B sites (yellow)

Figure 2.2……16

Schematics of the high pressure reaction cell used at APS (above left) and NSLS(above right) X-ray photograph of the cell showing the sample pellet with two reaction mixtures (in this case both containing Ta) separated by MgO (below)

Figure 2.3…… 19

In situ x-ray diffraction data of the high pressure reaction of ZrO_2 and Zr_2ON_2

Figure 2.4 …….. 21

In situ x-ray diffraction data of the high pressure reaction of Y_2O_3/ Zr_2ON_2 system (above) and Y_2O_3/ Hf_2ON_2 system (below)

Figure 2.5 ……... 23

XRD data of products obtained by reacting Y_2O_3 and Zr_2ON_2 (top) Y_2O_3 and Hf_2ON_2 (bottom) at 1 GPa and 1300^0C

Figure 2.6 …… 25

In situ x-ray diffraction data of the high pressure reaction of Sc_2O_3/ Zr_2ON_2 system (above) and Sc_2O_3/ Hfr_2ON_2 system (below)

Figure 2.7 …….. 26

In situ x-ray diffraction data of the high pressure reaction of InN/Nb_2O_5 system

Figure 2.8 …….. 28

In situ x-ray diffraction data of the high pressure reaction of InN/TaON system

Figure 2.9……. 30

In situ x-ray diffraction data of the high pressure reaction of Zr_2ON_2/Ba_3N_2 system

Figure 2.10 …….. 31

In situ x-ray diffraction data of the high pressure reaction of Zr_2ON_2/GaN system

Chapter 3

Figure 3.1……. 41

XRD patterns Ga-O-N spinel products synthesized with Ga-BDC precursor at 350°C and500°C and with $Ga(NO_3)_3.xH_2O$ at 550°C

Figure 3.2 (a)…… 43

XRD pattern (background subtracted) of gallium oxynitride spinel products synthesized from $Ga(NO_3)_3 \cdot \times H_2O$ at 550ºC with calculated reflections shown for Ga_3O_3N with a cell parameter of 8.25 Å.

Figure 3.2 (b) …… 44

XRD patterns of gallium oxynitride spinel products synthesized from $Ga(NO_3)_3 \cdot \times H_2O$ at in the temperature range 400ºC-600ºC

Figure 3.3 (a) …… 47

Regimes over which gallium oxynitride spinel exhibits direct (bottom, blue lines) optical gap, as shown for the relative absorption data obtained by the Kubleka-Munk transform of diffuse reflectance (above) and for the same data rescaled to appear linear when the functional form for this absorption is obeyed (below)

Figure 3.3 (b) …… 48

Regimes over which gallium oxynitride spinel exhibits an indirect optical gap, as shown for the relative absorption data obtained by the Kubleka-Munk transform of diffuse reflectance (above) and for the same data rescaled to appear linear when the functional form for this absorption is obeyed (below)

Figure 3.4 …… 49

Relative absorption (α_{KM}) on a log scale for gallium oxynitride spinel synthesized by ammonolyzing $Ga(NO_3)_3 \cdot xH_2O$. Fit to the low-energy Urbach tail is overlaid (black line)

Figure 3.5 ……. 51

Evolution of hydrogen from spinel gallium oxynitride suspension over a 20% methanol in water solution irradiated with a 300 W UV lamp (320 nm)

Figure 3.6 ……. 53

The UV-Visible diffuse reflectance spectra of GOS as prepared (black), after 6hrs in 20% methanol solution in dark (red) and after 6 hrs in solution under irradiation (green)

Figure 3.7 ……. 54

The XRD patterns of GOS, as prepared (black), after 6 hrs in 20% methanol solution in dark (red) and after 6 hrs in 20% methanol solution under irradiation (green). The calculated pattern for GaO(OH) is shown in blue

Chapter 4

Figure 4.1 ……. 64

The X-ray diffraction patterns of the products obtained by reacting GaN and ZnO at 1 GPa ,1150-1200 °C

Figure 4.2 (a) …… 67

The lattice parameters calculated for high pressure synthesized $(GaN)_{1-x}(ZnO)_x$ with the values predicted by Liu et al. Errors are smaller than markers. Dashed lines represent ideal variation of lattice parameters.

Figure 4.2 (b) …… 68

Cell volumes calculated for high pressure synthe-sized $(GaN)_{1-x}(ZnO)_x$ with the values predicted by Liu et al. Errors are smaller than markers. Dashed lines represent ideal variation of lattice parameters

Figure 4.3 (a) …… 71

Kubelka-Munk transformed diffuse reflectance data for $(GaN)_{1-x}(ZnO)_x$ with x= 0.07, 0.24 and 0.51, showing regions that show absorption behaviours of direct band gap (yellow) and Urbach tail (red)

Figure 4.3 (b) …….. 72

Kubelka-Munk transformed diffuse reflectance data for $(GaN)_{1-x}(ZnO)_x$ with x= 0.76and 0.90, showing regions that show absorption behaviours of direct band gap (yellow) and Urbach tail (red)

Figure 4.4 …… 74

Comparison of band gaps of $(GaN)_{1-x}(ZnO)_x$ synthesized at high pressure in this study (black squares, errors are smaller than the symbol), with those of nanorods synthesized by Rienart et al. (red circles), nanoparticles synthesized by Feygenson et al. (green triangles) and $(GaN)_{1-x}(ZnO)_x$ obtained using layered double hydroxide precursors by Wang et al. (blue diamonds). Dashed lines mark the band gap values of GaN and ZnO as marked.

Figure 4.5 (a) …… 76

Hydrogen evolution for $(GaN)_{1-x}(ZnO)_x$ solid solution members for 5 hours

Figure 4.5 (b) …… 76

Hydrogen evolution rates for first hour (blue) and 5 hour average (red)

Figure 4.6 (a) …… 78

The XRD data of $(GaN)_{1-x}(ZnO)_x$ (x=0.53) sample before and after the photocatalytic activity test

Figure 4.6 (b) …… 78

Photocatalytic activity of the same sample

List of Tables

Chapter 2

Table 2.1 …… 12

Perovskite oxynitride tolerance and octahedral factors predicted by Li et al and their predicted band gaps (this study)

Chapter 3

Table 3.1 …….. 52

Comparison of gallium oxynitride spinel H_2 evolution activity under UV radiation (methanol sacrificial reagent) with that of Ga based oxides

Chapter 4

Table 4.1 …… 65

Cell parameters of $(GaN)_{1-x}(ZnO)_x$, weight percentages of $(GaN)_{1-x}(ZnO)_x$ and $ZnGa_2O_4$ obtained by Rietveld refinements, and final calculated compositions

Table 3.2 ……... 73

Calculated band caps and Urbach energies for $(GaN)_{1-x}(ZnO)_x$ synthesized at high pressure

Acknowledgments

Firstly, I would like to thank my advisor, Prof. John B Parise, for providing this wonderful opportunity to learn. I am extremely grateful for his guidance for the past six years. I would also like to thank Prof. Robert Mayanovic for persuading me to go a step beyond a master's degree. Furthermore, I would like to thank Prof. John B Parise, Prof Dilip Gersappe, Prof. Tadanori Koga and Dr. Matthew Whitaker for serving on my defense committee and for their suggestions on improving this dissertation.

Special thanks extend to Dr. William Woerner for mentoring me during the early years of my dissertation research and bringing me up to speed. I would like to thank all other collaborators in Parise group who contributed to the research mentioned in this dissertation: Mr. Alwin James, Dr. Alexandra Sinclair, Ms. Xianyin Chen and Dr. Anna Plonka. I am also grateful to Dr. Mathew Whitaker, Dr. Haiyan Chen, Dr. Tony Yu, Dr. Yanbin Wang Dr. Huafeng Huang and Mr. Qiyuan Wu for their guidance

I am very grateful for the resources provided for my research at the National Synchrotron Light Source at the Brookhaven National Laboratory and the Advanced Photon Source at the Argonne National Laboratory. I would also like to thank for the financial support provided to me by the Department of Materials Science and Engineering, Department of Geoscience, the Research Foundation for the State University of New York and the National Science Foundation.

Finally, I would like to thank my family and friends, especially my wife Uthpala, for the support and love provided through the years.

Chapter 1

Introduction

1.1 Overview

Harvesting energy efficiently from freely available sunlight has always been a pinnacle topic of alternative energy Research. However, its non-uniform availability is a hindrance for uninterrupted power generation. Developing practical and economical methods to store solar energy is crucial to meet the growing global energy demand. Storing solar energy generated through solar cell arrays (or other means) in chemical cells is very expensive due to high production costs and limited lifetime of cells. Solar light driven photocatalytic water splitting, a process where suspended semiconductor particles absorb light and split water into hydrogen and oxygen that can be stored for uninterrupted power generation, is a highly anticipated solution to the energy storage problem.[1, 2]

Photocatalytic water-splitting was first demonstrated using a TiO_2 semiconductor anode and Pt cathode by Honda and Fujishima in 1972.[3] Oxide photocatalysts, although known to spilt water under UV light, usually have band gaps above 3.0 eV and do not utilize the abundant visible light from solar radiation.[2] Oxynitrides compounds of d^0 and d^{10} cations tend to have the appropriate band structure for visible light absorption and water-splitting.[1, 2] Several oxynitrides (e.g. TaON and $LaTiO_2N$) were known to photocatalytically evolve hydrogen under visible light though most of them cannot perform water-splitting to produce both H_2 and O_2 simultaneously, and only reduce water in the presence of a sacrificial reagent.[4-7] The demonstration of 'overall

water splitting' by the solid solution between wurtzite type GaN and ZnO further enforced the idea that the oxynitrides promising candidates for solar energy conversion.[8]

1.2 The process of water splitting.

The overall water splitting is a thermodynamically "uphill reaction" with a positive change of Gibb's free energy.[1, 2] The process first involves irradiating a semiconductor material with light having photon energies greater than the band gap to excite electron and hole pairs. If not recombined, these electrons and holes then travel to the semiconductor/water interface which causes oxidation and reduction reactions to produce O_2 and H_2. To achieve overall water splitting, the conduction band of the material should have a potential less than $H+/H_2$ redox potential (0 V vs NHE- Normal Hydrogen Electrode) and the valance band should have a potential greater than the O_2/H_2O redox potential (1.23 V vs NHE, *see Figure 1.1(a)*).[1, 2]However, due to the activation energy required for the charge transfer process between the catalyst and water molecules, a larger band gap is necessary.[1]

The effects of nitrogen on the band structure of metal cations with d^0 or d^{10} electronic configurations are expected to be crucial in promoting visible light driven photocatalysis by oxynitrides.[1] In d^0/d^{10} oxynitrides, the d or sp orbitals of the cations form the bottom of the conduction band, which tend to have a more negative potential than the H^+/H_2 redox potential. The top of the valence bands correspond to N2p orbitals which tend to have higher potential than the redox potential of O_2/H_2O but still have lower potentials than an O2p orbitals, making band gaps of oxynitrides smaller compared to those of oxides.[1]

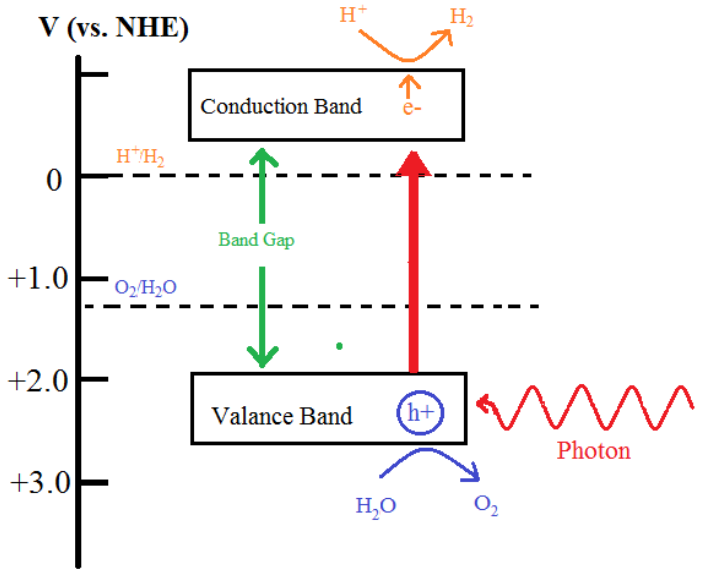

(a)

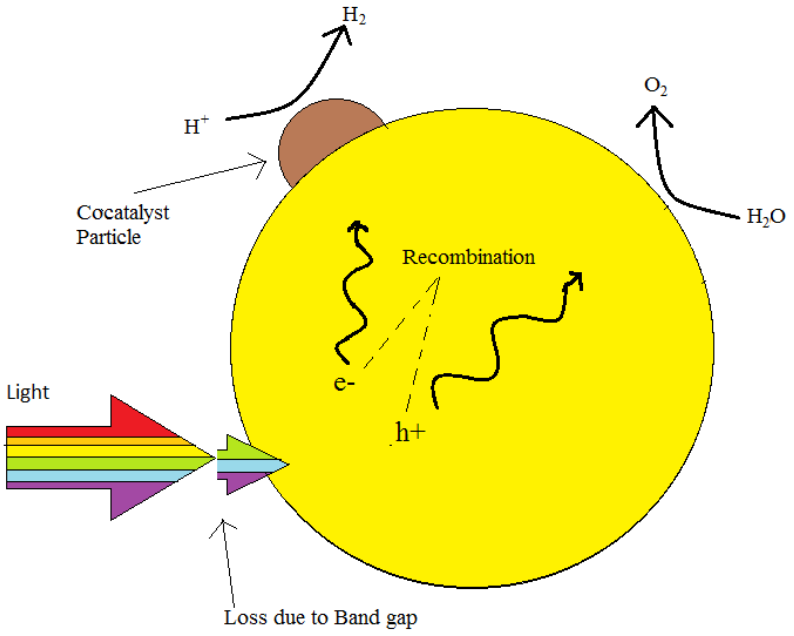

(b)

Figure 1.1 (a) The basic principles of water splitting (b) The process of overall water splitting by a particulate photo catalyst.

Several factors influence the photocatalytic process (*see Figure 1.1(b)*). As most of the energy in sunlight corresponds to photon energies less than 3eV, band gap must be sufficiently small to absorb a good portion of solar energy. Resistivity is another factor as the electron hole pairs needs to travel to the surface fast to avoid recombining. Also, crystal defects in photocatalytic material are considered to act as carrier recombination sites, hence higher crystallinity is expected to improve activity.

Surface medication of photocatalyst particles with co-catalysts are usually necessary to provide active sites for water splitting. Usually, the co-catalysts are either noble metals (e.g Pt,Rh) or metal oxides (e.g. NiO,RuO_2). Most oxide and oxynitride photocatalysts cannot split water without co-catalysts.[1, 2]

1.3 Research Objectives

For practical applications of visible light driven photocatalytic overall water splitting, a quantum efficiency of 10% is expected to be necessary. However, the maximum efficiency reported so far is only 5.9%, which was observed with GaN-ZnO solid solution.[9] Hence, investigations on synthesizing new oxynitride materials as well as improvements on existing materials remain necessary to make this green energy solution a reality, which we took as the basis for our research. The following chapters of this thesis explain outcomes of three projects concentrating on the synthesis/characterization of oxynitrides. The objectives of the works mentioned in each chapter are explained below in short.

Ammonolysis is the most extensively used method to synthesize oxynitrides with most of the viable options already tested. High pressure synthesis is an attractive alternative method to

synthesize oxynitrides as high pressure suppresses the decomposition of reactants to evolve gaseous products. However, this technique is still rarely used to synthesize oxynitrides. The objective of the research discussed in the second chapter of this thesis was to conduct exploratory synthesis of oxynitride materials at high pressure. There, we used *in situ* x-ray scattering to identify phase changes.

In the third chapter, we discuss an alternative synthesis route (ambient pressure) for nanocrystalline gallium oxynitride spinel, its optical properties and photocatalytic activity. This material was previously reported with high pressure synthesis and ambient pressure synthesis has been reported recently. However, neither a detailed optical analysis nor any photocatalytic activity studies has been reported for this system and providing such was the goal of this project.

Finally, in the fourth chapter we discuss the optical and photocatalytic properties of wurtzite type $(GaN)_{1-x}(ZnO)_x$ solid solution members synthesized at high-pressure in the entire composition range (up to x=0.9). Members of $(GaN)_{1-x}(ZnO)_x$ with x>0.3 are difficult to synthesize with ammonolysis at ambient pressure due to reduction and evaporation of zinc. Members with x>0.3 was first reported with high pressure synthesis but detailed studies on optical and photocatalytic properties was not carried out.[10] Such studies are specifically important as $(GaN)_{1-x}(ZnO)_x$ solid solution has the highest reported quantum efficiency plus it is the only materials known for overall water splitting under visible light.

References

1 K. Maeda and K. Domen, *New non-oxide photocatalysts designed for overall water splitting under visible light,* J. Phys. Chem. C., 2007, **111**, 7851-7861.

2 A. Kudo and Y. Miseki, *Heterogeneous photocatalyst materials for water splitting,* Chem. Soc. Rev., 2009, **38**, 253-278.

3 A. Fujishima and K. Honda, *Electrochemical Photolysis of Water at a Semiconductor Electrode,* Nature, 1972, **238**, 37-+.

4 K. Maeda and K. Domen, *Oxynitride materials for solar water splitting,* MRS Bull., 2011, **36**, 25-31.

5 M. Hara, G. Hitoki, T. Takata, J. N. Kondo, H. Kobayashi and K. Domen, *TaON and Ta3N5 as new visible light driven photocatalysts,* Catal. Today, 2003, **78**, 555-560.

6 A. Kasahara, K. Nukumizu, G. Hitoki, T. Takata, J. N. Kondo, M. Hara, H. Kobayashi and K. Domen, *Photoreactions on LaTiO2N under visible light irradiation,* J. Phys. Chem. A, 2002, **106**, 6750-6753.

7 A. Kasahara, K. Nukumizu, T. Takata, J. N. Kondo, M. Hara, H. Kobayashi and K. Domen, *LaTiO2N as a visible-light (<= 600 nm)-driven photocatalyst (2),* J. Phys. Chem. B, 2003, **107**, 791-797.

8 K. Maeda, T. Takata, M. Hara, N. Saito, Y. Inoue, H. Kobayashi and K. Domen, *GaN : ZnO solid solution as a photocatalyst for visible-light-driven overall water splitting,* J. Am. Chem. Soc., 2005, **127**, 8286-8287.

9 K. Maeda, K. Teramura and K. Domen, *Effect of post-calcination on photocatalytic activity of (Ga1-xZnx)(N1-xOx) solid solution for overall water splitting under visible light,* J. Catal., 2008, **254**, 198-204.

10 H. Y. Chen, L. P. Wang, J. M. Bai, J. C. Hanson, J. B. Warren, J. T. Muckerman, E. Fujita and J. A. Rodriguez, *In Situ XRD Studies of ZnO/GaN Mixtures at High Pressure and High Temperature: Synthesis of Zn-Rich (Ga1-xZnx)(N1-xOx) Photocatalysts,* J. Phys. Chem. C., 2010, **114**, 1809-1814.

Chapter 2

Exploratory synthesis for novel oxynitrides with *in situ* high pressure Techniques

2.1 Introduction

Oxynitride synthesis is typically carried out by ammonolysis which involves heating reagents, usually an oxide or an oxide mixture, under flowing ammonia at ambient pressure and temperatures up to 1200°C. However, decomposition and subsequent evaporation of materials at ambient pressure makes the controlling of the stoichiometry challenging. For example, members of wurtzite type $(GaN)_{1-x}(ZnO)_x$ solid solution with $x > 0.3$ are difficult to synthesize via ammonolysis due to the evaporation of Zn.[1-3]

High pressure can stabilize reactants by restricting decomposition to evolve gaseous products and can allow direct reactions of oxides and nitrides/oxynitrides making an interesting approach to synthesize oxynitrides. This advantage is well demonstrated with the $(GaN)_{1-x}(ZnO)_x$ solid solution, where members with $x>0.3$ were first reported with high pressure synthesis by reacting mixtures of GaN and ZnO at 6-7GPa and 1000 °C.[2] However, studies reporting high pressure synthesized oxynitrides are rare. Some examples include, $RZrO_2N$ (R = Pr, Nd, Sm) synthesized at 2-3 GPa,[4] and La_2AO_3N (A = Al, Nb, Ti, V) oxynitrides synthesized at 5 GPa.[5]

In ex-situ "cook and look" high pressure synthesis experiments, the only the information about the final product can be obtained. In contrast, *in situ* synchrotron x-ray scattering can provide information about phase changes in the entire pressure-temperature (P-T) range of an experiment, making it an ideal tool to conduct exploratory synthesis for novel oxynitrides. The

objective of the research reported in this chapter is to attempt to produce novel oxynitrides materials predicted in theoretical studies via *in situ* high pressure synthesis.

2.2 Theoretical studies

The d^0 and/or d^{10} cations are necessary for an oxynitride to have the appropriate band structure for overall water splitting (see chapter 1). There are a large number of elements that can form cations with d^0 and d^{10} configuration. A single element may form several oxynitrides, for an example Ga forms wurtzite type and spinel type oxynitrides.[6, 7] Due to these reasons, a virtually unlimited amount of compositions and structures can be assumed for oxynitrides containing d_0/d_{10} cations. Given the limited time and resources available for *in situ* experiments, it is important to look in to theoretical studies to rank order promising candidate oxynitride compositions that are both likely to form and have an appropriate band structure for solar water splitting. The main theoretical studies referred to in this chapter are summarized below.

2.2.1 First Principle high throughput screening of oxynitrides by Wu et al

A report by Wu et al attempts to predict novel and stable oxynitride compositions using density functional theory.[8] There, the focus was given to determine three important factors for a good oxynitride for photocatalytic water splitting (1) the crystal structure and its thermodynamic phase stability (*versus* competing solids and gases); (2) the band gap; (3) the conduction band (CB) and valence band (VB) edge positions relative to the H_2/H_2O and O_2/H_2O levels in water. These properties were used to define suitability and the DFT determined synthesizability at ambient pressure by computational methods with low enough computational costs. Stable phases were determined by low instability energy ΔH, which is described as negative of the

decomposition reaction energy to the stable phases. Only the phases with ΔH less than 36 meV were considered as stable.[8]

The study was able to predict six known oxynitrides, $CaTaO_2N$, $SrTaO_2N$, $LaTaO_2N$, $LaTiO_2N$, and $BaNbO_2N$.[8]

Wu et al[8] also mention some quaternary(i.e. containing four elements, two metal elements O and N) oxynitride compounds that were predicted to have instability energies higher than 36 meV (up to 200 meV) though exact compositions are not given. However, high pressure synthesis may drive the formation of these oxynitrides (instability energy <36 meV).

2.2.2 Formability of perovskite oxynitrides predicted from tolerance and octahedral factors by Li et al.

Li et al report plausibility of formation of perovskite-type oxynitrides by expanding on the principles used to predict the formability of perovskite-type oxides.[9] Perovskite-type oxides contain the unit formula ABO_3 where A is the larger cation and is 12 fold coordinated with oxygen anion while smaller cation B has 6 fold coordination with oxygen[10] (see figure 2.1). In the ideal case, perovskite oxides have cubic structure.[10]

The formability of perovskite oxides is generally assessed through tolerance and octahedral factors.[9] The tolerance factor t is expressed as follows.

$$t = \frac{r_A + r_O}{\sqrt{2}\,(r_B + r_O)} \qquad (2.1)$$

Where r_A r_B and r_O are ionic radii of A B and O respectively.[10] for an ideal cubic perovskite t is 1, while perovskite oxides form in the range 0.75 <t <1.0.

The Octahedral factor is defined simply as the ratio between ionic radii of B and oxygen[11] or r_B/r_O with the lowest limit being 0.425 .

Li et al extended these principles to predict the formability of perovskite oxynitrides of the form ABO_2N and $ABON_2$.[9] They considered both experimental cation- anion distances and ionic radii for the calculation. This study accurately predicted the formability of several known oxynitrides including $CaTaO_2N$, $SrTaO_2N$ and $LaTaON_2$.[9]

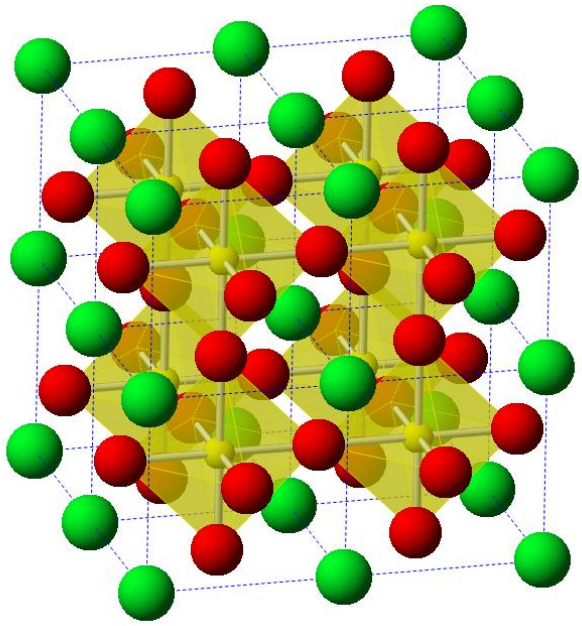

Figure 2.1. Structure of perovskite $SrTiO_3$ with Sr at A sites (green) and Ti at octahedral B sites (yellow)

2.2.3 Estimating band gaps

Li et al did not predict the bandgaps of the reported perovskite oxynitrides although that is necessary to single out most promising candidates for water splitting from a large number of predictions. To overcome this problem, a simple method of band gap determination was used in our studies. The method is based on a semi-empirical method of estimating bad gaps of ternary oxides as a function of the Pauling electronegativities of the elements, reported by Di Quarto et al.[12] The relationship they put forth is

$$E_g=2[E_I(X_M-X_O)+\Xi] \qquad (2.2)$$

Where E_I - Extraionic energy (1.08 for sp-metal oxides, 0.67 for d-metal oxides), X_M , X_O – Pauling electronegativities of the metal and oxygen, Ξ - A factor depending on metal and oxygen bond energies (-1.36 for sp-metal oxides, -0.75 for d-metal oxides)[12]

To check the feasibility of using this formula for an oxynitride with the composition $A_aB_bO_oN_n$ (A and B are metal cations) the form is modified

$$E_g=2[E_I(X_{Ci}-X_{Ai})+\Xi] \qquad (2.3)$$

Where Xci and Xai is the average electronegativity of cations and anions

$$X_{Ci}=\frac{aX_A+bX_B}{a+b} \qquad (2.4)$$

and

$$X_{Ai}=\frac{oX_O+nX_N}{o+n} \qquad (2.5)$$

The band gaps estimated for known oxynitrides using this method tend to fall within 0.5 eV of experimentally observed values. Note that this method will always predict band gaps in a linear (Vegard's law) variation between the end members for oxynitride solid solutions Oxynitride solid solutions of Zirconium and Tantalum do obey Vegard's law[13] however, as explained later in this thesis , $(GaN)_{1-x}(ZnO)_x$ solid solution does not.

Although not expected to be extremely accurate, the rough estimation provided by this method helps to narrow down favorable compositions. The selected perovskite compositions, which were attempted to synthesize in this study are shown in table 2.1

Table 2.1 Perovskite oxynitride tolerance and octahedral factors predicted by Li et al[9] and their predicted band gaps (this study)

Composition	Tolerance factor (t)[9]	Octahedral factor (r_B/r_O)[9]	Band Gap (eV)
$YZrO_2N$	0.881648	0.50259333	4.0
$YHfO_2N$	0.885764	0.49561287	4.1
$ScZrO_2N$	0.82866	0.50259333	3.6
$ScHfO_2N$	0.832528	0.49561287	3.7
$InNbON_2$	0.891214	0.47467148	1.7
$InTaON_2$	0.891214	0.47467148	2.0

2.3 Choosing compositions

Other than the studies mentioned above, few other factors were considered in choosing final compositions. The first consideration was simplicity. For an example $YZrO_2N$ can easily be made y with a 1:1 stoichiometric mixture of Y_2O_3 and Zr_2ON_2. Conversely, a stoichiometric reaction mixture for oxynitride composition $Sr_2Ti_6O_{11}N_2$, (predicted by Wu et al.[8]) is impossible to achieve with known compounds (i.e TiO_2, Sr_3N_2 and SrO_2) and such compositions were given less priority.

Anothert consideration when choosing compositions was about the similar compounds reported in literature. A preference was given to elements that were known to form oxynitrides capable of water splitting (e.g Zr, Ta). Compositions related to reported oxynitrides, such as a member beyond the known composition range of a solid solution, was also considered.

2.4 Experimental

2.4.1 High Pressure Synthesis

The synthesizability of target compositions at ambient pressure was first tested with ammonolysis and/or fused silica tube synthesis. High pressure synthesis experiments reported in this chapter were conducted at the beam line 13 BM-D of the Advanced Photon Source (APS), Argonne National Laboratory and beam line X17B2 of the National Synchrotron Light Source (NSLS), Brookhaven National laboratory. For each experiment, a sample pellet is made by pressing two reactant mixtures separated by a layer of MgO, which acted as the internal pressure standard. Small layers of BN were then put between MgO and reaction mixtures to prevent contact and unintended reactions. For APS experiments sample pellets were contained in a BN sleeve which is placed at the center of a cylindrical cavity drilled in to a cubic boron epoxy cell containing a graphite furnace used for heating (see figure 2.2). Two cylindrical alumina plugs wrer used to fill the remaining space of the cavity. A type C thermocouple ($W_{95}Re_5$–$W_{74}Re_{26}$) was attached to the cell with the junction placed closer to the sample. For NSLS experiments a pyrophyllite cell was used. In that case, the graphite furnace was encased within an alumina sleeve and MgO plugs was used to enclose the sample (see figure 2.2).

At the APS the cells were compressed in a 250 multi-anvil press. Heating was done by passing an electrical current through the graphite furnace while the temperature is being monitored. When a desired temperature point was reached, *in situ* XRD patterns were obtained on the sample (both reaction mixtures and MgO). Monochromatic x-ray beam with photon energy of 62 KeV (wavelength 0.1988Å) was used and diffraction data was collected by means

of an area detector. Two-dimensional x-ray diffraction data was integrated using the software DIOPTAS.[14] The pressure at each temperature point was calculated by using equation of state of MgO.[15]

At the NSLS the cells were compressed in a 200 multi-anvil press. *In situ* Energy dispersive x-ray diffraction data was collected with a polychromatic 'white' beam having photon energies between 20 and 100 keV. Heating was carried out in a similar manner to APS experiments.

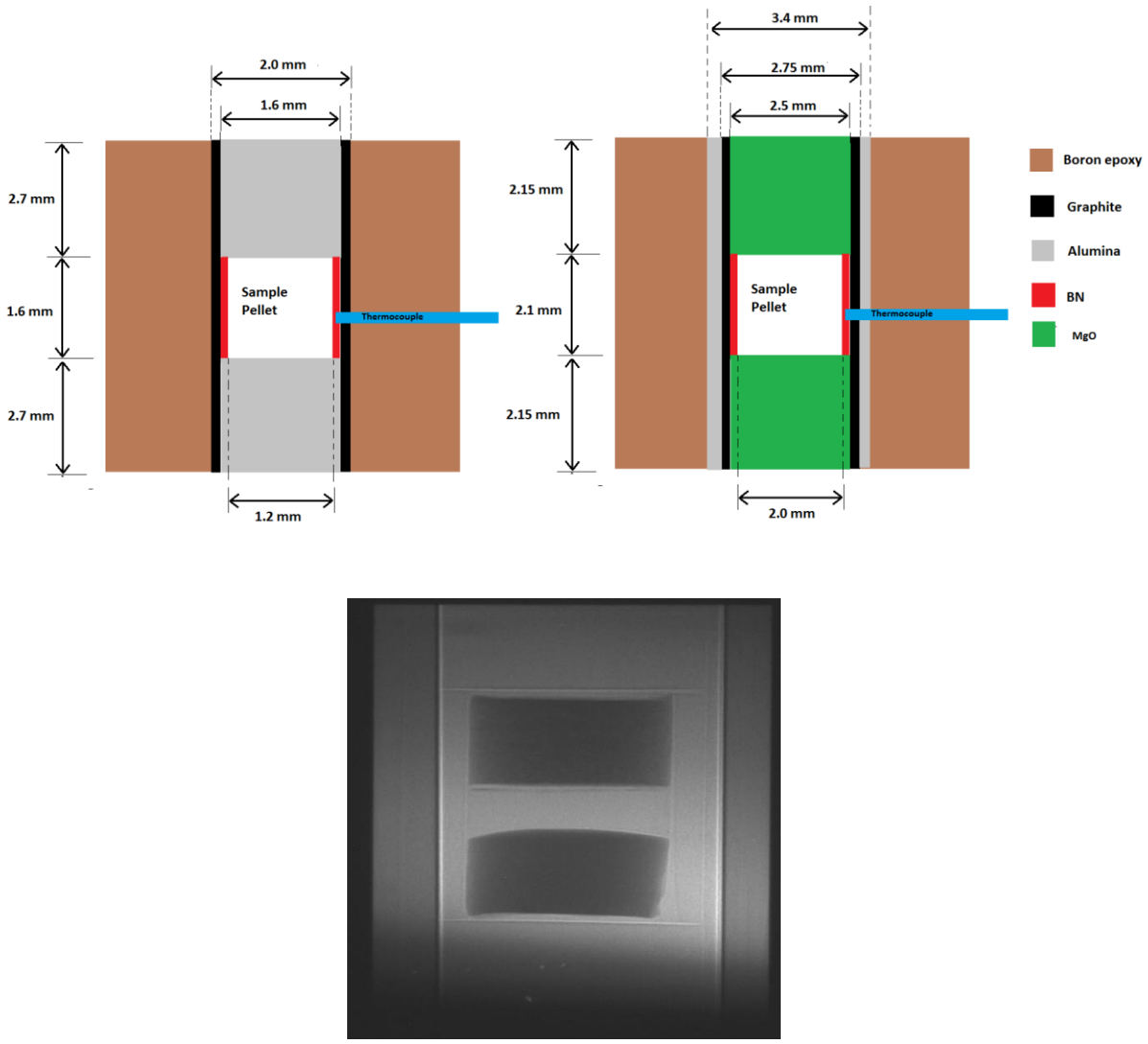

Figure 2.2 Schematics of the high pressure reaction cell used at APS (above left) and NSLS(above right) X-ray photograph of the cell showing the sample pellet with two reaction mixtures (in this case both containing Ta) separated by MgO (below).

2.4.2 Synthesis of Zr_2ON_2 and Hf_2ON_2

Zr_2ON_2 was synthesized by ammonolysing ZrO_2. About 0.2 grams of ZrO_2 was placed in a fused silica boat which was placed inside a quartz tube (Ø = 20mm) going through a tube furnace. Ammonia was flowed through the tube at a rate of 500 ml/min. Synthesis was carried out for 5 hrs at a temperature of 1050°C after which the sample was allowed to cool under flowing ammonia. Recovered product was ground and the whole process was repeated until only Zr_2ON_2 is present in XRD pattern and usually takes ~35 h of synthesis time.

2.4.3 Synthesis of TaON

TaON was synthesized with the method explained by Orhan et al.[16] About 1 gram of Ta_2O_5 was placed inside a tube furnace in the same way described in section 2.3.2. Ammonia gas was bubbled through water before entering the furnace at a rate of 500 ml/min. Synthesis was carried out at 800°C for 10 hours, after which the sample was recovered and XRD analysis was carried out. The whole process was repeated until only TaON is present and takes ~20hrs of synthesis time

2.5 Results and Discussion

In this section, *in situ* high pressure synthesis attempts on several oxynitride systems are discussed. In each case, the justifications for the selection of the system (in par with above mentioned theoretical studies), experimental conditions and observed phases are described.

2.5.1 $Zr_3O_3N_2$

Several oxynitride phases of zirconium are known and numerous studies, namely β phase ($Zr_7O_8N_4$), β' phase ($Zr_7O_{11}N_2$), β'' phase ($Zr_7O_{9.5}N_{3.0}$) and γ phase (Zr_2ON_2).[17] The β phases are solid solutions between $Zr_7O_8N_4$ and ZrO_2.[17, 18] The γ phase has a band gap of 2.6 eV and is known to photocatalytically split water under visible light.[19]

A new zirconium oxynitride phase, $Zr_3O_3N_2$, has been predicted to be formable in Ta_3N_5 (*Cmcm*) structure by Wu et al. The solid solution between $Zr_3O_3N_2$ and Ta_3N_5 is known to exist, but so far reported only up to 20% Zr.[13] It makes an interesting case to see if high pressure can drive the formation of the end member $Zr_3O_3N_2$.

For the synthesis experiment, the reaction mixture was made by mixing ZrO_2 and Zr_2ON_2 in 1:1 molar ratio. In-situ x-ray diffraction data observed in the reaction are showed in figure 2.3. Above 700°C ZrO_2 Slowly begins to disappear and by 1100°C it is completely absent, and only a cubic phase remained. This phase was identified to be β Zirconium oxynitride phase ($Zr_7O_8N_4$).

The result shows that $Zr_7O_8N_4$ is stable in the pressure and temperature range (up to 3.2 GPa and 1100°C) of the experiment and is known to form at ambient pressure. Another important fact is that $Zr_7O_8N_4$ and $Zr_3O_3N_2$ have close stoichiometries with Zr to O ratios being 1.14 and 1 , Zr:N ratios being 0.57 and 0.67 respectively. This strongly suggests the formation of $Zr_3O_3N_2$ below 3.2 GPa is unlikely.

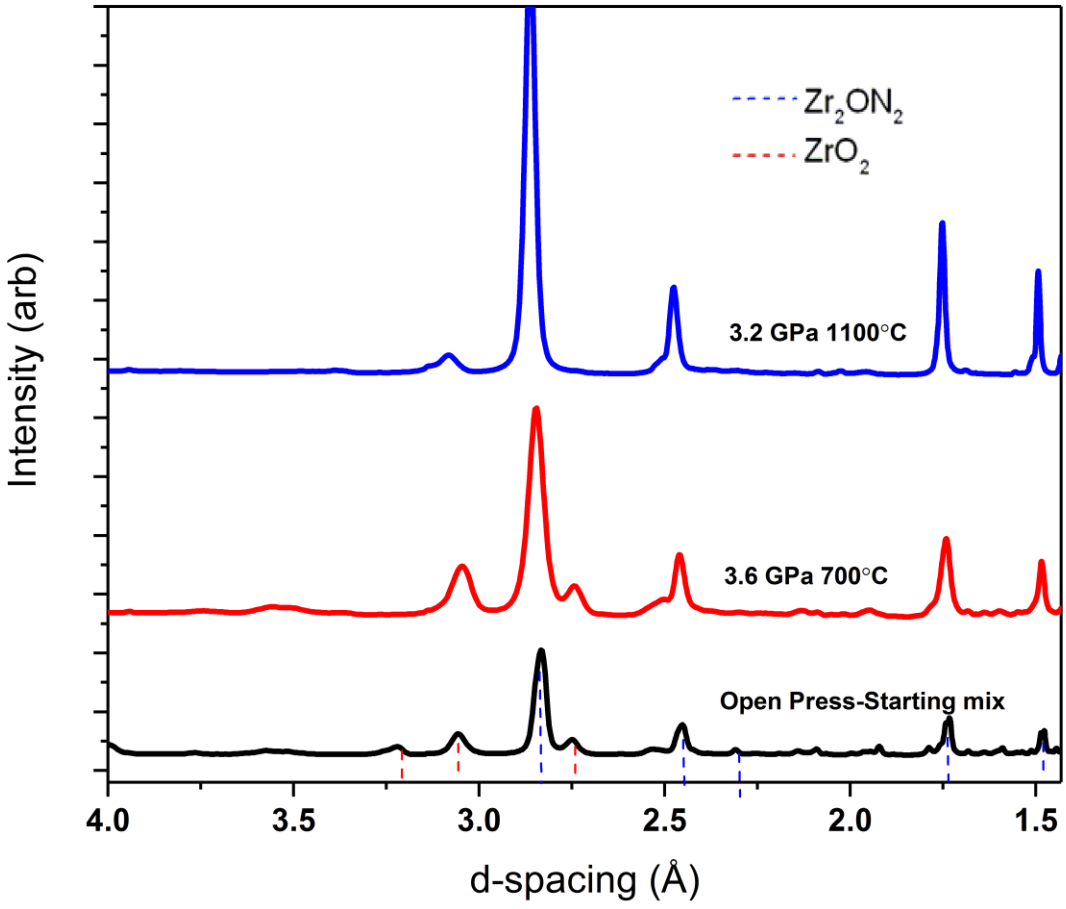

Figure 2.3. *In situ* x-ray diffraction data of the high pressure reaction of ZrO_2 and Zr_2ON_2

2.5.2 Zr_2ON_2-Y_2O_3 and Hf_2ON_2 –Y_2O_3

Zr_2ON_2, Hf_2ON_2 and Y_2O_3 are isostructural (Ia-3) and have cell parameters of 10.22 Å, 9.88 Å and 10.601 Å respectively. This makes them ideal candidates to form solid solutions. However, solid solution members of only 20% Y have been achieved with ambient pressure synthesis.[17]

Li et al report that the perovskites $YZrO_2N$ and $YHfO_2N$ are marginally stable with octahedral factors 0.49, 0.51 and tolerance factors 0.881, 0.885 respectively. Wu et al also reports of a Y-Zr oxynitride phase of with stability energy of about 140 meV/atom, which was beyond their study's considered limit of 36 meV/atom and the exact stoichiometry was not given.

Apart from being known to produce members of solid solutions that are difficult to make at ambient pressure, high pressure synthesis is also known to drive the formation of perovskite-type materials with smaller tolerance factors. In the case of perovskite type solid solution (1 - *x*)$BiScO_3$-*x*$PbTiO_3$ members with $x<0.5$ and $t<0.96$ have been first reported with high pressure synthesis.[20, 21] Although the predicted band gaps for these systems are very high (4.0 eV for $YZrO_2N$ and 4.1 eV for $YHfO_2N$) given the above factors, these systems make interesting cases for high pressure synthesis and was considered.

For synthesis, Zr_2ON_2/Y_2O_3 and Hf_2ON_2/Y_2O_3 1:1 molar mixtures were made. Both samples were reacted in the same cell. Upon compression, this cell reached a pressure of 4.7 GPa which subsequently decreased to 3.5 GPa upon heating (see figure 2.4). At 900°C and 3.5 GPa,

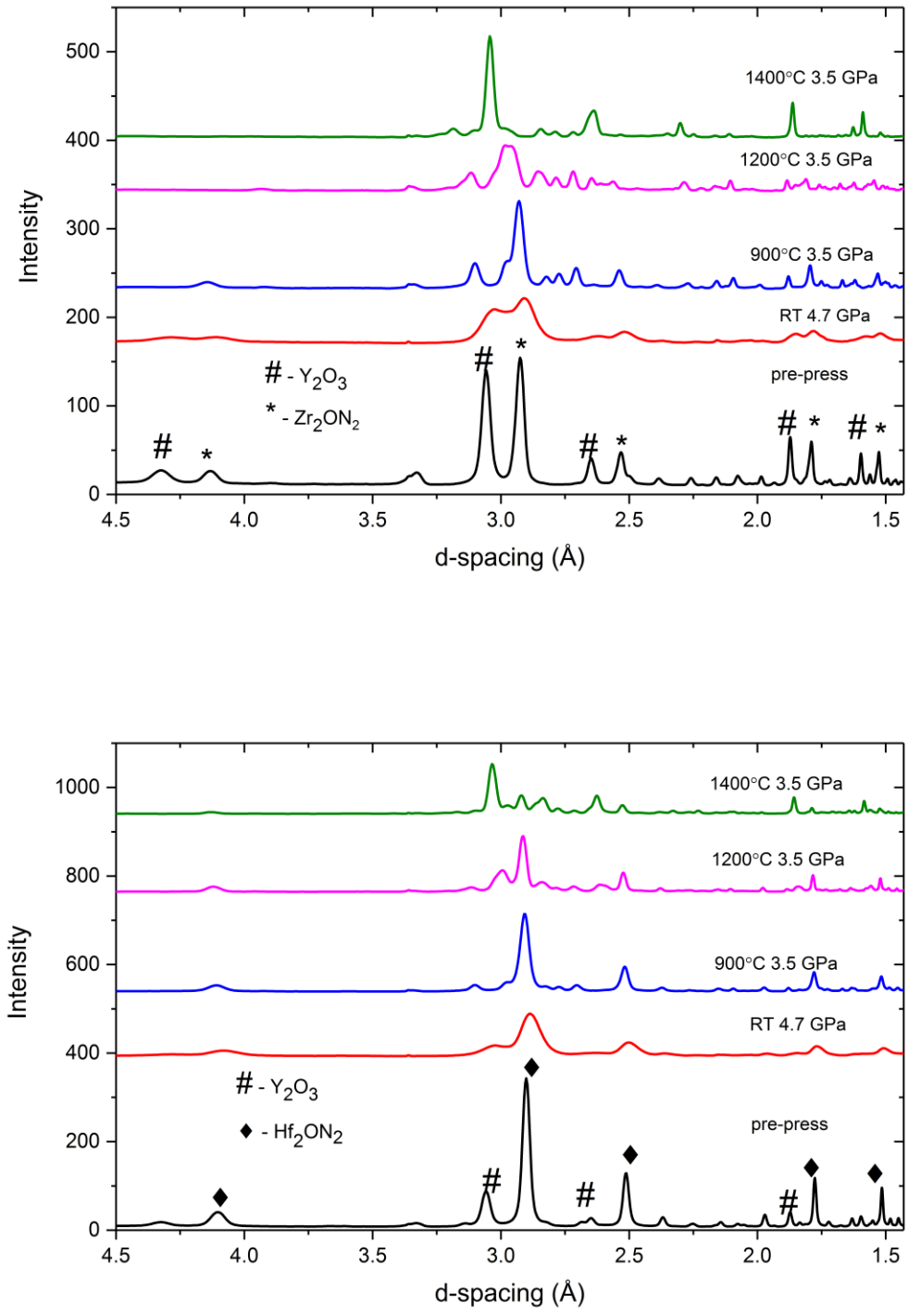

Figure 2.4 *In situ* x-ray diffraction data of the high pressure reaction of Y_2O_3/ Zr_2ON_2 system (above) and Y_2O_3/ Hf_2ON_2 system (below)

Y_2O_3 appears to be diminishing in both mixtures. By 1400°C dominant phases present in both systems appears to be cubic.

The diffraction patterns obtained in-situ experiments are of poor quality with a significant background noise. In order to obtain sufficient amount of sample for a detailed analysis, large sample synthesis was attempted with a piston-cylinder apparatus. About 0.5 g mixtures of each Zr_2ON_2/Y_2O_3 and Hf_2ON_2/Y_2O_3 (1:1 molar) were used. The synthesis was carried out at 1300°C, 1 GPa and higher pressures and temperatures were not possible due to equipment restrictions. X-ray diffractions on samples after the synthesis show that the reactants are largely intact (figure 2.5).

In the case of Hf_2ON_2/Y_2O_3 a small diffraction peak is present at around a d-spacing 3Å,. A similar peak appears for Zr_2ON_2/Y_2O_3 which could correspond to $Zr_2Y_2O_7$. In the Zr-Y sample, ZrN is present indicating reduction of Zr^{+3}. HfN was not observed.

These results indicate that the cubic phases observed in the in-siu experiments form above 1 GPa.

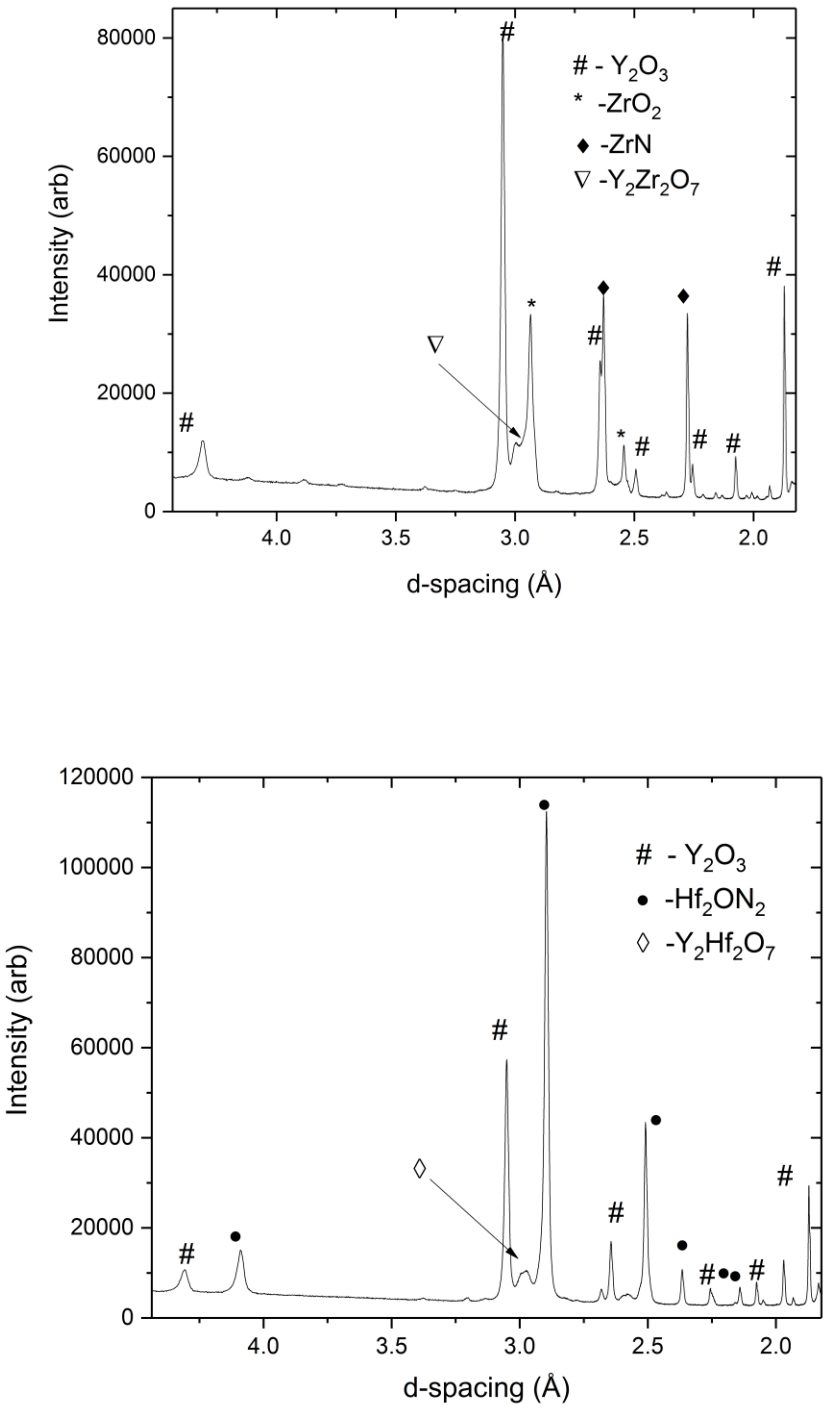

Figure 2.5 XRD data of products obtained by reacting Y_2O_3 and Zr_2ON_2 (top) Y_2O_3 and Hf_2ON_2 (bottom) at 1 GPa and 1300^{0}C

2.5.3 Zr_2ON_2-Sc_2O_3 and Hf_2ON_2 –Sc_2O_3

Sc_2O_3 is also isostructural to Hf_2ON_2 and Zr_2ON_2.[22] According to the report of Li et al. $ScZrO_2N$ and $ScHfO_2N$ perovskites are predicted to have tolerance factors 0.829 and 0.832 respectively with octahedral factors closer to 0.5, making them more unlikely to form than perovskite-type $YZrO_2N$ and $YHfO_2N$. However, Sc_2O_3 has a cell parameter of 9.844 Å that is closer to the isostructural Hf_2ON_2 and Zr_2ON_2 than Y_2O_3 making it a better candidate to form solid solutions. Predicted band gaps for $ScZrO_2N$ and $ScHfO_2N$ are 3.6 eV and 3.7 eV which are more favorable than those of $YZrO_2N$ and $YHfO_2N$ (see table 2.1)

The high pressure synthesis experiments were carried out with Sc_2O_3/Hf_2ON_2 and Sc_2O_3/Zr_2ON_2 1:1 molar mixture. A maximum pressure of 2.7 GPa was achieved during synthesis. Samples were heated to 1100°C before quenching. Sc_2O_3 did not react in both cases. Other end products were found to be $Zr_7O_8N_4$ and $Hf_7O_8N_4$.

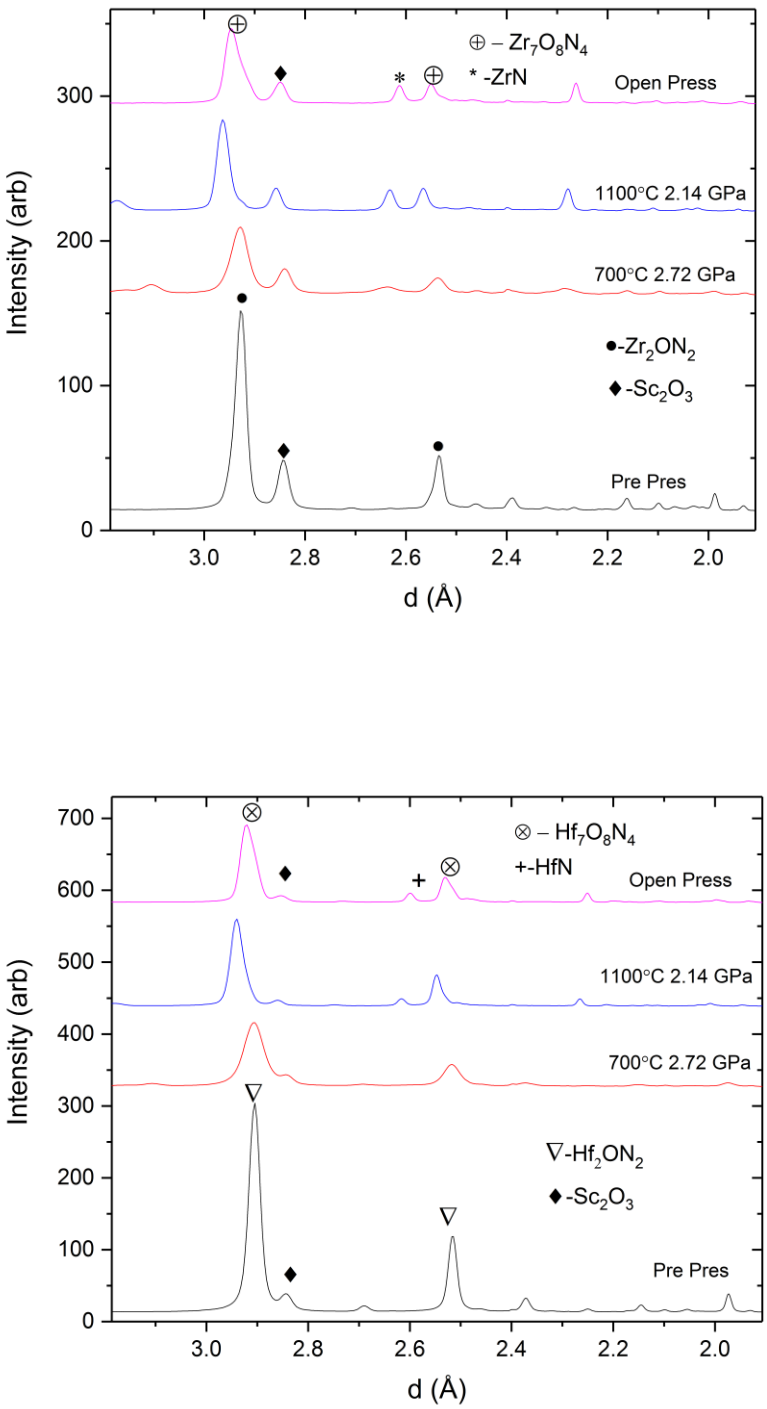

Figure 2.6 *In situ* x-ray diffraction data of the high pressure reaction of Sc_2O_3/ Zr_2ON_2 system (above) and Sc_2O_3/ Hfr_2ON_2 system (below)

2.4.4 InN-Nb_2O_5

Two oxynitrides in the GaN-Nb_2O_5 system have been recently reported with high pressure synthesis.[23] InN has wurtzite type structure (*$P6_3mc$*) with cell parameters a,b= 3.501Å and c=5.6690Å.[24] It is isostructural to GaN (a,c= 3.190 Å c=5.189 Å). [24] Since In and Ga are both group 13 elements, it is compelling to see if InN will react with Nb_2O_5 in a similar manner to GaN. Also, report of Li et al. predicts an $InNbON_2$ perovskite to have a tolerance factor of 0.89 and an octahedral factor of 0.47 while the predicted band gap being 1.7 eV.

The reaction was carried out with 2:1 mixture of InN and Nb_2O_5. The cell reached a pressure of 2.8 GPa (at 600^0C) and reduced to 2.5 GPa at 1000^0C.(figure 2.7)

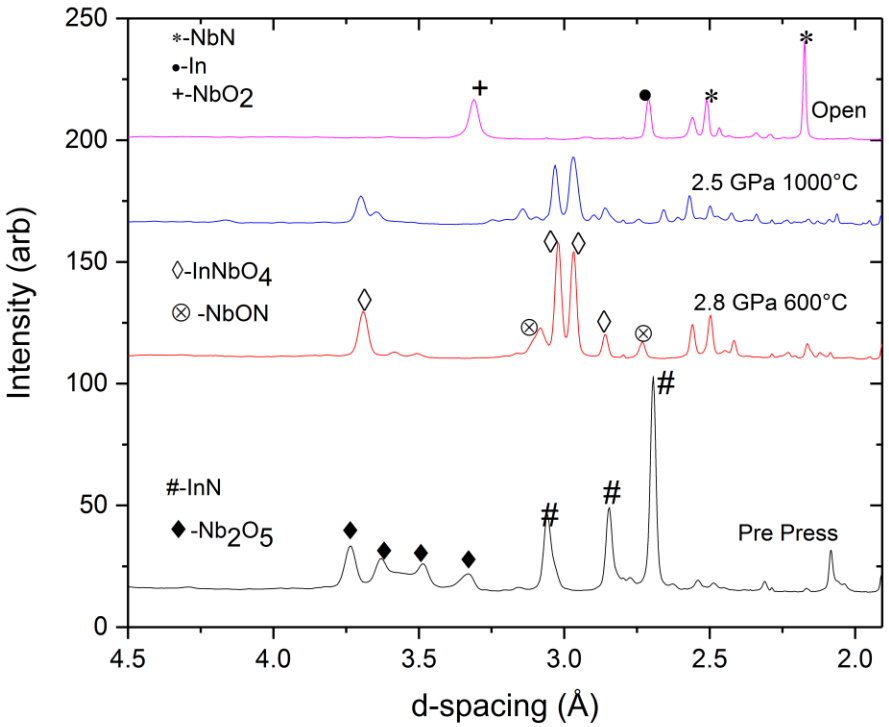

Fig 2.7 *In situ* x-ray diffraction data of the high pressure reaction of InN/Nb_2O_5 system

At 600^0C 2.8GPa, InN and Nb_2O_5 have reacted to form $InNbO_4$ and NbON where Nb and In still exist in +5 and +3 oxidation states respectively. Upon heating to 1000^0C NbON disappears. After quenching and subsequent decompression, the end products was found to be NbN, NbO_2, where Nb exist in +3 and +4 oxidation states, and metallic In.

2.5.5 InN-TaON.

TaON has baddeleyite type structure with a band gap of 2.5 eV and is known for photocatalytic hydrogen evolution activity.[25] Several visible light absorbing Ta-Zr oxynitrides are also known.[13] This suggests that Ta containing systems are likely to have right band structure for visible light driven water splitting. Report by Li et al predicts perovskite $InTaON_2$ to have a tolerance factor of 0.89 and an octahedral factor of 0.47 , putting it right below of the stable range.[9] Band gap of $InTaON_2$ is predicted to be a very favorable 2.0 eV.

An attempt was made to synthesize the perovskite at high pressure with an 1:1 molar mix of InN and TaON. During the experiment, InN began to disappear upon heating and is completely disappeared around 600°C. TaON did not decompose and survives heating, quenching and decompression. In_2O_3 appears after quenching. (see Figure 2.8).

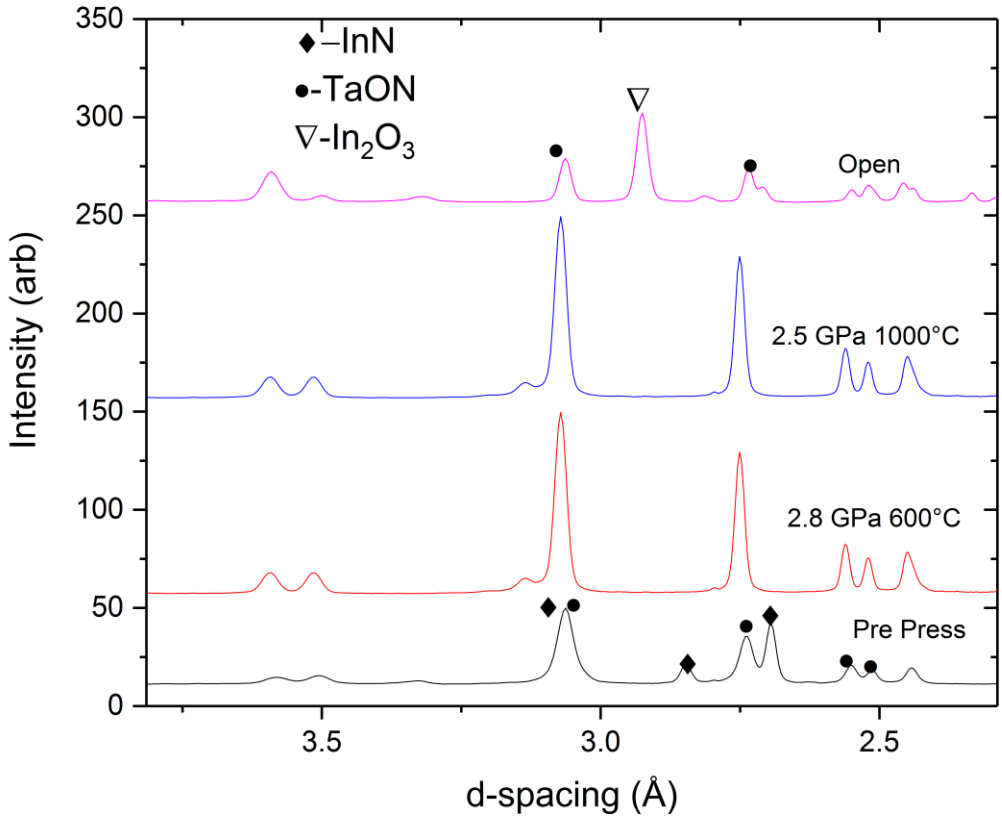

Figure 2.8 *In situ* x-ray diffraction data of the high pressure reaction of InN/TaON system

2.5.6 $Zr_2ON_2 – Ba_3N_2$

Wu et al.'s predictions mention a possible Zr-Ba oxynitride with instability energy of about 90 meV, though more details were not given. [8] We carried out a synthesis experiment to check possible formation Zr-Ba oxynitride by reacting Zr_2ON_2 and Ba_3N_2 in 1:1 molar ratio. The starting material are nitrogen rich with N:O ratio of 4:1and, it was expected that the system will retain more N, and so contrast previous experiments where considerable replacement of N with O was observed.

Ba_3N_2 is hygroscopic, reacting with moisture to form $Ba(OH)_2$, so the reaction mixture was prepared and loaded under a dry N_2 environment in a glove box. The diffraction patterns obtained on the sample (loaded cell) before compression did not indicate any Ba containing compounds (see figure 2.9) other than the reactant. The cell was heated to 1000°C after which the pressure dropped to 0.6 GPa. The final product was $BaZrO_3$ with some Zr_2ON_2 remaining and this survived quenching.

2.5.7 $Zr_2ON_2 – GaN$

Although oxynitride materials containing Ga and Zr are known to be water splitters[19, 26] no known oxynitride containing both the elements has been reported. The study by Wu et al does not report a Ga-Zr oxynitride within the considered stability range and the perovskite tolerance factor predicted for $ZrGaO_2N$ is very small at 0.825 compared to the ideal 1.0, suggesting that ambient pressure synthesis of such an oxynitride may not be viable.

We carried out a high pressure synthesis experiment with a 1:1 mixture of Zr2ON2 and GaN. The cell was heated to a temperature of 800°C where pressure dropped rapidly(see figure 2.10).No reaction was observed with Zr_2ON_2 and GaN remaining intact.

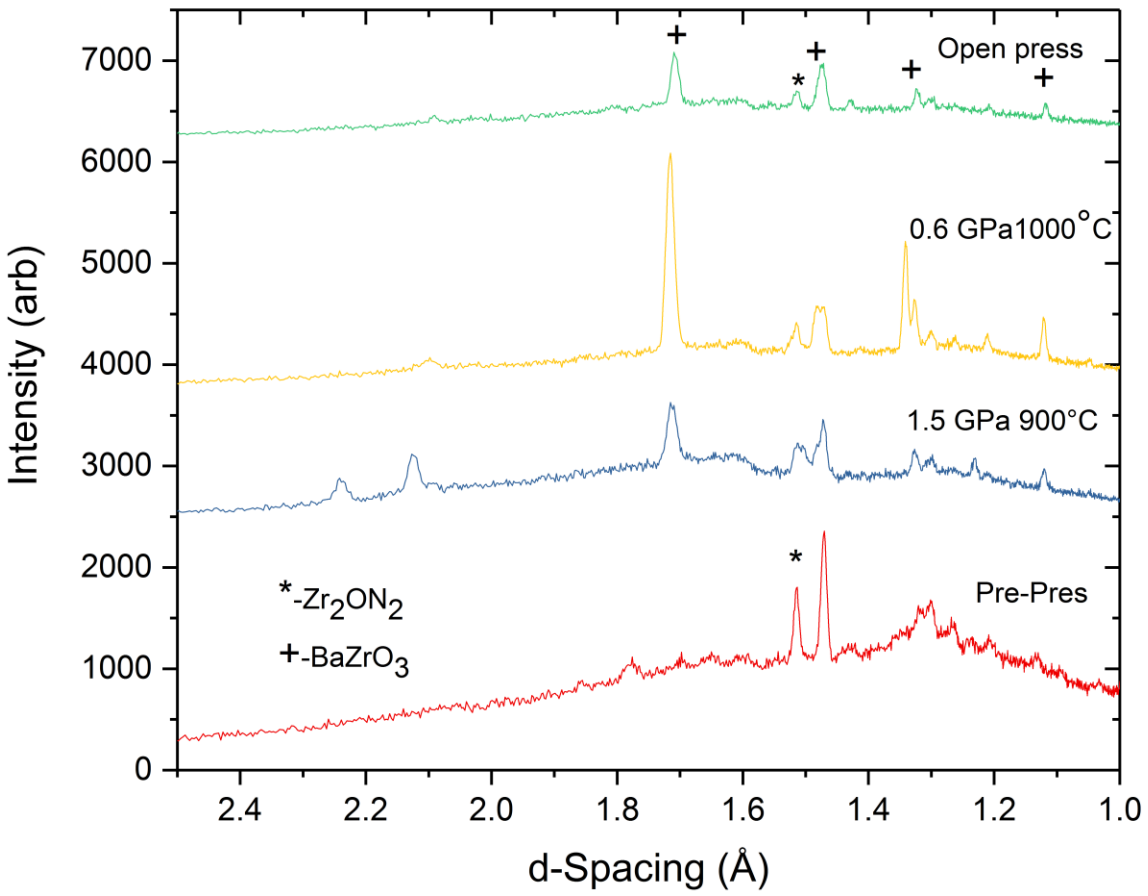

Figure 2.9 *In situ* x-ray diffraction data of the high pressure reaction of Zr_2ON_2/Ba_3N_2 system

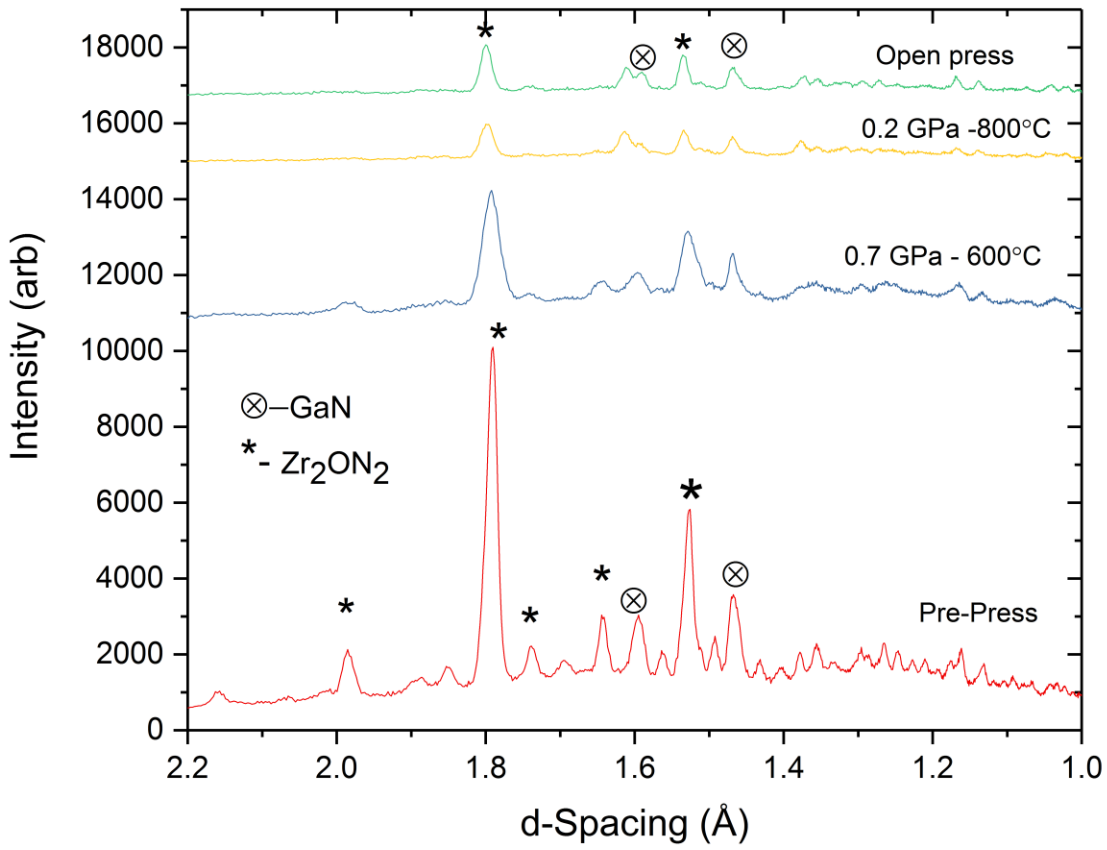

Figure 2.10 *In situ* x-ray diffraction data of the high pressure reaction of Zr_2ON_2/GaN system

2.5.8 Identified issues and suggestions for future research

One major problem observed with the *in situ* high pressure synthesis experiments is the replacement of N by O in the reaction environment. Such replacement has been observed before in the high pressure synthesis of GaN-ZnO solid solution, although to a much smaller extent.[2] In the above-reported experiments replacement of N is very significant. In the case of Zr_2ON_2/Sc_2O_3 and the formation of $Zr_7O_8N_4$ indicate a loss of 43% of N originally in the reaction mixture. In the case InN/TaON all InN has been oxidized to In_2O_3. Out of the materials in the high pressure reaction cell, alumina BN and graphite cannot provide O and Al_2O_3 is stable, so the most likely source oxygen is the boron-epoxy cell itself, presumably due to the decomposition of epoxy resin at high temperature as the inner cell surface is in direct contact with the graphite furnace. It can also be that in the process of affixing fixing the thermocouples, BN sleeves might have fractured, exposing samples to oxygen..

Another main issue is the reduction of cations to lose the $d^{0/}d^{10}$ configurations. Cations with d_0/d_{10} electronic configurations are necessary for an oxynitride to have the appropriate band structure to both absorb visible light and to water split.[27] In the above- mentioned experiments all of In^{3+} and Nb^{5+} in the systems were observed to reduce. Nb^{5+} has been reported to partially reduce in the high pressure synthesis experiments on GaN-Nb2O5 system.[23] In comparison Ta^{5+} although being in the group as Nb (group 5) did not reduce. In the case of Zr^{4+} and Hf^{4+} only a fraction of the ions reduced. In order to avoid oxygen association, a different cell arrangement containing a layer of insulation (preferably BN) between furnace and cell is advisable for future experiments. Also the use of thermocouples may be avoided by doing a calibration for temperature as a function of applied voltage.

Also, in order to minimize reduction and N loss, a Pt capsule could be used to cover sample pellet. This method has been used to synthesize single crystals of Nb_2O_5 without Nb^{5+} reduction.[28] The capsule could be expected to prevent O in the reaction environment from reaching the sample. However, in future research, avoiding In and Nb and prioritizing Zr,Hf and Ta containing systems is suggested to maximize the chances of discovering a novel oxynitride. One problem with Pt is its high x-ray absorption cross section, which can make getting reasonable quality data difficult, especially when sample contain strongly absorbing elements such as Ta.

It is evidently clear from this research effort is that theoretical predictions on oxynitrides that specifically consider high pressure and temperature conditions are necessary. Even though pressures beyond 5 GPa were not used for the reported research, It can also be suggested to explore possibilities at pressures beyond 5 GPa for future theoretical and experimental studies to expand the probability of success.

2.6 Summary and Conclusions

Attempts were made to synthesize oxynitrides at high pressure based on reported theoretical predictions. Reacting Zr_2ON_2 and ZrO_2 at 3.6 GPa yielded $Zr_7O_8N_4$ suggesting that the target phase $Zr_3O_3N_2$ is unlikely to form below that pressure. Two cubic like phases phase formed in Y_2O_3-Zr_2ON_2 and Y_2O_3-Zr_2ON_2 at 1400°C and 3.5 GPa but could not be synthesized in bulk at 1 GPa. Other experiments show that Nb^{5+} and In^{3+} tend to reduce at high pressure reaction environment while Ta^{5+} was stable. Considerable replacement of N with O was observed in all experiment with O possibly coming from the decomposition of epoxy resin. A

modified cell configuration may be necessary to avoid N replacement. Also, using a platinum capsule to prevent both N loss, and cation reduction is suggested. Theoretical predictions that specifically consider high pressure and temperature conditions are necessary for future studies.

2.6 Acknowledgements

The selection of compositions, preparation of samples and collection of *in situ* data was carried out by H A N Dharmagunawardhane. Special thanks go to Mr. Alwin James of the Department of Chemistry, Dr. Alexandra Sinclair and Mr. William Woerner of the Department of Geosciences for providing assistance in sample preparation. Dr. Yanbin Wang and Dr. Tony Yu of GSECARS provided support for *in situ* experiments at APS. Dr. Matthew Whittaker and Dr. Haiyan Chen provided support for *in situ* experiments at NSLS

References

1 L. L. Jensen, J. T. Muckerman and M. D. Newton, *First-principles studies of the structural and electronic properties of the (Ga1-xZnx)(N1-xOx) solid solution photocatalyst,* J. Phys. Chem. C., 2008, **112**, 3439-3446.

2 H. Y. Chen, L. P. Wang, J. M. Bai, J. C. Hanson, J. B. Warren, J. T. Muckerman, E. Fujita and J. A. Rodriguez, *In Situ XRD Studies of ZnO/GaN Mixtures at High Pressure and High Temperature: Synthesis of Zn-Rich (Ga1-xZnx)(N1-xOx) Photocatalysts,* J. Phys. Chem. C., 2010, **114**, 1809-1814.

3 A. A. Reinert, C. Payne, L. M. Wang, J. Ciston, Y. M. Zhu and P. G. Khalifah, *Synthesis and Characterization of Visible Light Absorbing (GaN)(1-x)(ZnO)(x) Semiconductor Nanorods,* Inorg. Chem., 2013, **52**, 8389-8398.

4 M. H. Yang, J. A. Rodgers, L. C. Middler, J. Oro-Sole, A. B. Jorge, A. Fuertes and J. P. Attfield, *Direct Solid-State Synthesis at High Pressures of New Mixed-Metal Oxynitrides: RZrO2N (R = Pr, Nd, and Sm),* Inorg. Chem., 2009, **48**, 11498-11500.

5 I. O. Troyanchuk, N. V. Kasper, O. S. Mantytskaya and E. F. Shapovalova, *High-Pressure Synthesis of Some Perovskite - Like Compounds with a Mixed Anion Type,* Mater. Res. Bull., 1995, **30**, 421-425.

6 C. C. Hu and H. S. Teng, *Gallium Oxynitride Photocatalysts Synthesized from Ga(OH)(3) for Water Splitting under Visible Light Irradiation,* J. Phys. Chem. C., 2010, **114**, 20100-20106.

7 E. Soignard, D. Machon, P. F. McMillan, J. J. Dong, B. Xu and K. Leinenweber, *Spinel-structured gallium oxynitride (Ga(3)O(3)N) synthesis and characterization: An experimental and theoretical study,* Chem. Mater., 2005, **17**, 5465-5472.

8 Y. B. Wu, P. Lazic, G. Hautier, K. Persson and G. Ceder, *First principles high throughput screening of oxynitrides for water-splitting photocatalysts,* Energ Environ Sci, 2013, **6**, 157-168.

9 W. J. Li, E. Ionescu, R. Riedel and A. Gurlo, *Can we predict the formability of perovskite oxynitrides from tolerance and octahedral factors?,* J Mater Chem A, 2013, **1**, 12239-12245.

10 M. A. Pena and J. L. G. Fierro, *Chemical structures and performance of perovskite oxides,* Chem. Rev., 2001, **101**, 1981-2017.

11 C. Li, K. C. K. Soh and P. Wu, *Formability of ABO(3) perovskites,* J. Alloys Compd., 2004, **372**, 40-48.

12 F. DiQuarto, C. Sunseri, S. Piazza and M. C. Romano, *Semiempirical correlation between optical band gap values of oxides and the difference of electronegativity of the elements. Its importance for a quantitative use of photocurrent spectroscopy in corrosion studies,* J. Phys. Chem. B, 1997, **101**, 2519-2525.

13 E. Guenther and M. Jansen, *Optical properties of Ta(3-x)Zr(x)N(5-x)O(x) semiconductor pigments,* Mater. Res. Bull., 2001, **36**, 1399-1405.

14 C. Prescher and V. B. Prakapenka, *DIOPTAS: a program for reduction of two-dimensional X-ray diffraction data and data exploration,* High Pressure Res, 2015, **35**, 223-230.

15 P. I. Dorogokupets and A. Dewaele, *Equations of state of MgO, au, pt, NaCl-B1, and NaCl-B2: Internally consistent high-temperature pressure scales,* High Pressure Res, 2007, **27**, 431-446.

16 E. Orhan, F. Tessier and R. Marchand, *Synthesis and energetics of yellow TaON,* Solid State Sci, 2002, **4**, 1071-1076.

17 I. Molodetsky, A. Navrotsky, F. DiSalvo and M. Lerch, *Energetics of oxidation of oxynitrides: Zr-N-O, Y-Zr-N-O, Ca-Zr-N-O, and Mg-Zr-N-O,* J. Mater. Res., 2000, **15**, 2558-2570.

18 T. Bredow and M. Lerch, *On the anion distribution in Zr7O8N4,* Z. Anorg. Allg. Chem., 2007, **633**, 2598-2602.

19 T. Mishima, M. Matsuda and M. Miyake, *Visible-light photocatalytic properties and electronic structure of Zr-based oxynitride, Zr2ON2, derived from nitridation of ZrO2,* Appl Catal a-Gen, 2007, **324**, 77-82.

20 Y. Inaguma, A. Miyaguchi, M. Yoshida, T. Katsumata, Y. Shimojo, R. P. Wang and T. Sekiya, *High-pressure synthesis and ferroelectric properties in perovskite-type BiScO3-PbTiO3 solid solution*, J. Appl. Phys., 2004, **95**, 231-235.

21 M. Alguero, J. Ricote, T. Hungria and A. Castro, *High-sensitivity piezoelectric, low-tolerance-factor perovskites by mechanosynthesis*, Chem. Mater., 2007, **19**, 4982-4990.

22 T. Schleid and G. Meyer, *Single-Crystals of Rare-Earth Oxides from Reducing Halide Melts*, J Less-Common Met, 1989, **149**, 73-80.

23 W. R. Woerner, G. R. Qian, A. R. Oganov, P. W. Stephens, H. A. N. Dharmagunawardhane, A. Sinclair and J. B. Parise, *Combined Theoretical and in Situ Scattering Strategies for Optimized Discovery and Recovery of High-Pressure Phases: A Case Study of the GaN-Nb2O5 System*, Inorg. Chem., 2016, **55**, 3384-3392.

24 A. F. Wright and J. S. Nelson, *Consistent Structural-Properties for Aln, Gan, and Inn*, Physical Review B, 1995, **51**, 7866-7869.

25 G. Hitoki, T. Takata, J. N. Kondo, M. Hara, H. Kobayashi and K. Domen, *An oxynitride, TaON, as an efficient water oxidation photocatalyst under visible light irradiation (lambda <= 500 nm)*, Chem. Commun., 2002, DOI: 10.1039/b202393h, 1698-1699.

26 K. Maeda, T. Takata, M. Hara, N. Saito, Y. Inoue, H. Kobayashi and K. Domen, *GaN : ZnO solid solution as a photocatalyst for visible-light-driven overall water splitting*, J. Am. Chem. Soc., 2005, **127**, 8286-8287.

27 K. Maeda and K. Domen, *New non-oxide photocatalysts designed for overall water splitting under visible light*, J. Phys. Chem. C., 2007, **111**, 7851-7861.

28 S. Tamura, K. Kato and M. Goto, *Single-Crystals of T-Nb2o5 Obtained by Slow Cooling Method under High-Pressures*, Z. Anorg. Allg. Chem., 1974, **410**, 313-315.

Chapter 3

Photocatalytic hydrogen evolution using nanocrystalline gallium oxynitride spinel

3.1 Introduction

Commercialization of materials produced at high pressure suffers from the cost of production. It is vital to develop strategies for the production of promising functional materials in higher volumes than might be available at high pressure (HP). In this chapter[1], we report *chimie douce* methods to synthesize a phase produced at HP, gallium oxynitride spinel (GOS), from ammonolysis of gallium nitrate hydrate and of gallium-based metal organic frameworks. The photocatalytic hydrogen evolution activity was monitored from the former. Since first being predicted by Lowther et al.,[2] there have been numerous reports of the synthesis of GOS. The phase was first synthesized as an impurity in GaN thin films.[3, 4] It has also been synthesized at high pressures,[5-9] by ammonolysis of gallium nitrate[6] and solvothermally.[10] Products obtained solvothermally have large reported band gaps, varying from 4.1 eV to 4.9 eV,[11] while the GOS synthesized at high pressure is dark brown in color, indicating absorption in the visible range.[5] These results suggest that the band gap might be tuned by varying synthetic conditions. While there are no reports that GOS is a photocatalyst until this study, the reported band gaps and its appearance suggest that the material might be a good candidate for water splitting and may be useful as a platform for further study of the relationships between stoichiometry, order/disorder and local structure on photocatalytic activity.

[1]Content reported in this chapter are published in the Journal of Materials Chemistry A.[1]

3.2. Experimental

3.2.1 Synthesis of Gallium Oxynitride Spinel

Nanocrystalline GOS was prepared in a tube furnace by ammonolyzing ~0.5 g of finely ground gallium nitrate hydrate ($Ga(NO_3)_3$•×H_2O Sigma-Aldrich 99.9%) in a fused silica boat. Ammonolysis was carried out under an NH_3 flow (Praxair inc., 99.99%) of 100 mL/min. The sample was heated to the desired temperature at a rate of 40 °C/min and held at the temperature for 3 hrs. The furnace was then switched off and the sample allowed to cool over ~1 hr to 200 °C under flowing ammonia. At 200 °C the atmosphere was switched to extra-dry nitrogen (General Welding Supply Corp, 99.99%, 100 mL/min) and the product was quenched to room temperature. The recovered product was reground and the ammonolysis was repeated once using the conditions described above to obtain the final product. Ga-BDC(benzenedicarboxylic)based GOS products were synthesized by ammonolyzing 0.5 g of Ga-BDC under the same conditions mentioned above.

3.2.2 Characterization

X-ray diffraction (XRD) patterns were collected using a Rigaku Ultima IV diffractometer with CuKα radiation. Chemical analyses for oxygen and nitrogen were carried out using inert gas fusion by Luvak Inc., Boylston, MA, USA. Samples were heated to 120 °C for 20 min prior to analysis to remove any adsorbed species.

Photocatalytic reactions were carried out in a customized Pyrex reactor, with a closed gas evacuation and circulation system. 100 mg of sample were dispersed in 100 mL of aqueous solution containing 20 vol% methanol. The suspension was purged and degassed with argon while being stirred in the dark for 30 min, before adjusting the pressure to 40 Torr of argon (to

serve as a carrier gas). Afterwards, the suspension was irradiated by a 300 W Xe lamp (Newport, Model 66984), equipped with a 10 cm water filter to eliminate IR radiation ($\lambda > 800$ nm) and a cut-off filter to eliminate light with $\lambda < 320$ nm. The amount of evolved hydrogen was detected by an inline GC-TCD system (Agilent, 7890A).

UV-Vis diffuse reflectance data were collected in a PerkinElmer Lambda 950 spectrometer over a range of 200-860 nm with a scan rate of 182 nm/min using $BaSO_4$ (Alfa Aesar, 99.998%) as a 100% reflectance standard. Powder samples were loaded into a cylindrical powder holder with a circular quartz window 16.60 mm in diameter and 1.50 mm thick mounted vertically adjacent to a 60 mm diameter Spectralon-coated integrating sphere.

For stability tests, two suspensions of 400 mg of GOS dispersed in 400 mL of aqueous solution containing 20 vol% methanol were prepared. One suspension was exposed to light for 6 hrs under the same conditions as used for the photocatalytic reaction testing. The other suspension was kept in the dark for 6 hrs. Both samples were recovered and dried at 50°C for 2 hrs.

3.3 Results and Discussion

3.3.1 Synthesis

Previously, nanocrystalline GOS at ambient pressure has been achieved by using gallium based metalorganic compounds as precursors.[11, 12] In our initial synthesis attempts, we ammonolyzed Ga-BDC (benzenedicarboxylic) and the products obtained at 350 °C and 550 °C show very low degree of crystallinity (fig 3.1). In comparison, the GOS synthesized by

ammonolysing $Ga(NO_3)_3 \bullet \times H_2O$ show a higher degree of crystallinity, and was selected for further studies.

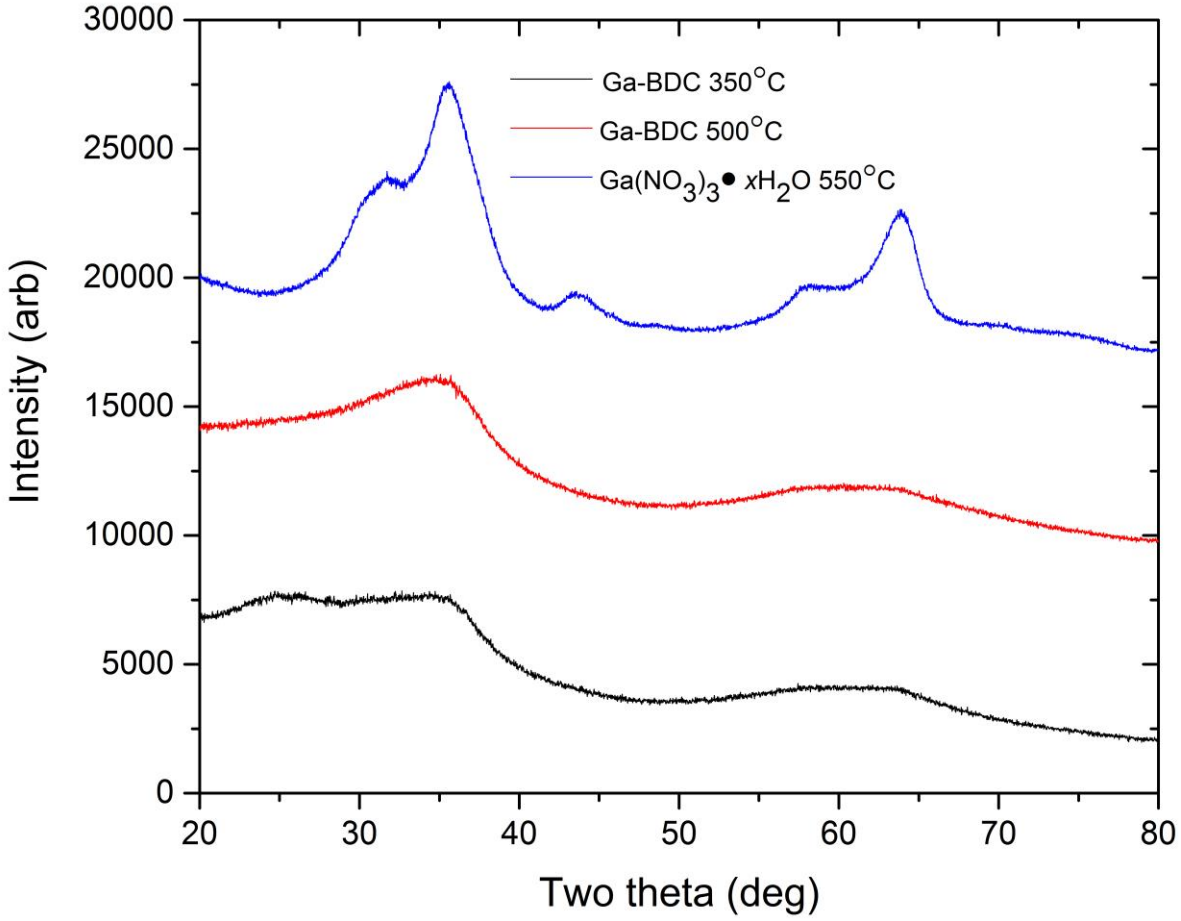

Figure 3.1 XRD patterns Ga-O-N spinel products synthesized with Ga-BDC precursor at 350°C and500°C and with $Ga(NO_3)_3.xH_2O$ at 550°C

An ammonolysis temperature of 550 °C was initially chosen for the synthesis of GOS from $Ga(NO_3)_3 \bullet \times H_2O$ based upon several observations gleaned from the literature, since a reaction temperature was not specified in the original report.[6] Thermal treatments of the solvothermally produced spinel show that the structure is retained even after heating to 500 °C[11] while it is known that ammonolyzing $Ga(NO_3)_3 \bullet \times H_2O$ above 600 °C[13] will produce wurtzite GaN. The XRD pattern (Figure 3.2 (a)) acquired for gallium oxynitride spinel produced at 550 °C (GOS-550) indicates the presence of only the nanocrystalline spinel phase. Later, we carried out a series of synthesis experiments in the temperature range 400°C-600°C to check the formability of GOS and observed more crystalline products at lower temperatures (see figure 3.2. (b)). However, compared to yellow GOS-550, samples produced at 450°C and 500°C were white indicating poor visible light absorption, possibly due to lower N content.

The chemical analysis obtained for the GOS-550 sample shows N and O mass percentages of 1.85% and 24.1%, respectively, yielding a stoichiometry close to $Ga_{2.78}O_{3.65}N_{0.35}$ if a filled anion model is assumed. There are a number of stoichiometries for GOS reported in the literature, and these vary depending on the method of synthesis. For GOS obtained at 5 GPa and 1250 °C the reported stoichiometry is nitrogen rich, $Ga_{2.79}\square_{0.21}(O_{3.05}N_{0.76}\square_{0.19})$ (□ = vacancy).[8] A wide variation in stoichiometry (N molar composition 0.6% to 13.9%) was observed in solvothermally prepared GOS products after subjecting to thermal treatment under air, argon and ammonia.[11] However, these values may be limited in accuracy due to the presence of absorbates.[11]

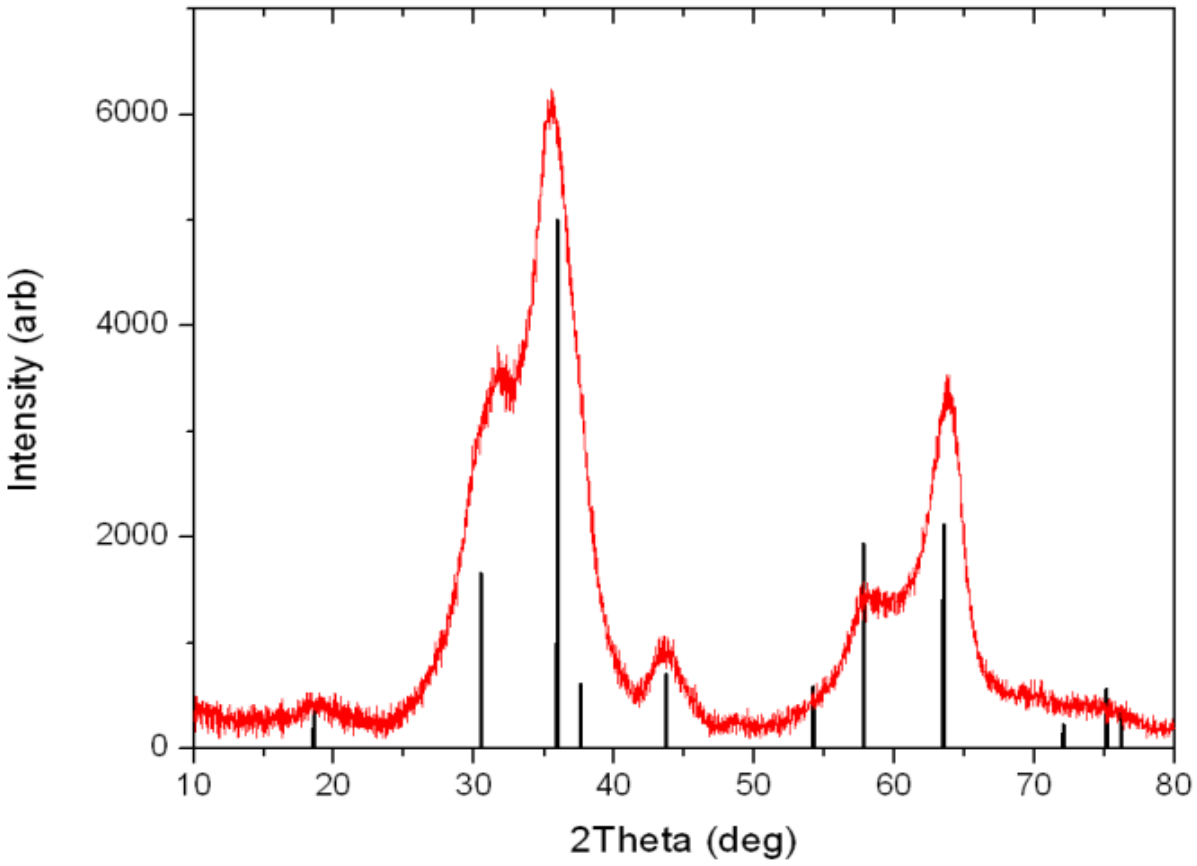

Figure 3.2 (a). XRD pattern (background subtracted) of gallium oxynitride spinel products synthesized from $Ga(NO_3)_3 \cdot \times H_2O$ at 550ºC with calculated reflections shown for Ga_3O_3N with a cell parameter of 8.25 Å.

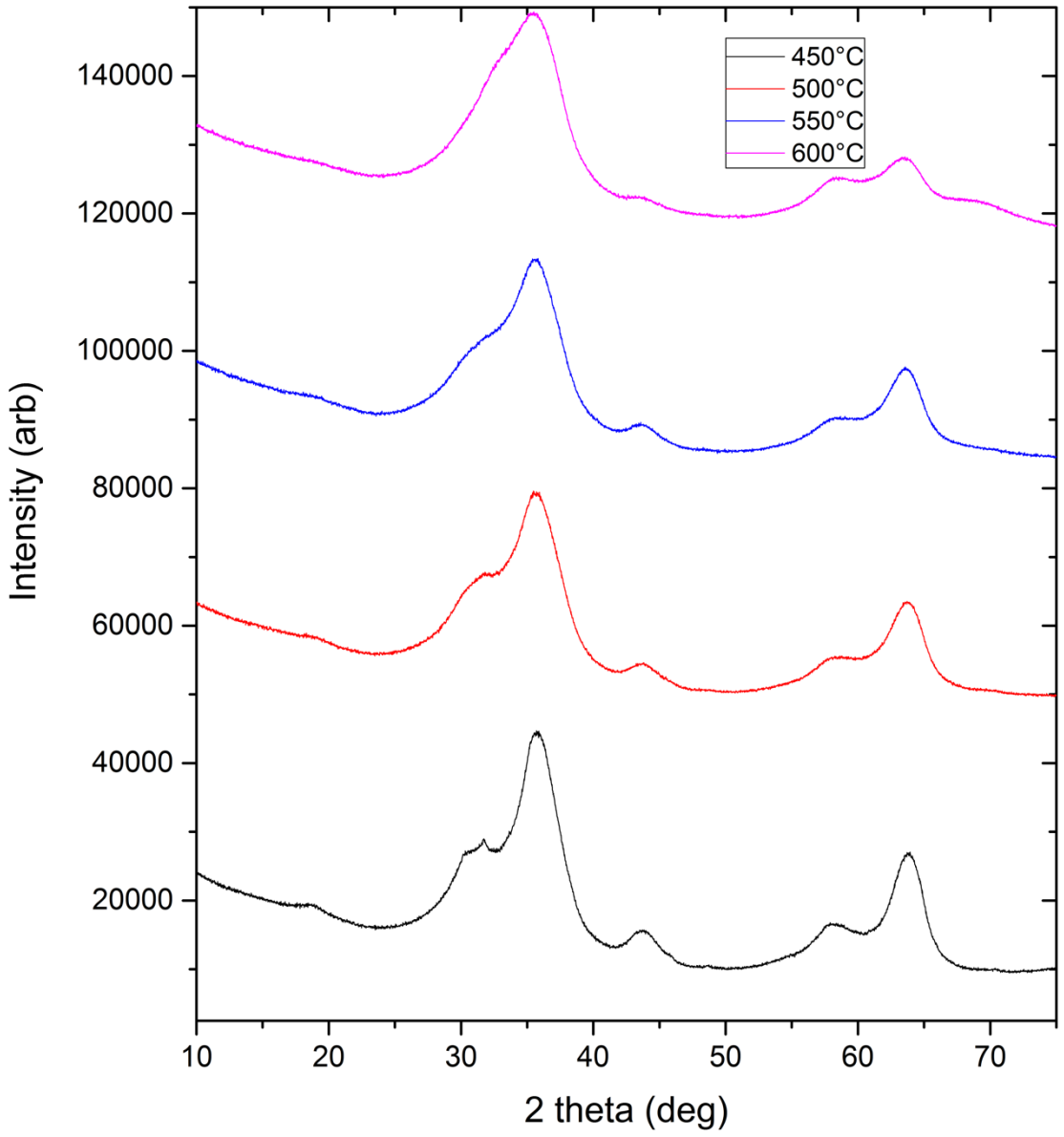

Figure 3.2.(b). XRD patterns of gallium oxynitride spinel products synthesized from $Ga(NO_3)_3{\cdot}\times H_2O$ at in the temperature range 400ºC-600ºC

3.3.2 Optical Properties:

The UV-Vis diffuse reflectance data for GOS-550 indicate the absorption of visible light (Figure 3.3 (a) and (b)), with $0.1 < \alpha_{KM} < 1$ for energies (E) between 2.5 eV and 3 eV. The relative absorption is obtained by the Kubelka-Munk transform of the diffuse reflectance data, R, through the formula (3.1).

$$\alpha_{KM}(E) = (1-R)^2/(2R) \qquad (3.1)$$

The absorption below 2.5 eV can be fit to an Urbach tail that precedes the optical gap, and has the functional form of (3.2),

$$\alpha_{Urbach} = A_U \exp[(E - E_g)/E_U] \qquad (3.2)$$

where E_U is a characteristic Urbach energy which reflects the degree of broadening, E_g is a characteristic gap energy which is slightly (direct) or substantially (indirect) larger than the optical gap energy, and A_U is a scaling prefactor.

The fit shows a modest degree of Urbach broadening (E_U = 0.16 eV), and the characteristic gap energy is substantially higher in energy than the regime over which Urbach scaling is followed, suggesting that the present system has an indirect gap (Figures 3.4).

Optical transitions typically follow the scaling relationship (3.3),

$$\alpha_{KM} = A\,(E - E_g)^n / E \qquad (3.3)$$

with a power n = 2 for indirect excitations and n = 0.5 for direct excitations, where E_g is the gap energy, and A is a prefactor related to the intensity of the transition.[14] When data is appropriately rescaled for the relationship, The absorption will appear linear over the energies where the band

gap absorption occur (figure 3.2) and indicates that the lowest energy optical gap is indirect for this system. Absorption at higher energies suggests an allowed direct gap optical transition (figure 3.3.(b)). Quantitative fits (figure 3.3, solid lines) to data indicate that the indirect gap is 2.50 eV while the direct gap is 3.69 eV.

Based on analogues with other oxynitride compounds such as the wurtzite $(GaN)_{1-x}(ZnO)_x$ solid solution, we hypothesize that the lower energy indirect transitions originate in localized limited minority N 2p anion states while the more intense direct states are associated with strongly hybridized O 2p anion states that are about 1 eV lower in energy due to the higher electronegativity of O relative to N. These band gaps are substantially lower than those previously reported for solvothermally-prepared GOS (4.1– 4.9 eV direct gap).[11] It is not known if the difference in the determined optical gaps is due to differences in the quantification methodology or in the different sample stoichiometries that may result from different synthesis routes. Optical properties of high-pressure GOS have not been reported. Because of their increased N content, high-pressure GOS samples are expected to have stronger visible light absorption relative to ammonolyzed products. In contrast to the GOS product reported here nitrogen rich wurtzite type gallium oxynitrides were found to have direct band gaps.[15] Similarly, a direct band gap of 2.7 eV has been reported for a bimetallic zinc gallium oxynitride spinel.[16]

Indirect band gap materials can be efficient water splitters despite their lower light absorption rates compared to materials with direct band gaps. For example, a significant difference in photocatalytic activity was observed between two polymorphs of $NaTaO_3$, one with a direct band gap (~4.0 eV) and the other having an indirect gap (~4.1 eV).[17] The polymorph with the indirect band gap showed about 150 times higher H_2 evolution rate than the other

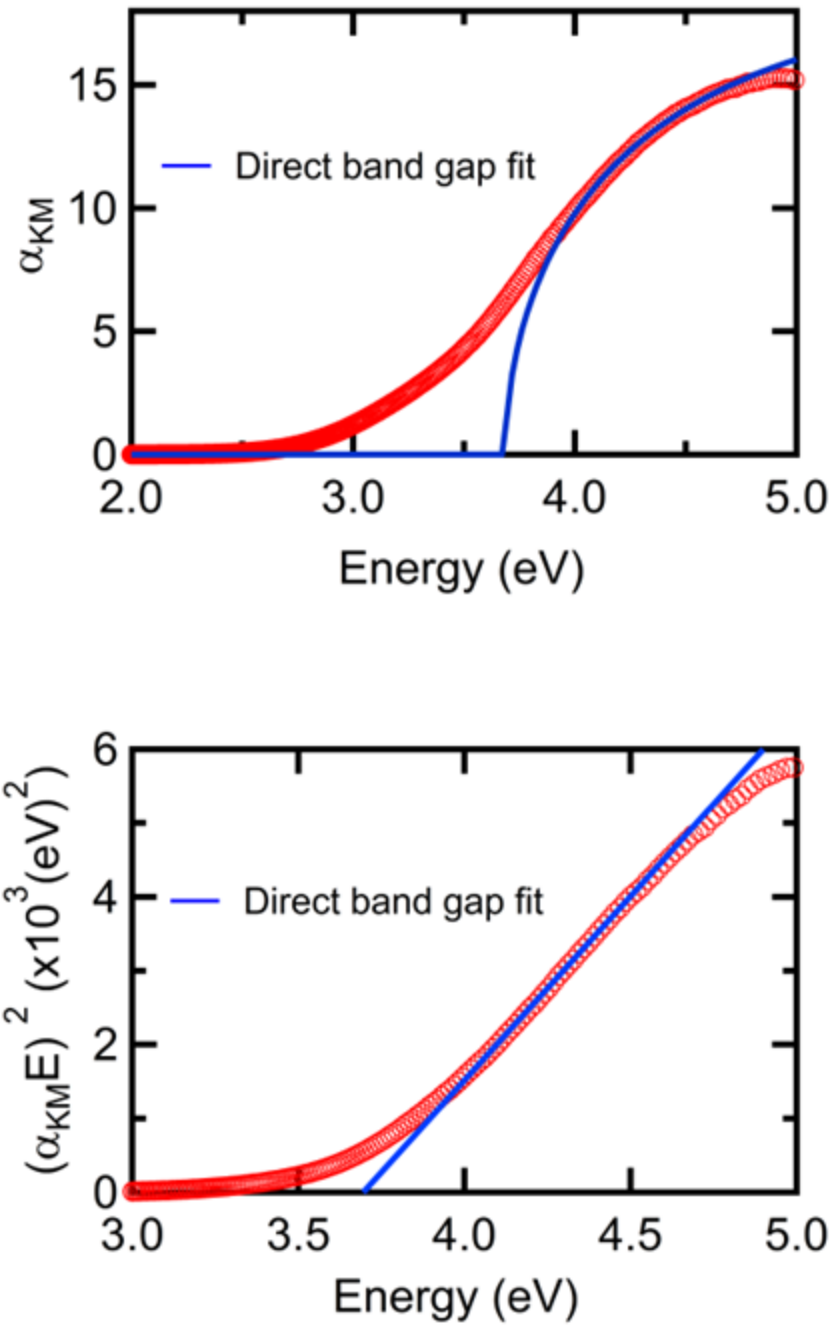

Figure 3.3.(a) Regimes over which gallium oxynitride spinel exhibits direct (bottom, blue lines) optical gap, as shown for the relative absorption data obtained by the Kubleka-Munk transform of diffuse reflectance (above) and for the same data rescaled to appear linear when the functional form for this absorption is obeyed (below).

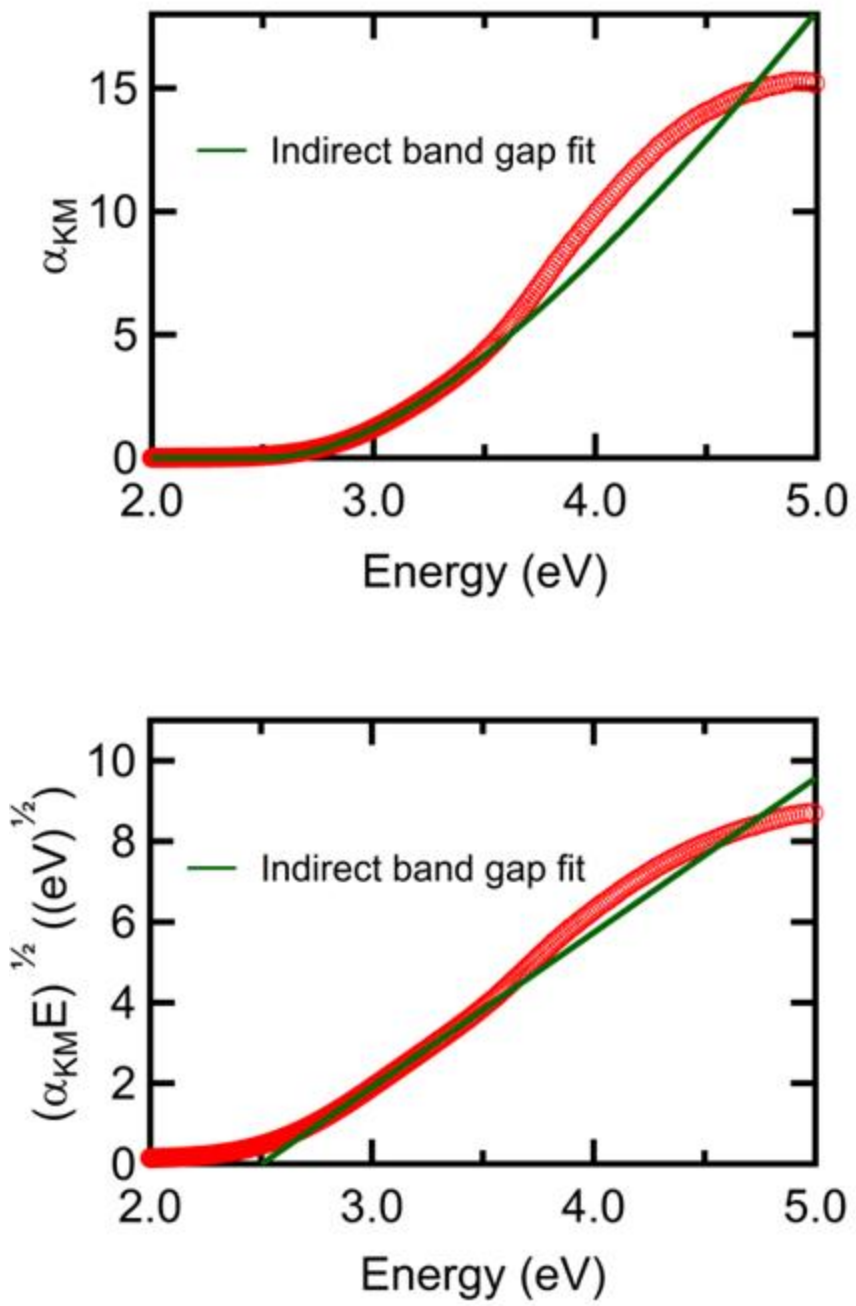

Figure 3.3 (b) Regimes over which gallium oxynitride spinel exhibits an indirect optical gap, as shown for the relative absorption data obtained by the Kubleka-Munk transform of diffuse reflectance (above) and for the same data rescaled to appear linear when the functional form for this absorption is obeyed (below).

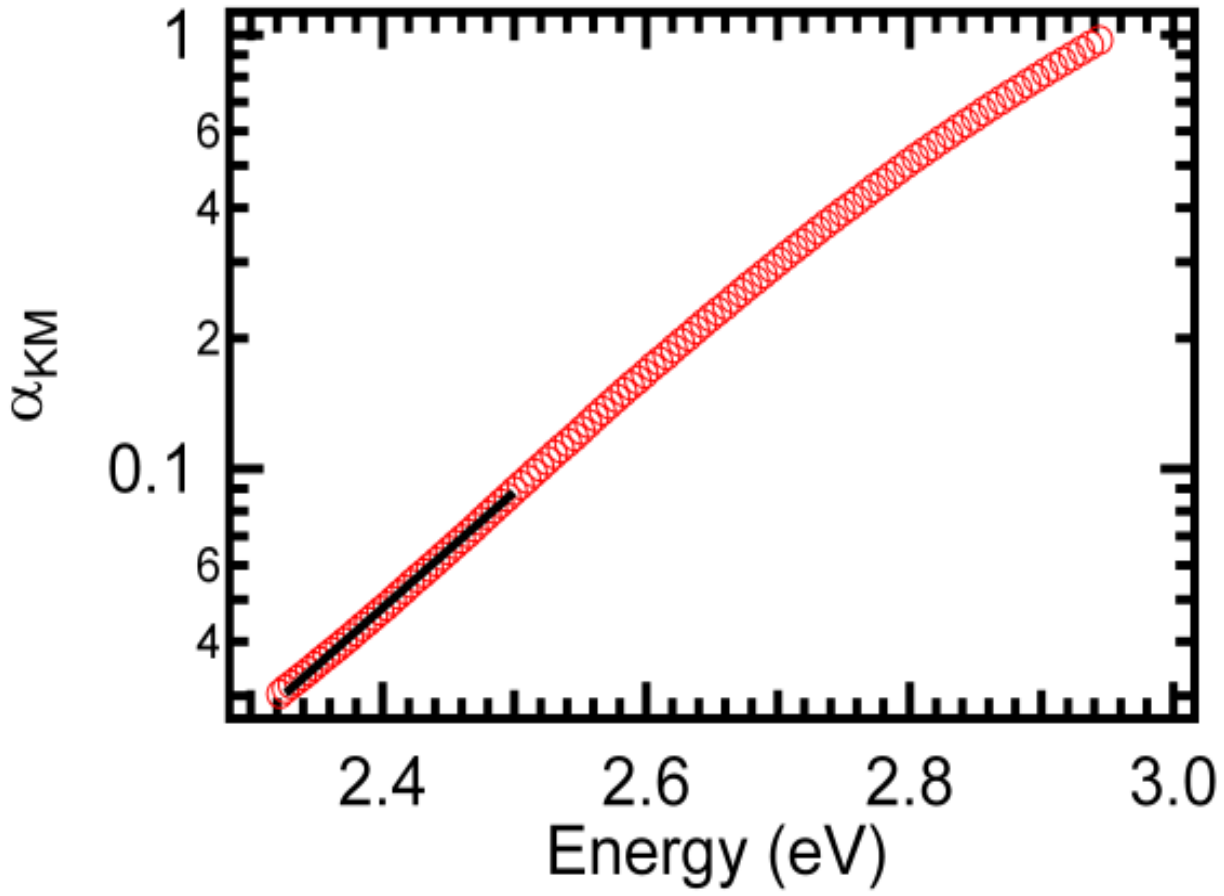

Figure 3.4 Relative absorption (α_{KM}) on a log scale for gallium oxynitride spinel synthesized by ammonolyzing $Ga(NO_3)_3 \cdot xH_2O$. Fit to the low-energy Urbach tail is overlaid (black line).

polymorph under same conditions.[17] The same phenomena is observed with anatase (direct band gap ~3.2 eV) and rutile (indirect band gap ~3.0 eV) TiO_2.[18] It has been suggested that the longer charge carrier life arising from the lower recombination rate of hole-electron pairs in indirect band gap materials is one of the contributing factors for higher activity,[17, 18] and thus higher internal quantum efficiencies may be expected for indirect gap semiconductors.

3.3.3 Photocatalytic H_2 production and stability in water

The photocatalytic activity for GOS-550 was tested under simulated solar light irradiation (320 nm < λ < 800 nm) with methanol as a sacrificial reagent. GOS-550 has a maximum H_2 evolution rate of 8 μmol/hr, although there was a slight induction delay in photocatalytic activity (Figure 3.5). The observed photocatalytic activity confirms that the conduction band edge of $Ga_{2.78}O_{3.65}N_{0.35}$ is low enough for H^+ reduction. It is also important to note that this activity was measured without loading the surface with co-catalysts often used to increase the H_2 production rate. For example, TiO_2, a well-known semiconductor exhibiting high photocatalytic activity under UV irradiation, does not produce hydrogen without the loading of co-catalysts.[19] A comparison between maximum activities for H_2 evolution for the catalyst produced in this project and other Ga-based oxides described in literature (under UV irradiation with methanol as a sacrificial reagent) is shown in Table 3.1. GOS-550 compares favourably with these photocatalysts considering that no surface modification was performed.

Despite the promising initial photocatalytic activity, the longer term activity of GOS decreases sharply after 4 hours. Further experiments were carried out to investigate the reason for this change. Optical analysis of the GOS sample irradiated in a 20% methanol solution for 6

hours shows a complete loss of band gap absorption in the visible region (Figure 3.5). Photo-degradation

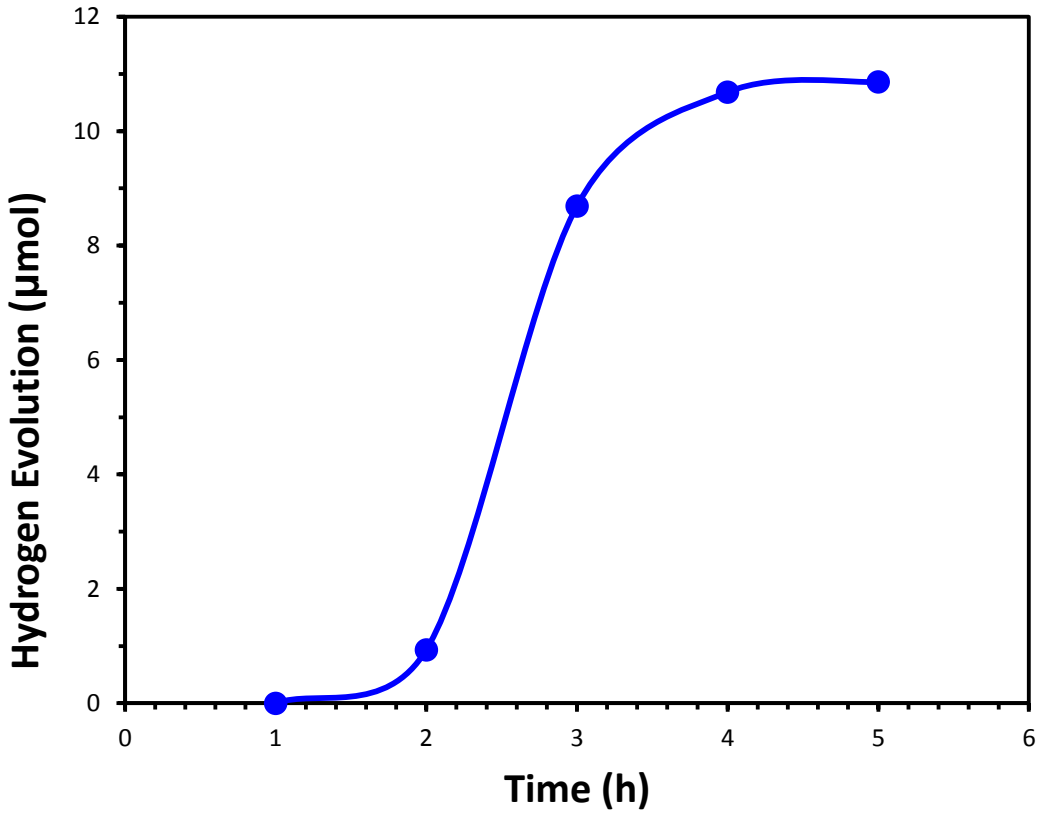

Figure 3.5 Evolution of hydrogen from spinel gallium oxynitride suspension over a 20% methanol in water solution irradiated with a 300 W UV lamp (320 nm).

Table 3.1. Comparison of gallium oxynitride spinel H_2 evolution activity under UV radiation (methanol sacrificial reagent) with that of Ga based oxides

Oxide	Band Gap (eV)	Co-catalyst	H_2 evolution rate (μmol/h)	References
$Ga_{2.78}O_{3.65}N_{0.35}$	2.50	None	8	This work
$ZnGa_2O_4$	4.3	None	1.5	Ref. [20]
$ZnGa_2O_4$	4.3	RuO_2	10	Ref. [20]
β–Ga_2O_3	4.6	Pt	50	Ref. [21]
$Ga_{1.14}In_{0.86}O_3$	3.7	Pt	30	Ref. [21]

occurring due to photo-generated holes is a common issue with many non-oxide semiconductors, including other previously studied oxynitrides.[22-24] However, GOS is unusual in that nearly complete degradation occurs even without irradiation (Figure 3.6), suggesting that GOS also slowly reacts with aqueous solutions. The loss of nitrogen due to both photo-oxidation and water corrosion rapidly diminishes the ability of GOS powders to absorb light in the visible region, stopping the photocatalytic reaction. The XRD patterns for degraded samples show that gallium oxide hydroxide, GaO(OH) forms in the irradiated sample, but not in the dark sample (Figure 3.7). The degradation mechanism is ascribed to the initial water-induced loss of N from the GOS, followed by the photo-induced degradation producing GaO(OH).

In order to improve the stability and the photocatalytic activity of GOS, several strategies can be pursued. In a recent study Hu et al demonstrated that Si, GaAs, and GaP photo anodes can

be stabilized in water by depositing thin TiO_2 films over the catalyst, eliminating direct contact with the aqueous solution.[25] Also, introduction of a co-catalyst is known to improve the

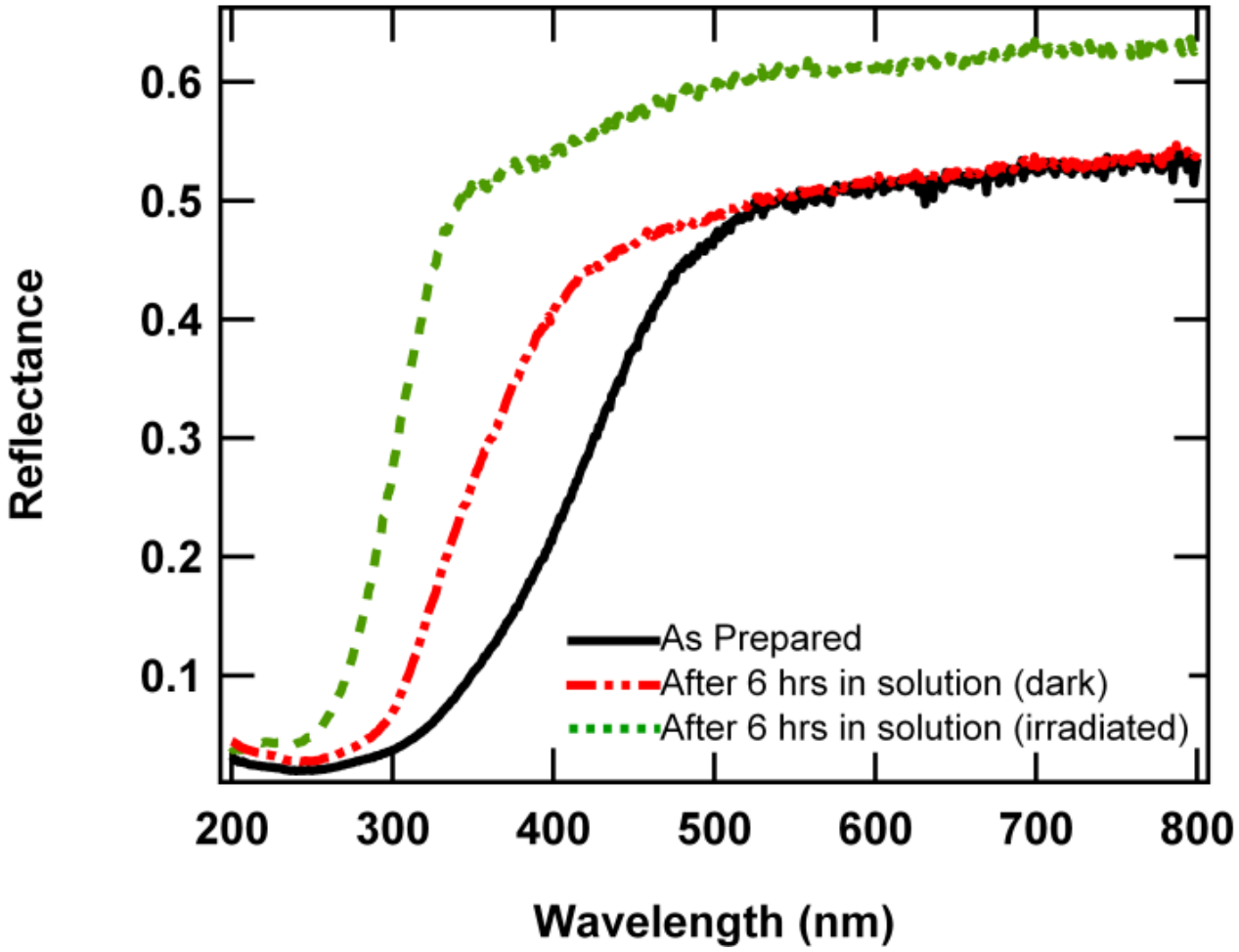

Figure 3.6 The UV-Visible diffuse reflectance spectra of GOS as prepared (black), after 6hrs in 20% methanol solution in dark (red) and after 6 hrs in solution under irradiation (green)

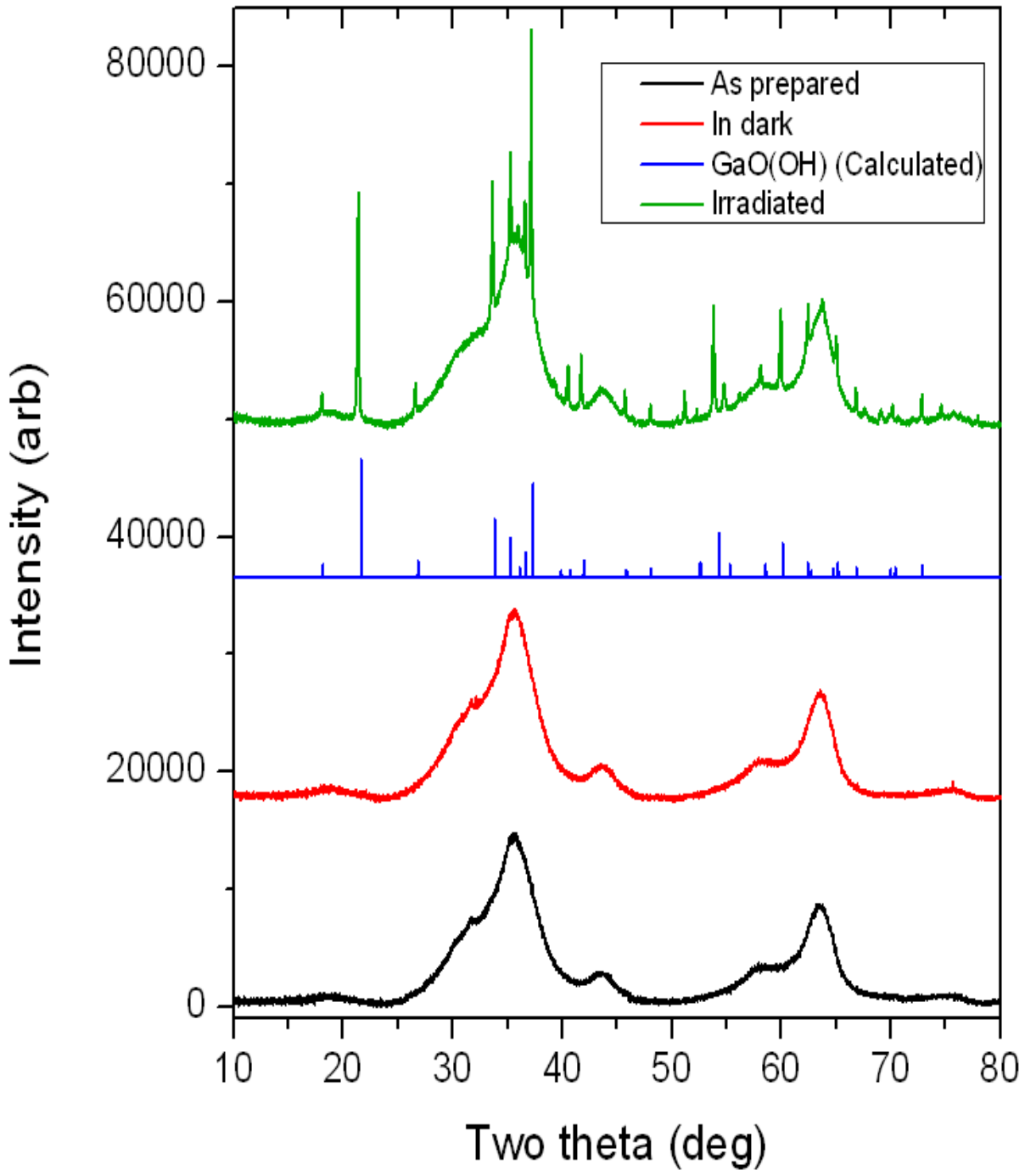

Figure 3.7. The XRD patterns of GOS, as prepared (black), after 6 hrs in 20% methanol solution in dark (red) and after 6 hrs in 20% methanol solution under irradiation (green). The calculated pattern for GaO(OH) is shown in blue.

photostability of oxynitrides.[22-24] In the case of TaON adding IrO_2 as a co-catalyst substantially decreased the rate of N loss due to photo-oxidation.[22]

Increasing the crystallinity is a possible approach to increase the activity of GOS. Higer degree of crystallinity is often correlated to high photocatalytic activity as crystal defects can act as recombination sites for photo-generated holes and electrons, thereby preventing the carriers from reaching the surface of the particle. As a result, crystal defects are often linked to reduction in the overall quantum efficiency of photocatalysts.[19] For example, the photocatalytic water splitting activity of GaN-ZnO solid solution showed about threefold increase after calcination at 873 K and the associated decrease of recombination between photogenerated carriers due to reduced defect concentration was suggested as the cause.[26] In $NaTaO_3$ the crystallinity was improved by adjusting the concentrations of NaOH in the reaction mixture which corresponded to about seven fold increase in photocatalytic H_2 production activity.[27] Even in highly crystalline materials surface defects can reduce photocatalytic activity as observed in nanoparticulate ZrO_2-TaON solid solution where activity was improved by the reduction of surface defect density.[28] Along with improving its crystallinity and decreasing surface defect concentrations, surface modifications with a co-catalyst (Table 3.1) may also improve photocatalytic activity for GOS. There are few systems with both strong visible light absorption and conduction band levels appropriate positioned to enable the production of H_2 gas, so it is of great interest to determine if the activity of the GOS can be further improved by these methods for optimization.

3.4 Conclusions

A visible light absorbing gallium oxynitride spinel is demonstrated to be capable of photocatalytically evolving hydrogen. A maximum H_2-evolution rate of about 8 μmol/hr was observed without the use of co-catalysts on the nanocrystalline gallium oxynitride spinel synthesized by ammonolyzing $Ga(NO_3)_3 \bullet \times H_2O$. The GOS was identified to have an indirect band gap of ~2.50 eV and the absorption at photon energies higher than 3.5 eV is consistent with a direct band gap of ~3.7 eV. Stability tests indicate that GOS is susceptible to corrosion from water and photo-oxidation, which produces GaO(OH). Further improvement of this system must begin with the development of good coating procedures, such as the ALD titanate films that have proved effective in improving the performance of other non-oxide semiconductors.

3.5 Acknowledgements

H A N Dharmagunawardhane carried out the synthesis, X-ray data collection and determination of bandgaps. UV-Vis diffuse reflectance data reported in this chapter were collected by Mr. Huafeng Huang from the Department of Chemistry Stony, Brook University. Photocatalytic activity data collection was carried out by Mr. Qiyuan Wu from the department of Materials Science and Engineering.

References

1 H. A. N. Dharmagunawardhane, W. R. Woerner, Q. Y. Wu, H. F. Huang, X. Y. Chen, A. Orlov, P. G. Khalifah and J. B. Parise, *Photocatalytic hydrogen evolution using nanocrystalline gallium oxynitride spinel,* J Mater Chem A, 2014, **2**, 19247-19252.

2 J. E. Lowther, T. Wagner, I. Kinski and R. Riedel, *Potential gallium oxynitrides with a derived spinel structure*, J. Alloys Compd., 2004, **376**, 1-4.

3 S. D. Wolter, J. M. DeLucca, S. E. Mohney, R. S. Kern and C. P. Kuo, *An investigation into the early stages of oxide growth on gallium nitride*, Thin Solid Films, 2000, **371**, 153-160.

4 M. Puchinger, D. J. Kisailus, F. F. Lange and T. Wagner, *Microstructural evolution of precursor-derived gallium nitride thin films,* J. Cryst. Growth, 2002, **245**, 219-227.

5 E. Soignard, D. Machon, P. F. McMillan, J. J. Dong, B. Xu and K. Leinenweber, *Spinel-structured gallium oxynitride (Ga(3)O(3)N) synthesis and characterization: An experimental and theoretical study,* Chem. Mater., 2005, **17**, 5465-5472.

6 I. Kinski, G. Miehe, G. Heymann, R. Theissmann, R. Riedel and H. Huppertz, *High-pressure synthesis of a gallium oxonitride with a spinel-type structure,* Zeitschrift Fur Naturforschung Section B-a Journal of Chemical Sciences, 2005, **60**, 831-836.

7 P. Kroll, R. Dronskowski and M. Martin, *Formation of spinel-type gallium oxynitrides: a density-functional study of binary and ternary phases in the system Ga-O-N*, J. Mater. Chem., 2005, **15**, 3296-3302.

8 H. Huppertz, S. A. Hering, C. E. Zvoriste, S. Lauterbach, O. Oeckler, R. Riedel and I. Kinski, *High-Pressure Synthesis, Electron Energy-Loss Spectroscopy Investigations, and Single Crystal Structure Determination of a Spinel-Type Gallium Oxonitride Ga-2.79 square(0.21)(O3.05N0.76 square(0.19)),* Chem. Mater., 2009, **21**, 2101-2107.

9 C. E. Zvoriste, L. Dubrovinsky, S. A. Hering, H. Huppertz, R. Riedel and I. Kinski, *Diamond anvil cell syntheses and compressibility studies of the spinel-structured gallium oxonitride*, High Pressure Res, 2009, **29**, 389-395.

10 C. C. Tang, Y. Bando, Y. Huang, C. Y. Zhi, D. Golberg, X. W. Xu, J. L. Zhao and Y. X. Li, *Synthesis of nanoporous spheres of cubic gallium oxynitride and their lithium ion intercalation properties,* Nanotechnology, 2010, **21**, 115705.

11 A. Oberlander, I. Kinski, W. L. Zhu, G. Pezzotti and A. Michaelis, *Structure and optical properties of cubic gallium oxynitride synthesized by solvothermal route,* J. Solid State Chem., 2013, **200**, 221-226.

12 I. Kinski, F. Scheiba and R. Riedel, *Advances in gallium oxonitride ceramics: A new class of materials in the system Ga-O-N,* Adv. Eng. Mater., 2005, **7**, 921-927.

13 W. S. Jung, *Preparation of gallium nitride powders and nanowires from a gallium(III) nitrate salt in flowing ammonia,* Bull. Korean Chem. Soc., 2004, **25**, 51-54.

14 A. C. Malingowski, P. W. Stephens, A. Huq, Q. Z. Huang, S. Khalid and P. G. Khalifah, *Substitutional Mechanism of Ni into the Wide-Band-Gap Semiconductor InTaO4 and Its Implications for Water Splitting Activity in the Wolframite Structure Type,* Inorg. Chem., 2012, **51**, 6096-6103.

15 C. C. Hu and H. S. Teng, *Gallium Oxynitride Photocatalysts Synthesized from Ga(OH)(3) for Water Splitting under Visible Light Irradiation,* J. Phys. Chem. C., 2010, **114**, 20100-20106.

16 V. B. R. Boppana, D. J. Doren and R. F. Lobo, *A Spinel Oxynitride with Visible-Light Photocatalytic Activity,* Chemsuschem, 2010, **3**, 814-817.

17 W. H. Lin, C. Cheng, C. C. Hu and H. S. Teng, *NaTaO3 photocatalysts of different crystalline structures for water splitting into H-2 and O-2,* Appl. Phys. Lett., 2006, **89**, 211904.

18 T. Luttrell, S. Halpegamage, J. G. Tao, A. Kramer, E. Sutter and M. Batzill, *Why is anatase a better photocatalyst than rutile? - Model studies on epitaxial TiO2 films,* Scientific Reports, 2014, **4**, 4043.

19 A. Kudo and Y. Miseki, *Heterogeneous photocatalyst materials for water splitting,* Chem. Soc. Rev., 2009, **38**, 253-278.

20 K. Ikarashi, J. Sato, H. Kobayashi, N. Saito, H. Nishiyama and Y. Inoue, *Photocatalysis for water decomposition by RuO2-dispersed ZnGa2O4 with d(10) configuration,* J. Phys. Chem. B, 2002, **106**, 9048-9053.

21 A. Kudo and I. Mikami, *Photocatalytic activities and photophysical properties of Ga2-xInxO3 solid solution,* Journal of the Chemical Society-Faraday Transactions, 1998, **94**, 2929-2932.

22 M. Higashi, K. Domen and R. Abe, *Fabrication of efficient TaON and Ta3N5 photoanodes for water splitting under visible light irradiation,* Energ Environ Sci, 2011, **4**, 4138-4147.

23 A. Kasahara, K. Nukumizu, T. Takata, J. N. Kondo, M. Hara, H. Kobayashi and K. Domen, *LaTiO2N as a visible-light (<= 600 nm)-driven photocatalyst (2),* J. Phys. Chem. B, 2003, **107**, 791-797.

24 A. Kasahara, K. Nukumizu, G. Hitoki, T. Takata, J. N. Kondo, M. Hara, H. Kobayashi and K. Domen, *Photoreactions on LaTiO2N under visible light irradiation,* J. Phys. Chem. A, 2002, **106**, 6750-6753.

25 S. Hu, M. R. Shaner, J. A. Beardslee, M. Lichterman, B. S. Brunschwig and N. S. Lewis, *Amorphous TiO2 coatings stabilize Si, GaAs, and GaP photoanodes for efficient water oxidation,* Science, 2014, **344**, 1005-1009.

26 K. Maeda, K. Teramura and K. Domen, *Effect of post-calcination on photocatalytic activity of (Ga1-xZnx)(N1-xOx) solid solution for overall water splitting under visible light,* J. Catal., 2008, **254**, 198-204.

27 J. W. Liu, G. Chen, Z. H. Li and Z. G. Zhang, *Hydrothermal synthesis and photocatalytic properties of ATaO(3) and ANbO(3) (A = Na and K),* Int. J. Hydrogen Energy, 2007, **32**, 2269-2272.

28 K. Maeda, H. Terashima, K. Kase, M. Higashi, M. Tabata and K. Domen, *Surface modification of TaON with monoclinic ZrO2 to produce a composite photocatalyst with enhanced hydrogen evolution activity under visible light,* Bull. Chem. Soc. Jpn., 2008, **81**, 927-937.

Chapter 4

Optical properties and photocatalytic activity of $(GaN)_{1-x}(ZnO)_x$ solid solution synthesized at high pressure in the entire composition range.

4.1 Introduction

The wurtzite type (space group $P6_3mc$) solid solution between GaN and ZnO, a material that can perform photocatalytic overall water splitting under visible light, was first discovered by Maeda et al.[1] The members of the solid solution $(GaN)_{1-x}(ZnO)_x$ have lower band gaps than the end members GaN (3.4 eV) and ZnO (3.2 eV).[1] The quantum efficiency of the system was later optimized by calcination at 873 K, which resulted in an efficiency of 5.9% at $x = 0.18$.[2] Since then there have been numerous studies to improve the photocatalytic activity of the system.[2-5] Initial density functional theory (DFT) studies predicted the solid solution to have a minimum band gap of 2.4 eV at $x \sim 0.5$.[6] However this stoichiometry was difficult to achieve at first with ambient pressure synthesis due to the reduction of Zn^{2+} and subsequent evaporation at high temperatures.[6-8] Chen et al. synthesized $(GaN)_{1-x}(ZnO)_x$ with $x > 0.3$ for the first time using high pressure synthesis at around 5 GPa and 1000°C and observed that the most visible light absorption occurs at $x = 0.5$ though exact band gap estimations and photocatalytic activity studies were not performed.[7] Later studies report synthesis of compositions up to $x = 0.9$ under ambient pressure conditions.[8, 9]

Several theoretical studies attempting to predict the band gaps and order/disorder of $(GaN)_{1-x}(ZnO)_x$ have been reported.[6, 10, 11] However, complementing experimental reports

covering the entire composition range are scarce. In this study, we report on the optical and photocatalytic properties of $(GaN)_{1-x}(ZnO)_x$ up to x=0.9 synthesized at high pressure.

4.2 Experimental

4.2.1 GaN synthesis

GaN reagent was synthesized by ammonolysing Ga_2O_3. About 0.5 g of Ga_2O_3 (Alfa Aeser 99.9%) was placed in two fused silica boats (0.25 g in each boat) which were placed inside a quartz tube (Ø = 20mm) going through a tube furnace so that the boats straddle the hot spot of the furnace. Ammonia was passed over the boats at a rate of ~600ml/min while the temperature was raised to 950 °C at a rate of 40 °C/min and left for 3hrs before quenching. The powder product was recovered, ground and the process was repeated until reaction is complete. Completion of the reaction was confirmed by x-ray powder diffraction.

4.2.2 High Pressure synthesis

High pressure reactions were conducted on a ~ 1g scale with a piston-cylinder apparatus and 19 mm diameter cylindrical talcum pressure cell. All solid solution compositions were reacted under the same high pressure and high temperature conditions - 1 GPa at 1150 -1200 °C for 45 mins.

Dried powdered reagents ZnO and GaN were combined in stoichiometric ratios depending on the target composition and ground intimately for 30 mins. The talc sleeve encircles a cylindrical graphite resistive heater, into which the powder was loaded, capped with two BN disks and centered within the cell by two pyrophyllite spacers. Previously the spacers were dried at 1000 °C for 20 mins. A Pt/Pt90-Rh10 thermocouple was placed in contact with the BN disk to monitor the sample temperature.

Once loaded the cell was pressurized to a maximum of 1 GPa over 45 mins and then heated. First at 200 °C/min up to 1000 °C, then slowed to 100 °C/min up to 1100 °C and finally 50 °C/min until the maximum temperature reach between 1150 °C- 1200 °C. The maximum temperature was held for 45 mins, before being quenched to room temperature followed by slow decompression over 1 h.

Samples were recovered as dense sintered pellets, which were cleaned with sandpapers to remove any residual graphite and ground into a fine powder. All x-ray diffraction analysis was done on a Rigaku Ultima IV diffractometer in Bragg- Brentano geometry with a Cu tube and D-tex Ultra solid-state detector.

4.2.3 Optical properties and photocatalytic activity

UV-Vis diffuse reflectance data were collected on a Thermo Evolution 300 spectrometer at a range of 300-900 nm. $BaSO_4$ was used as the 100% reflectance standard.

Photocatalytic water splitting reactions were carried out under visible light illumination in a customized reactor equipped with a quartz window. For each experiment, 100 mg sample

was dispersed in 180 mL DI water. The suspension was then illuminated by a 300W Xe lamp which was equipped with a high pass cutoff filter (>420 nm, Hoya, L42) to eliminate UV light and a 10 cm water filter (> 800 nm) to eliminate IR irradiation. Determination of the amount of evolved gases was carried out with an inline GC-TDC system (Agilent, 7890A).

4.3 Results and Discussion

4.3.1 Compositional analysis

X-ray diffraction patterns of the products obtained are shown in figure 4.1. The optimum synthetic temperature range of 1150 °C -1200 °C, where ZnO completely react, was determined by several trial experiments. The x-ray data were analyzed using whole pattern Rietveld refinement to obtain lattice constants, *a* and *c*, and unit cell volume (see table 4.1 and supporting information). In our samples, Zn metal was noticeably present only at $x = 0.51$ (i.e. 50% ZnO reaction mixture) and Rietveld refinements show this is below 1% by weight. All samples have $ZnGa_2O_4$ (spinel- $Fd\bar{3}m$) present as a second phase (figure 4.1 and table 4.1). Chen et al. previously observed $ZnGa_2O_4$ impurity forming though their products had less than 1% $ZnGa_2O_4$.[7] The $ZnGa_2O_4$ was presumed to arise from the reaction between ZnO and Ga_2O_3, which may form from partial oxidation of GaN by O_2 in the reaction environment.[7] In our products, the amount of $ZnGa_2O_4$ steadily decreases with increasing ZnO content (see table 4.1).

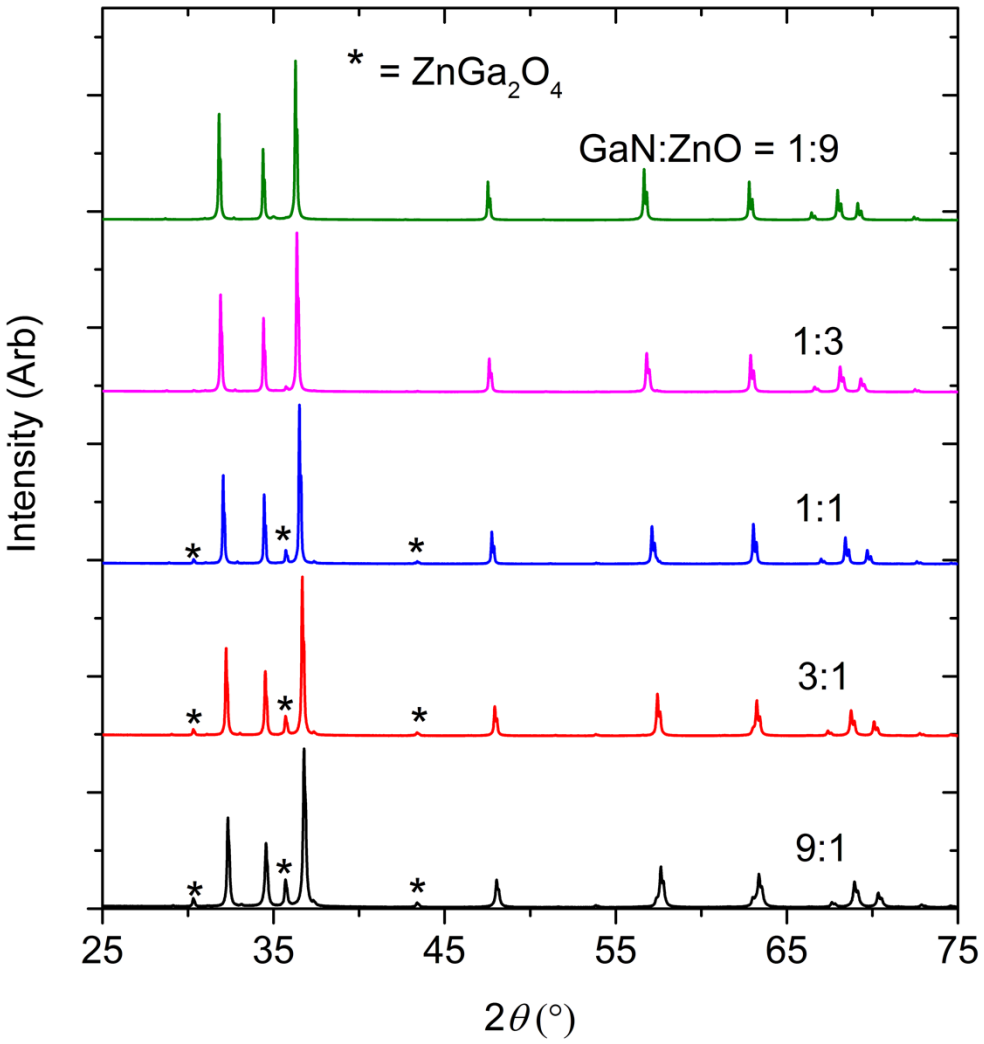

Figure 4.1. The X-ray diffraction patterns of the products obtained by reacting GaN and ZnO at 1 GPa ,1150-1200 °C

Table 4.1: Cell parameters of $(GaN)_{1-x}(ZnO)_x$, weight percentages of $(GaN)_{1-x}(ZnO)_x$ and $ZnGa_2O_4$obtained by Rietveld refinements, and final calculated compositions.

Composition of reaction mixture (GaN:ZnO moles)	$(GaN)_{1-x}(ZnO)_x$ (weight %)	$ZnGa_2O_4$ (weight %)	Lattice Parameters (wurtzite, $P6_3mc$)		R_{wp} %	GOF	Calculated composition of $(GaN)_{1-x}(ZnO)_x$ Phase (x)
			a (Å)	c(Å)			
GaN(Ref[7])	-	-	3.186	5.181	-	-	-
9:1	87.25(5)	12.75(5)	3.19673(3)	5.18998(6)	7.00	2.20	0.07
3:1	89.58(5)	10.42(5)	3.20721(2)	5.19614(4)	6.94	2.23	0.24
1:1	92.75(4)*	6.96(4)*	3.22432(1)	5.20620(6)	6.25	2.21	0.51
1:3	98.15(2)	1.85(2)	3.24060(1)	5.21358(2)	6.27	3.87	0.76
1:9	99.48(3)	0.52(3)	3.24844(2)	5.21665(3)	10.85	6.47	0.90
ZnO[7]	-	-	3.249	5.198	-	-	-

* This product contain 0.291 wt% Zn (see supporting information)

The formation of $ZnGa_2O_4$ causes the final composition of $(GaN)_{1-x}(ZnO)_x$ to vary from the intended. Determination of the composition x from the refinement is particularly difficult since the x-ray scattering contrasts between Ga^{3+} and Zn^{2+} as well as between N^{3-} and O^{2-} are small. Another approach to determine x is possible since that molecular masses of $(GaN)_{1-x}(ZnO)_x$ members vary very little with x as GaN and ZnO have very similar molecular masses (3% difference). Hence, a rough approximation of the value of x in $(GaN)_{1-x}(ZnO)_x$ was adjusted from the stoichiometry of the starting materials using the weight % of the secondary phases determined from Rietveld refinements (see table 4.1 for values).

In contrast to the difficulty of synthesizing the complete $(GaN)_{1-x}(ZnO)_x$ solid solution at ambient pressure, due to the reduction of Zn^{2+} during ammonolysis[2, 8, 12] , the closed reaction

environment of the high pressure system produces relatively pure samples, even for Zn-rich members of the solid solution

Chen et al. [7] observed that Lattice parameters of their $(GaN)_{1-x}(ZnO)_x$ show deviations from the linear variation expected for Vegard's law[13] showing an upward bowing trend. Lattice parameters calculated for our samples show an even higher degree of bowing (figure 4.2 (a),(b)). Theoretical studies show that the bowing depends on the degree of disorder and decreases when short-range order (SRO) is present.[6, 11] The SRO in $(GaN)_{1-x}(ZnO)_x$ is predicted to occur due to ZnO and GaN clustering driven by the preference for valance-matched Zn-O and Ga-N pairs and the degree of SRO tend to decrease with increasing synthesis temperature.[6, 11] Recently reported theoretical studies of Liu et al give a comparison of lattice parameters between short-range ordered ("special quasi-ordered structure"(SQoS) equilibrated at1123K) and disordered ("special quasi-disordered structure" (SQdS) equilibrated at 20000K) structures (see figure 4.2 (a),(b)).).[14] The trends of lattice parameters and cell volume of our samples generally tend to be less than the values predicted for the disordered structure suggesting some degree of SRO. Smaller lattice parameters reported by Chen et al. indicate a higher degree of SRO that corresponds to their lower synthesis temperature (1000^0C).[7]

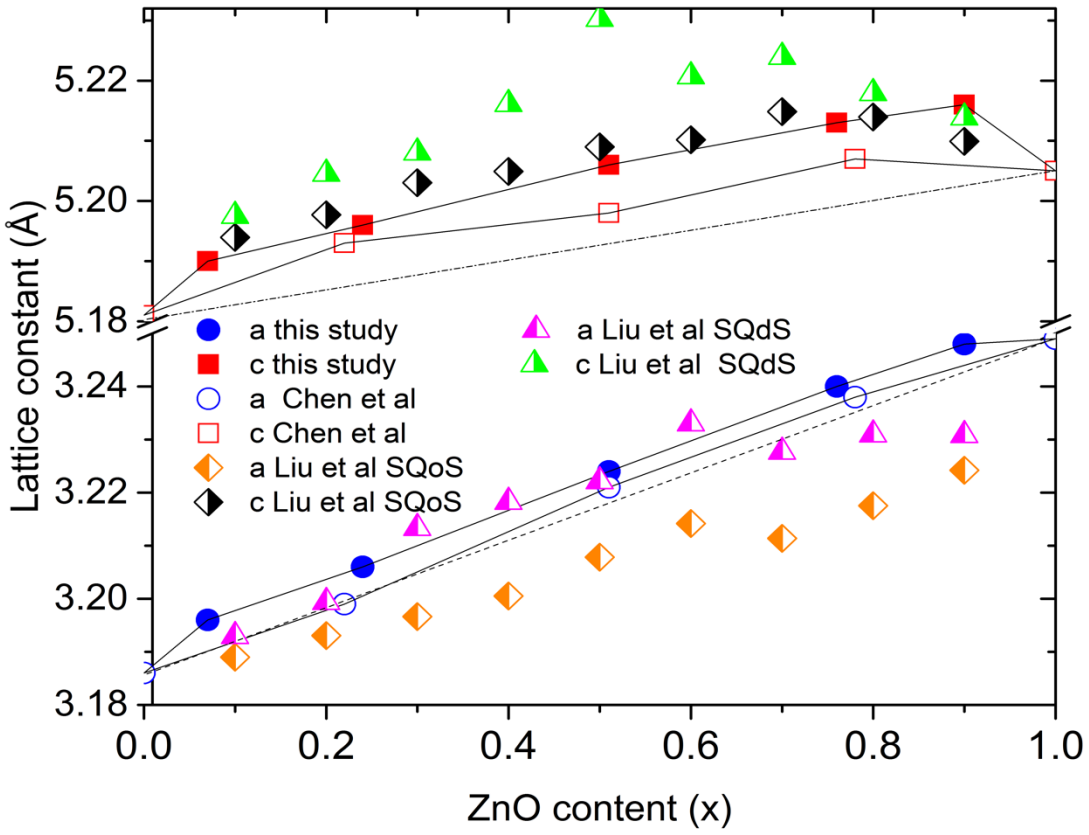

Figure 4.2 (a) The lattice parameters calculated for high pressure synthe-sized $(GaN)_{1-x}(ZnO)_x$ with the values predicted by Liu et al. Errors are smaller than markers. Dashed lines represent ideal variation of lattice parameters

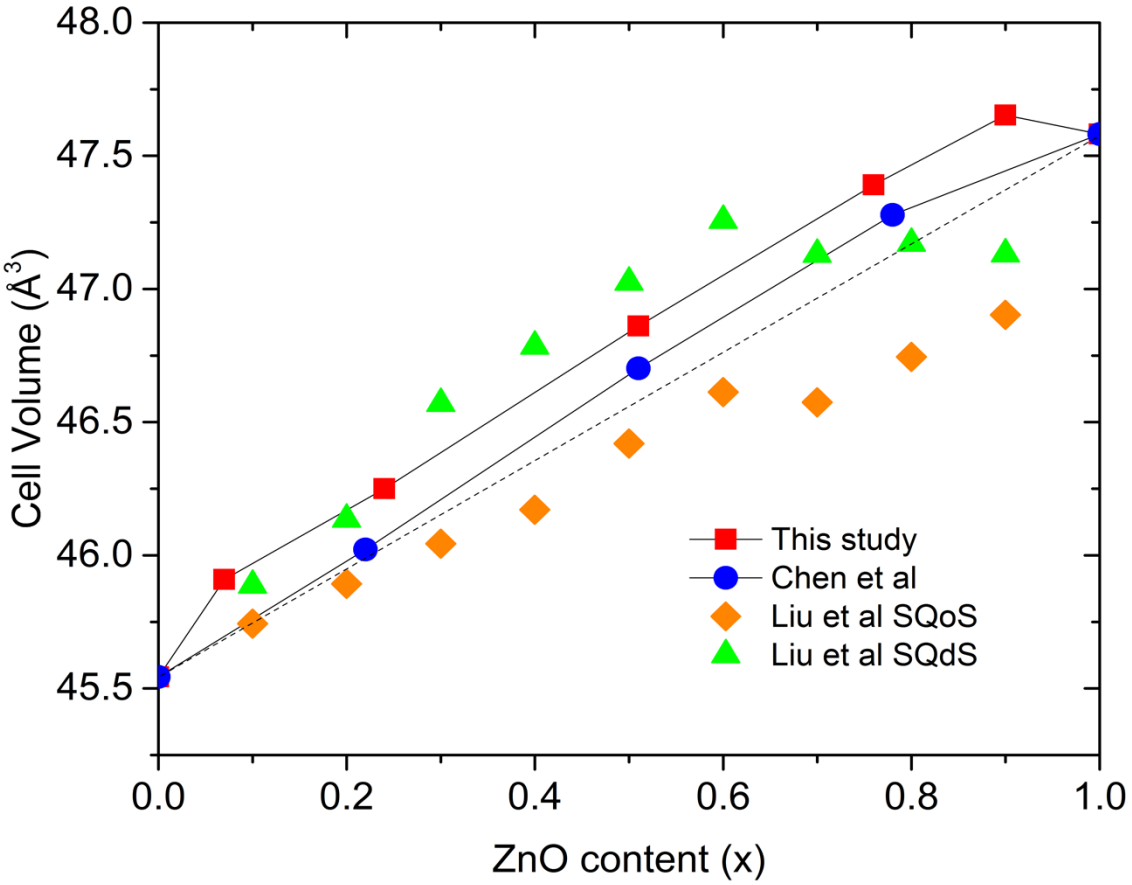

Figure 4.2 (b) Cell volumes calculated for high pressure synthe-sized $(GaN)_{1-x}(ZnO)_x$ with the values predicted by Liu et al.[14] Errors are smaller than markers. Dashed lines represent ideal variation of lattice parameters

4.3.2 Optical properties

The Kubelka-Munk transformed diffuse reflection data for samples are shown in figure 3. The highest absorption of light in the visible region is observed at x = 0.51. Since $(GaN)_{1-x}(ZnO)_x$ is known to have direct band gaps initial curve fits on our data were made assuming the same behavior. Direct band gaps take the form (also see form 3.3 in chapter 3)

$$\alpha_{KM} = A(E - E_g)^{0.5}/E \qquad (4.1)$$

where α_{KM} is the Kubeka-Munk transformed diffuse reflectance, A is a scaling factor, E is photon energy and E_g is the band gap energy. Fits done using formula (4.1) show direct band gap absorption in all samples in the regions where absorption is relatively high ($\alpha_{KM} > 0.5\alpha_{KM}$ max, see Figure 4.3 (a) and (b) yellow lines). The calculated band gaps are shown in table 4.2. $ZnGa_2O_4$ has a wide band gap (4.5 eV)[15] and is not expected to contribute to absorption in the visible region.

Absorption of $(GaN)_{1-x}(ZnO)_x$ below the band gap has been explained before as occurring due to Urbach tail behavior($\alpha \sim \exp[(E - E_g)/E_U]$ where E_U is Urbach energy, also see form 3.2) and free carrier absorption ($\alpha \sim E^{-3}$).[8] Urbach tail behavior is explained as the exponential increase in absorption just below band gap energy occurring due to factors such as impurities, excitons, compositional inhomogeneity and structural disorder.[8, 16] The regions below band gaps in our data were fitted with both Urbach tail behavior and free carrier absorption taken in to account. The combined effect takes the form

$$\alpha_{KM} = A \exp[(E - E_g)/E_U] + BE^{-3} + C \qquad (4.2)$$

where A,B and C are constants.[8] The regions of absorption fitted with form 4.2 (substituting for E_g with values calculated using form 1) are shown with red lines in figure 4.3 and calculated Urbach energies are shown in table 4.2.

Our experimental results agree with previous DFT based theoretical studies predicting trends in $(GaN)_{1-x}(ZnO)_x$ band gaps to follow a downward bowing curve with x.[6, 11] Jensen et al. predicted a minimum band gap of 2.29 eV at x = 0.525.[6] Later Li et al. predicted a minimum band gap to be between 2.5eV and 2.7 eV at x~0.5 which agrees with our observations. [6, 11] A comparison of band gaps from our study with some other reports are shown in Figure 4. The lower band gaps observed on$(GaN)_{1-x}(ZnO)_x$ nanoparticles are explained as occurring due to high degree of disorder in nanoparticles.[17] Band gaps reported for $(GaN)_{1-x}(ZnO)_x$. synthesized at ambient pressure over the entire composition range do not tend to show the downward bowing curve behavior. For example, Lee et al. report onsets of absorption continuously decreasing with increasing Zn content, with onset dropping to 2.2 eV at x = 0.87.[9] However, as shown in this study, band gaps determined on $(GaN)_{1-x}(ZnO)_x$ based on just the onset of absorption alone may not be accurate due to Urbach broadening.

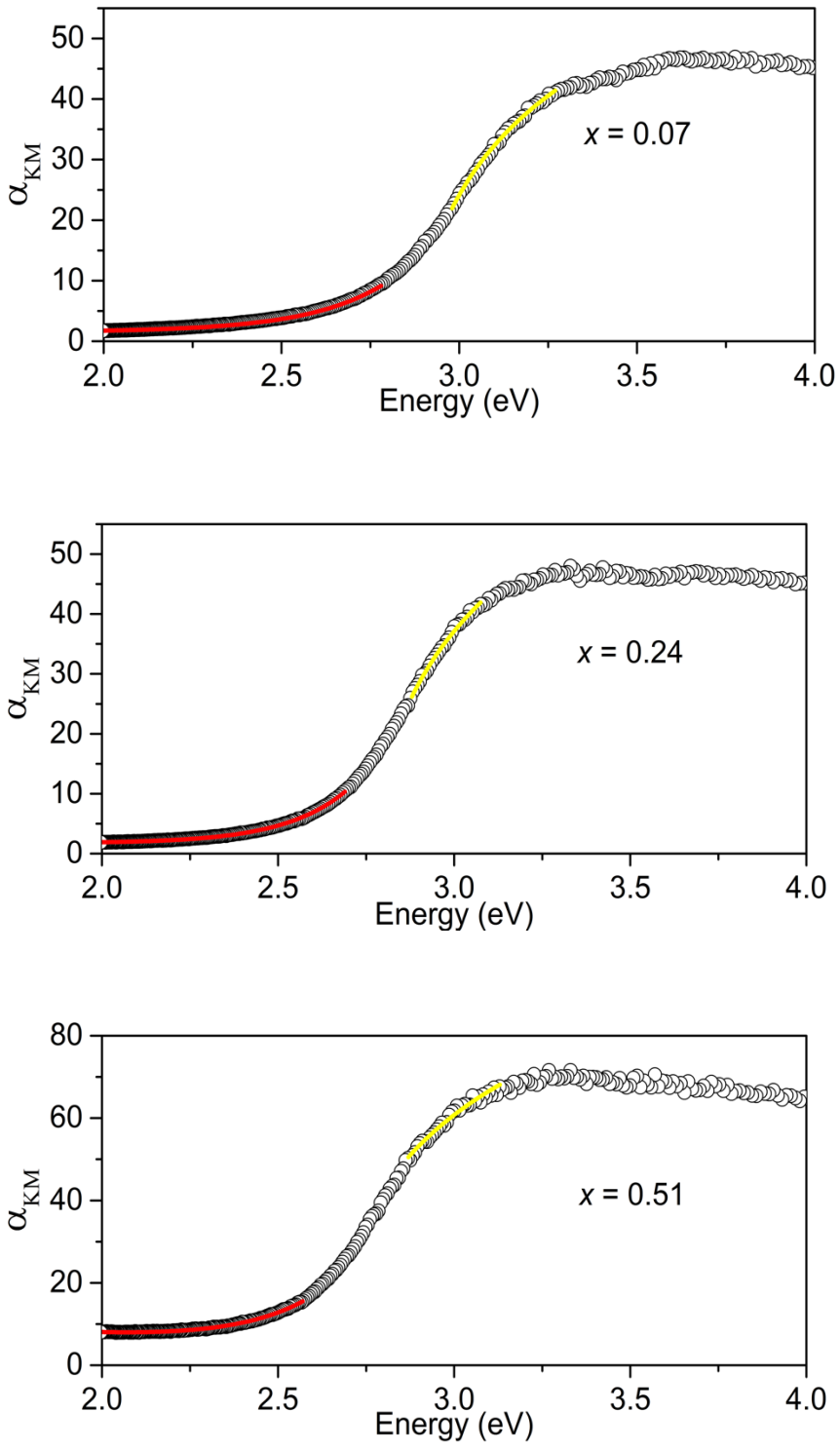

Figure 4.3(a) Kubelka-Munk transformed diffuse reflectance data for $(GaN)_{1-x}(ZnO)_x$ with x= 0.07, 0.24 and 0.51, showing regions that show absorption behaviours of direct band gap (yellow) and Urbach tail (red)

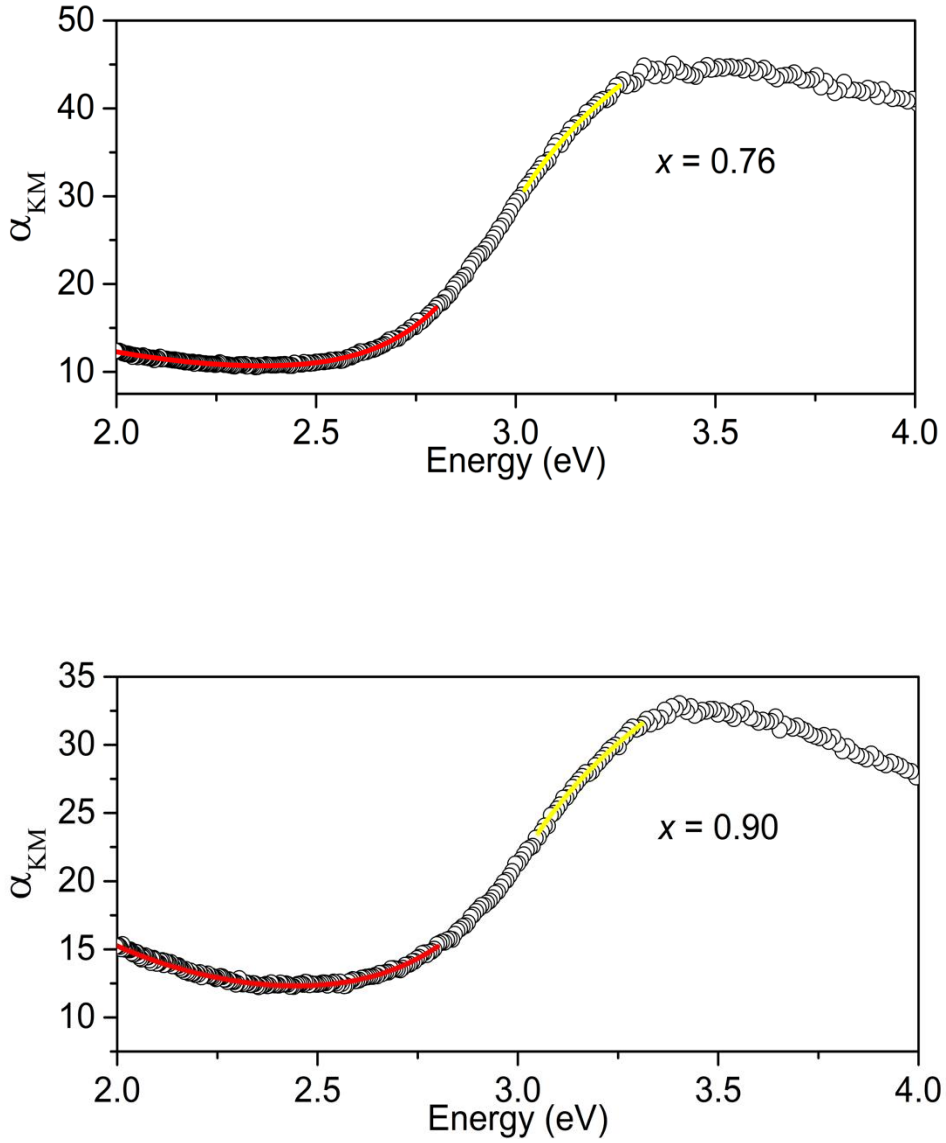

Figure 4.3.(b) Kubelka-Munk transformed diffuse reflectance data for $(GaN)_{1-x}(ZnO)_x$ with x= 0.76and 0.90, showing regions that show absorption behaviours of direct band gap (yellow) and Urbach tail (red)

Table 4.2 Calculated band caps and Urbach energies for $(GaN)_{1-x}(ZnO)_x$ synthesized at high pressure

Composition (x)	Band Gap (eV)	Urbach energy (eV)
0.07	2.892(5)	0.216(1)
0.24	2.778(4)	0.179(1)
0.51	2.646(8)	0.203(2)
0.76	2.829(3)	0.185(3)
0.90	2.818(7)	0.27(1)

Another study reports a similar pattern in materials synthesized from layered double hydroxide precursors with band gap dropping to 2.37 eV at $x = 0.81$.[18] Our calculated bandgaps tend to agree well with those reported by Reinert et al.[8] though it should be noted that we used the same method for band gap estimation. This significant variation of band gaps of $(GaN)_{1-x}(ZnO)_x$ reported by different studies may be explained by the fact that the band gaps depend on factors other than the composition including order/disorder and particle size[10, 11, 17] which may vary between materials synthesized under different conditions. Theoretical studies also shows that the bandgap of $(GaN)_{1-x}(ZnO)_x$ tend to be smaller with increasing disorder.[14]

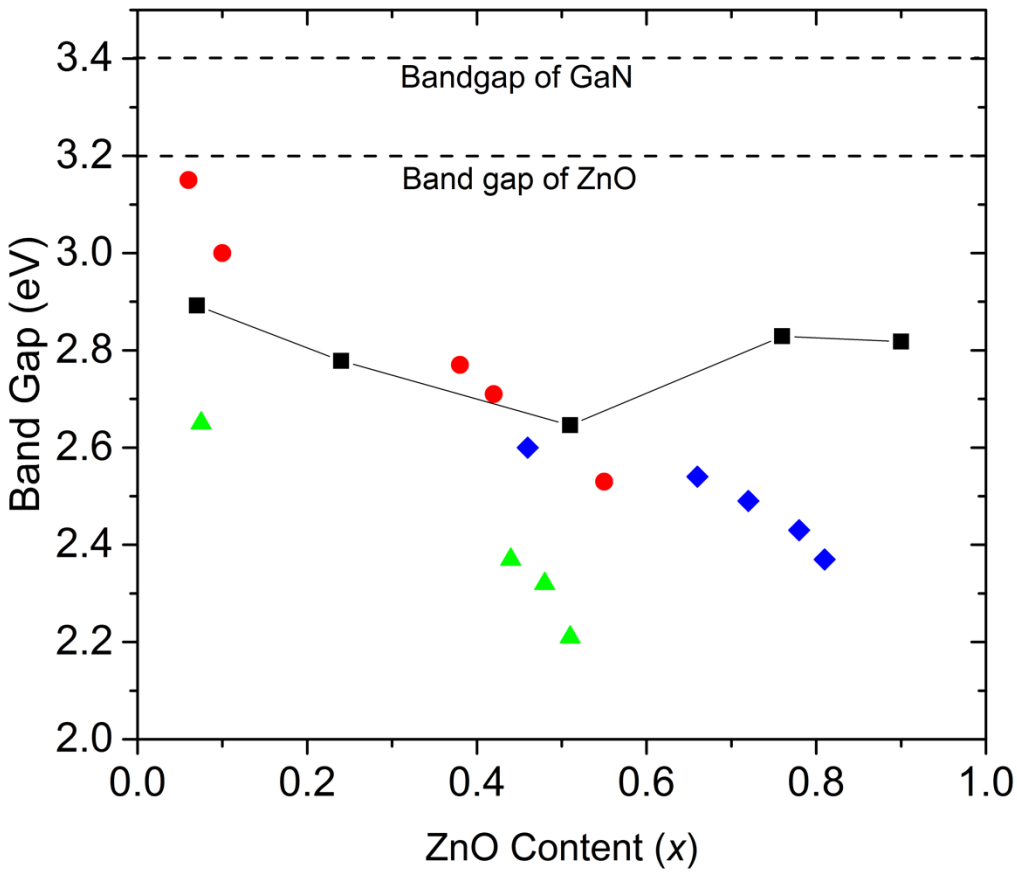

Figure 4.4 Comparison of band gaps of $(GaN)_{1-x}(ZnO)_x$ synthesized at high pressure in this study (black squares, errors are smaller than the symbol), with those of nanorods synthesized by Rienart et al.[8] (red circles), nanoparticles synthesized by Feygenson et al.[17] (green triangles) and $(GaN)_{1-x}(ZnO)_x$ obtained using layered double hydroxide precursors by Wang et al.[18] (blue diamonds). Dashed lines mark the band gap values of GaN and ZnO as marked.

The Urbach energies estimated for our samples vary between 0.17 eV and 0.2 eV and are larger than those observed before on $(GaN)_{1-x}(ZnO)_x$ nanorods (~0.1 eV) where it was considered to reflect compositional inhomogeneity and/or large concentrations of defects.[8] As compositional inhomogeneity can be expected due to GaN and ZnO clustering this can be viewed as another indication of the presence of SRO.

4.3.3 Photocatalytic Activity

We observed that the highest average rate of photocatalytic H_2 evolution under visible light was achieved by samples with x = 0.5 1 at 2.3 μmol/h without any cocatalysts, sacrificial reagents and pH modifiers (see Figure 4.5(a)) while samples with x =0.07, 0.22 and 0.76 showed initial evolution rates of 1.8, 1.1, 0.9 μmol/h respectively. Simultaneous O_2 evolution was not observed for any sample indicating that hydrogen peroxide might be the oxidation product. Since UV light was filtered out, the wide band gapped $ZnGa_2O_4$ is not expected to contribute to photocatalytic activity. The sample with x = 0.9 showed no activity though its estimated band gap of 2.82 eV was similar to that of the sample with x = 0.76. For the sample x = 0.07 the rate of evolution of hydrogen was stable for five hours while for x = 0.24 and 0.76 the rates dropped after one hour and remained steady thereafter. A slight decrease in rate was observed for x = 0.51 after 4 hrs.

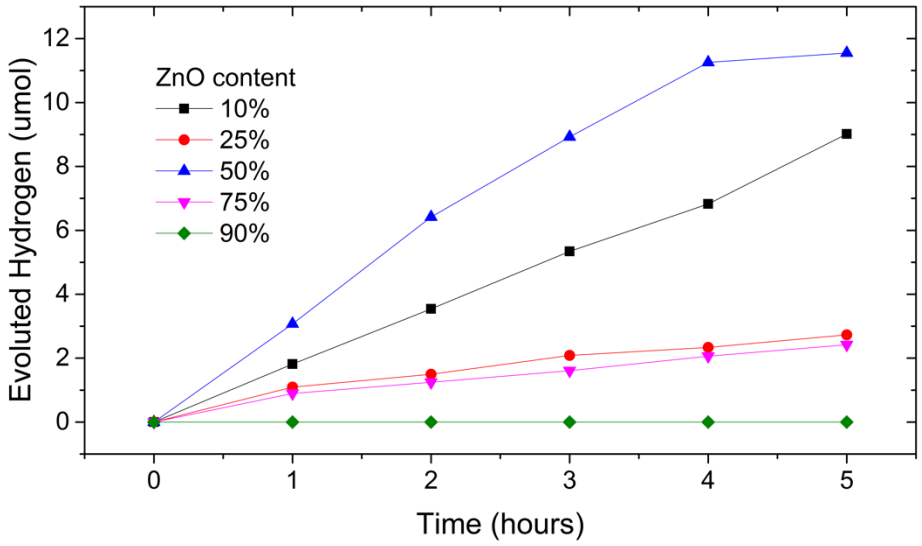

(a)

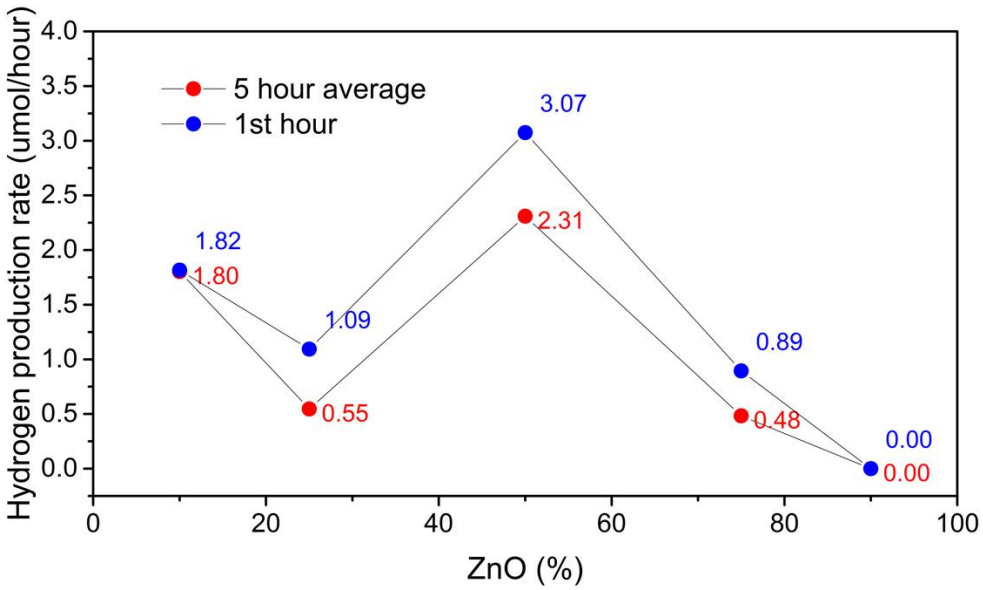

(b)

Figure 4.5 (a) Hydrogen evolution for $(GaN)_{1-x}(ZnO)_x$ solid solution members for 5 hours. (b) Hydrogen evolution rates for first hour (blue) and 5 hour average (red)

The observed average photocatalytic activities show a complex co-relation with x with the rate of activity decreasing from x = 0.07 to 0.24 and then increasing to a maximum at 0.51 (see Figure 4.5.(b)). Similar behavior has been observed in $(GaN)_{1-x}(ZnO)_x$ solution before in the x = 0.15 to 0.3 range[2, 12] but a cause for these observations was not provided.

To investigate stability of $(GaN)_{1-x}(ZnO)_x$, we carried out an extended photocatalytic activity test. For this test, a new $(GaN)_{1-x}(ZnO)_x$ sample was synthesized with 1:1 GaN: ZnO mixture at 2GPa, 1150°C with a multi anvil-press. The product had 15.71% by weight $ZnGa_2O_4$ corresponding to an end $(GaN)_{1-x}(ZnO)_x$ composition of x=0.53 (figure 4.6 (a)). The photocatalytic activity test was carried out for 20hrs with breaks (illumination stopped) at 5 and 10 hours.

The H_2 evolution rates at the beginning of the experiment and after each break were very similar (2.42 μmol/h , 2.46 μmol/h and 2.45 μmol/h respectively *see* figure 4.6 (b)). However, long term evolution rate decreased from 1.86 μmol/h during the first five hour run to 1.47 μmol/h in the next five hour run and finally decreasing to 0.722 μmol/h in the last ten hour run. Again, simultaneous O_2 evolution was not observed. The XRD analysis on post-reaction sample show little change with slight increase of $ZnGa_2O_4$ to 16% by weight. No other by-products were observed. The rate of reduction of activity observed here is significant and in comparison, Ohno et al. report $(GaN)_{1-x}(ZnO)_x$ activity test periods of 6 months before 50% reduction.[19] However, in that case, $Rh_{2-y}Cr_yO_3$, was used as a cocatalyst to provide active sites for H_2 evolution. [19] In our case, it can be hypothesized that the bare $(GaN)_{1-x}(ZnO)_x$ surface might have deteriorated faster, losing active sites.

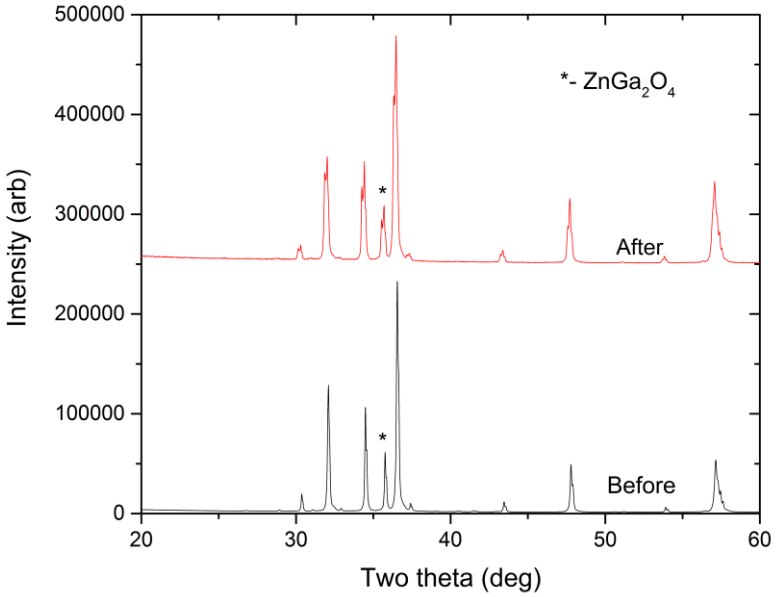

(a)

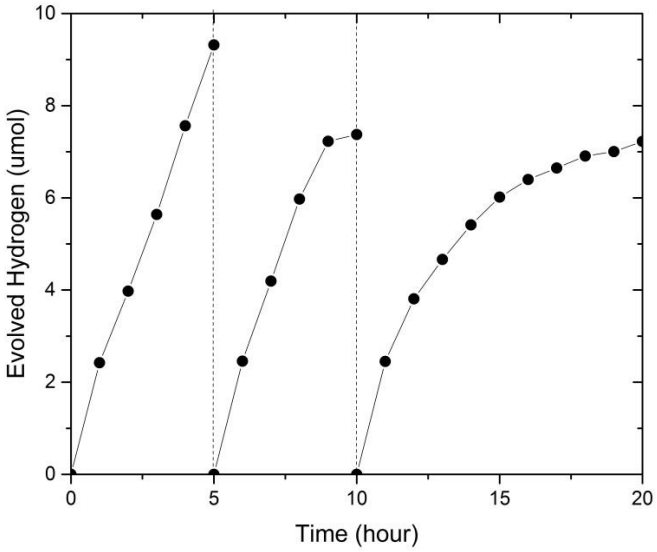

(b)

Figure 4.6 (a) The XRD data of $(GaN)_{1-x}(ZnO)_x$ (x=0.53) sample before and after the photocatalytic activity test (b) Photocatalytic activity of the same sample

In original work on $(GaN)_{1-x}(ZnO)_x$ solid solution system by Maeda et al. used RuO_2 as a cocatalyst for overall water splitting.[1] Later a Rh and Cr mixed oxide cocatalyst was determined to be the most effective for photocatalytic activity on $(GaN)_{1-x}(ZnO)_x$.[5, 20, 21] The photocatalytic activity of $(GaN)_{1-x}(ZnO)_x$ solid solution (prepared by ammonolysis of Ga_2O_3 and ZnO mixtures) is determined to be negligible in the absence of cocatalysts.[12] The photocatalytic H_2 evolution activity observed in this study is the first report on $(GaN)_{1-x}(ZnO)_x$, where cocatalysts, sacrificial reagents and pH modifiers were not used altogether indicating that high pressure synthesized $(GaN)_{1-x}(ZnO)_x$ is highly active for water splitting. It can be expected that cocatalyst loading on high pressure synthesized $(GaN)_{1-x}(ZnO)_x$, solid solution products to improve the rate of activity ,induce overall water splitting and sustain activity longer.

4.4 Conclusions

Members of the $(GaN)_{1-x}(ZnO)_x$ solid solution, synthesized up to $x = 0.9$ at $p = 1$ GPa and $1150 > T < 1200$ °C, were used without surface modification to photocatalytically evolve H_2 under visible light. HP synthesis promotes more complete reaction and allows the determination of bandgaps and photocatalytic activity for the entire composition range. In agreement with theoretical predictions, lattice parameters and band gaps deviate from Vegard's law, showing an upward and downward bowing trend, respectively with x. The lowest band gap of 2.65 eV and highest average photocatalytic H_2 evolution activity of 2.3 μmol/h was observed at $x = 0.51$. Reduction of activity was observed over 20 hours presumably due to deterioration of active sites for H_2 evolution.

4.5 Acknowledgements

H A N Dharmagunawardhane carried out the XRD data collection and analysis of optical and photocatalytic activity data . High pressure synthesis of the Materials reported in this chapter was carried out by Mr. William R. Woerner from the Department of Geosciences, Stony Brook University. The sample synthesis for extended activity test and Rietveld refinements over X-ray diffraction data were carried out by Mr. Alwin James from the Department of Chemistry, Stony Brook University. UV-Vis diffuse reflectance and hydrogen evolution activity data was collected by Mr. Qiyuan Wu from Department of Materials Science and Engineering, Stony Brook University.

References

1 K. Maeda, T. Takata, M. Hara, N. Saito, Y. Inoue, H. Kobayashi and K. Domen, *GaN : ZnO solid solution as a photocatalyst for visible-light-driven overall water splitting,* J. Am. Chem. Soc., 2005, **127**, 8286-8287.

2 K. Maeda, K. Teramura and K. Domen, *Effect of post-calcination on photocatalytic activity of (Ga1-xZnx)(N1-xOx) solid solution for overall water splitting under visible light,* J. Catal., 2008, **254**, 198-204.

3 K. Maeda, K. Teramura, D. L. Lu, T. Takata, N. Saito, Y. Inoue and K. Domen, *Photocatalyst releasing hydrogen from water - Enhancing catalytic performance holds promise for hydrogen production by water splitting in sunlight.,* Nature, 2006, **440**, 295-295.

4 T. Hirai, K. Maeda, M. Yoshida, J. Kubota, S. Ikeda, M. Matsumura and K. Domen, *Origin of visible light absorption in GaN-Rich (Ga1-xZnx)(N1-xOx) photocatalysts,* J. Phys. Chem. C., 2007, **111**, 18853-18855.

5 K. Maeda, K. Teramura, D. L. Lu, N. Saito, Y. Inoue and K. Domen, *Roles of Rh/Cr2O3 (core/shell) nanoparticles photodeposited on visible-light-responsive (Ga1-xZnx)(N1-xOx) solid solutions in photocatalytic overall water splitting,* J. Phys. Chem. C., 2007, **111**, 7554-7560.

6 L. L. Jensen, J. T. Muckerman and M. D. Newton, *First-principles studies of the structural and electronic properties of the (Ga1-xZnx)(N1-xOx) solid solution photocatalyst,* J. Phys. Chem. C., 2008, **112**, 3439-3446.

7 H. Y. Chen, L. P. Wang, J. M. Bai, J. C. Hanson, J. B. Warren, J. T. Muckerman, E. Fujita and J. A. Rodriguez, *In Situ XRD Studies of ZnO/GaN Mixtures at High Pressure and High Temperature: Synthesis of Zn-Rich (Ga1-xZnx)(N1-xOx) Photocatalysts,* J. Phys. Chem. C., 2010, **114**, 1809-1814.

8 A. A. Reinert, C. Payne, L. M. Wang, J. Ciston, Y. M. Zhu and P. G. Khalifah, *Synthesis and Characterization of Visible Light Absorbing (GaN)(1-x)(ZnO)(x) Semiconductor Nanorods,* Inorg. Chem., 2013, **52**, 8389-8398.

9 K. Lee, B. M. Tienes, M. B. Wilker, K. J. Schnitzenbaumer and G. Dukovic, *(Ga1-xZnx)(N1-xOx) Nanocrystals: Visible Absorbers with Tunable Composition and Absorption Spectra,* Nano Lett., 2012, **12**, 3268-3272.

10 S. Z. Wang and L. W. Wang, *Atomic and Electronic Structures of GaN/ZnO Alloys,* Phys. Rev. Lett., 2010, **104**.

11 L. Li, J. T. Muckerman, M. S. Hybertsen and P. B. Allen, *Phase diagram, structure, and electronic properties of (Ga1-xZnx)(N1-xOx) solid solutions from DFT-based simulations,* Physical Review B, 2011, **83**.

12 K. Maeda and K. Domen, *Solid Solution of GaN and ZnO as a Stable Photocatalyst for Overall Water Splitting under Visible Light,* Chem. Mater., 2010, **22**, 612-623.

13 L. Vegard, *The constitution of the mixed crystals and the filling of space of the atoms,* Z. Phys., 1921, **5**, 17-26.

14 J. Liu, M. V. Fernandez-Serra and P. B. Allen, *Special quasiordered structures: Role of short-range order in the semiconductor alloy (GaN)(1-x)(ZnO)(x),* Physical Review B, 2016, **93**.

15 V. B. R. Boppana, D. J. Doren and R. F. Lobo, *A Spinel Oxynitride with Visible-Light Photocatalytic Activity,* Chemsuschem, 2010, **3**, 814-817.

16 R. C. Rai, *Analysis of the Urbach tails in absorption spectra of undoped ZnO thin films,* J. Appl. Phys., 2013, **113**.

17 M. Feygenson, J. C. Neuefeind, T. A. Tyson, N. Schieber and W. Q. Han, *Average and Local Crystal Structures of (GaZn)(NO) Solid Solution Nanoparticles,* Inorg. Chem., 2015, DOI: 10.1021/acs.inorgchem.5b01605.

18 J. P. Wang, B. B. Huang, Z. Y. Wang, P. Wang, H. F. Cheng, Z. K. Zheng, X. Y. Qin, X. Y. Zhang, Y. Dai and M. H. Whangbo, *Facile synthesis of Zn-rich (GaN)(1-x)(ZnO)(x) solid solutions using layered double hydroxides as precursors,* J. Mater. Chem., 2011, **21**, 4562-4567.

19 T. Ohno, L. Bai, T. Hisatomi, K. Maeda and K. Domen, *Photocatalytic Water Splitting Using Modified GaN:ZnO Solid Solution under Visible Light: Long-Time Operation and Regeneration of Activity,* J. Am. Chem. Soc., 2012, **134**, 8254-8259.

20 K. Maeda, K. Teramura, H. Masuda, T. Takata, N. Saito, Y. Inoue and K. Domen, *Efficient overall water splitting under visible-light irradiation on (Ga1-xZnx)(N1-xOx) dispersed with Rh-Cr mixed-oxide nanoparticles: Effect of reaction conditions on photocatalytic activity,* J. Phys. Chem. B, 2006, **110**, 13107-13112.

21 K. Maeda and K. Domen, *Oxynitride materials for solar water splitting,* MRS Bull., 2011, **36**, 25-31.

Complete Bibliography

Chapter 1

1 K. Maeda and K. Domen, *New non-oxide photocatalysts designed for overall water splitting under visible light,* J. Phys. Chem. C., 2007, **111**, 7851-7861.

2 A. Kudo and Y. Miseki, *Heterogeneous photocatalyst materials for water splitting,* Chem. Soc. Rev., 2009, **38**, 253-278.

3 A. Fujishima and K. Honda, *Electrochemical Photolysis of Water at a Semiconductor Electrode,* Nature, 1972, **238**, 37-+.

4 K. Maeda and K. Domen, *Oxynitride materials for solar water splitting,* MRS Bull., 2011, **36**, 25-31.

5 M. Hara, G. Hitoki, T. Takata, J. N. Kondo, H. Kobayashi and K. Domen, *TaON and Ta3N5 as new visible light driven photocatalysts*, Catal. Today, 2003, **78**, 555-560.

6 A. Kasahara, K. Nukumizu, G. Hitoki, T. Takata, J. N. Kondo, M. Hara, H. Kobayashi and K. Domen, *Photoreactions on LaTiO2N under visible light irradiation,* J. Phys. Chem. A, 2002, **106**, 6750-6753.

7 A. Kasahara, K. Nukumizu, T. Takata, J. N. Kondo, M. Hara, H. Kobayashi and K. Domen, *LaTiO2N as a visible-light (<= 600 nm)-driven photocatalyst (2),* J. Phys. Chem. B, 2003, **107**, 791-797.

8 K. Maeda, T. Takata, M. Hara, N. Saito, Y. Inoue, H. Kobayashi and K. Domen, *GaN : ZnO solid solution as a photocatalyst for visible-light-driven overall water splitting,* J. Am. Chem. Soc., 2005, **127**, 8286-8287.

9 K. Maeda, K. Teramura and K. Domen, *Effect of post-calcination on photocatalytic activity of (Ga1-xZnx)(N1-xOx) solid solution for overall water splitting under visible light,* J. Catal., 2008, **254**, 198-204.

10 H. Y. Chen, L. P. Wang, J. M. Bai, J. C. Hanson, J. B. Warren, J. T. Muckerman, E. Fujita and J. A. Rodriguez, *In Situ XRD Studies of ZnO/GaN Mixtures at High Pressure and High Temperature: Synthesis of Zn-Rich (Ga1-xZnx)(N1-xOx) Photocatalysts,* J. Phys. Chem. C., 2010, **114**, 1809-1814.

Chapter 2

1 L. L. Jensen, J. T. Muckerman and M. D. Newton, *First-principles studies of the structural and electronic properties of the (Ga1-xZnx)(N1-xOx) solid solution photocatalyst,* J. Phys. Chem. C., 2008, **112**, 3439-3446.

2 H. Y. Chen, L. P. Wang, J. M. Bai, J. C. Hanson, J. B. Warren, J. T. Muckerman, E. Fujita and J. A. Rodriguez, *In Situ XRD Studies of ZnO/GaN Mixtures at High Pressure and High Temperature: Synthesis of Zn-Rich (Ga1-xZnx)(N1-xOx) Photocatalysts,* J. Phys. Chem. C., 2010, **114**, 1809-1814.

3 A. A. Reinert, C. Payne, L. M. Wang, J. Ciston, Y. M. Zhu and P. G. Khalifah, *Synthesis and Characterization of Visible Light Absorbing (GaN)(1-x)(ZnO)(x) Semiconductor Nanorods,* Inorg. Chem., 2013, **52**, 8389-8398.

4 M. H. Yang, J. A. Rodgers, L. C. Middler, J. Oro-Sole, A. B. Jorge, A. Fuertes and J. P. Attfield, *Direct Solid-State Synthesis at High Pressures of New Mixed-Metal Oxynitrides: RZrO2N (R = Pr, Nd, and Sm),* Inorg. Chem., 2009, **48**, 11498-11500.

5 I. O. Troyanchuk, N. V. Kasper, O. S. Mantytskaya and E. F. Shapovalova, *High-Pressure Synthesis of Some Perovskite - Like Compounds with a Mixed Anion Type,* Mater. Res. Bull., 1995, **30**, 421-425.

6 C. C. Hu and H. S. Teng, *Gallium Oxynitride Photocatalysts Synthesized from Ga(OH)(3) for Water Splitting under Visible Light Irradiation,* J. Phys. Chem. C., 2010, **114**, 20100-20106.

7 E. Soignard, D. Machon, P. F. McMillan, J. J. Dong, B. Xu and K. Leinenweber, *Spinel-structured gallium oxynitride (Ga(3)O(3)N) synthesis and characterization: An experimental and theoretical study,* Chem. Mater., 2005, **17**, 5465-5472.

8 Y. B. Wu, P. Lazic, G. Hautier, K. Persson and G. Ceder, *First principles high throughput screening of oxynitrides for water-splitting photocatalysts,* Energ Environ Sci, 2013, **6**, 157-168.

9 W. J. Li, E. Ionescu, R. Riedel and A. Gurlo, *Can we predict the formability of perovskite oxynitrides from tolerance and octahedral factors?,* J Mater Chem A, 2013, **1**, 12239-12245.

10 M. A. Pena and J. L. G. Fierro, *Chemical structures and performance of perovskite oxides,* Chem. Rev., 2001, **101**, 1981-2017.

11 C. Li, K. C. K. Soh and P. Wu, *Formability of ABO(3) perovskites,* J. Alloys Compd., 2004, **372**, 40-48.

12 F. DiQuarto, C. Sunseri, S. Piazza and M. C. Romano, *Semiempirical correlation between optical band gap values of oxides and the difference of electronegativity of the elements. Its importance for a quantitative use of photocurrent spectroscopy in corrosion studies,* J. Phys. Chem. B, 1997, **101**, 2519-2525.

13 E. Guenther and M. Jansen, *Optical properties of Ta(3-x)Zr(x)N(5-x)O(x) semiconductor pigments,* Mater. Res. Bull., 2001, **36**, 1399-1405.

14 C. Prescher and V. B. Prakapenka, *DIOPTAS: a program for reduction of two-dimensional X-ray diffraction data and data exploration,* High Pressure Res, 2015, **35**, 223-230.

15 P. I. Dorogokupets and A. Dewaele, *Equations of state of MgO, au, pt, NaCl-B1, and NaCl-B2: Internally consistent high-temperature pressure scales,* High Pressure Res, 2007, **27**, 431-446.

16 E. Orhan, F. Tessier and R. Marchand, *Synthesis and energetics of yellow TaON,* Solid State Sci, 2002, **4**, 1071-1076.

17 I. Molodetsky, A. Navrotsky, F. DiSalvo and M. Lerch, *Energetics of oxidation of oxynitrides: Zr-N-O, Y-Zr-N-O, Ca-Zr-N-O, and Mg-Zr-N-O,* J. Mater. Res., 2000, **15**, 2558-2570.

18 T. Bredow and M. Lerch, *On the anion distribution in Zr7O8N4,* Z. Anorg. Allg. Chem., 2007, **633**, 2598-2602.

19 T. Mishima, M. Matsuda and M. Miyake, *Visible-light photocatalytic properties and electronic structure of Zr-based oxynitride, Zr2ON2, derived from nitridation of ZrO2,* Appl Catal a-Gen, 2007, **324**, 77-82.

20 Y. Inaguma, A. Miyaguchi, M. Yoshida, T. Katsumata, Y. Shimojo, R. P. Wang and T. Sekiya, *High-pressure synthesis and ferroelectric properties in perovskite-type BiScO3-PbTiO3 solid solution,* J. Appl. Phys., 2004, **95**, 231-235.

21 M. Alguero, J. Ricote, T. Hungria and A. Castro, *High-sensitivity piezoelectric, low-tolerance-factor perovskites by mechanosynthesis,* Chem. Mater., 2007, **19**, 4982-4990.

22 T. Schleid and G. Meyer, *Single-Crystals of Rare-Earth Oxides from Reducing Halide Melts,* J Less-Common Met, 1989, **149**, 73-80.

23 W. R. Woerner, G. R. Qian, A. R. Oganov, P. W. Stephens, H. A. N. Dharmagunawardhane, A. Sinclair and J. B. Parise, *Combined Theoretical and in Situ Scattering Strategies for Optimized Discovery and Recovery of High-Pressure Phases: A Case Study of the GaN-Nb2O5 System,* Inorg. Chem., 2016, **55**, 3384-3392.

24 A. F. Wright and J. S. Nelson, *Consistent Structural-Properties for Aln, Gan, and Inn,* Physical Review B, 1995, **51**, 7866-7869.

25 G. Hitoki, T. Takata, J. N. Kondo, M. Hara, H. Kobayashi and K. Domen, *An oxynitride, TaON, as an efficient water oxidation photocatalyst under visible light irradiation (lambda <= 500 nm),* Chem. Commun., 2002, DOI: 10.1039/b202393h, 1698-1699.

26 K. Maeda, T. Takata, M. Hara, N. Saito, Y. Inoue, H. Kobayashi and K. Domen, *GaN : ZnO solid solution as a photocatalyst for visible-light-driven overall water splitting,* J. Am. Chem. Soc., 2005, **127**, 8286-8287.

27 K. Maeda and K. Domen, *New non-oxide photocatalysts designed for overall water splitting under visible light,* J. Phys. Chem. C., 2007, **111**, 7851-7861.

28 S. Tamura, K. Kato and M. Goto, *Single-Crystals of T-Nb2o5 Obtained by Slow Cooling Method under High-Pressures,* Z. Anorg. Allg. Chem., 1974, **410**, 313-315.

Chapter 3

1 H. A. N. Dharmagunawardhane, W. R. Woerner, Q. Y. Wu, H. F. Huang, X. Y. Chen, A. Orlov, P. G. Khalifah and J. B. Parise, *Photocatalytic hydrogen evolution using nanocrystalline gallium oxynitride spinel,* J Mater Chem A, 2014, **2**, 19247-19252.

2 J. E. Lowther, T. Wagner, I. Kinski and R. Riedel, *Potential gallium oxynitrides with a derived spinel structure,* J. Alloys Compd., 2004, **376**, 1-4.

3 S. D. Wolter, J. M. DeLucca, S. E. Mohney, R. S. Kern and C. P. Kuo, *An investigation into the early stages of oxide growth on gallium nitride,* Thin Solid Films, 2000, **371**, 153-160.

4 M. Puchinger, D. J. Kisailus, F. F. Lange and T. Wagner, *Microstructural evolution of precursor-derived gallium nitride thin films,* J. Cryst. Growth, 2002, **245**, 219-227.

5 E. Soignard, D. Machon, P. F. McMillan, J. J. Dong, B. Xu and K. Leinenweber, *Spinel-structured gallium oxynitride (Ga(3)O(3)N) synthesis and characterization: An experimental and theoretical study,* Chem. Mater., 2005, **17**, 5465-5472.

6 I. Kinski, G. Miehe, G. Heymann, R. Theissmann, R. Riedel and H. Huppertz, *High-pressure synthesis of a gallium oxonitride with a spinel-type structure,* Zeitschrift Fur Naturforschung Section B-a Journal of Chemical Sciences, 2005, **60**, 831-836.

7 P. Kroll, R. Dronskowski and M. Martin, *Formation of spinel-type gallium oxynitrides: a density-functional study of binary and ternary phases in the system Ga-O-N,* J. Mater. Chem., 2005, **15**, 3296-3302.

8 H. Huppertz, S. A. Hering, C. E. Zvoriste, S. Lauterbach, O. Oeckler, R. Riedel and I. Kinski, *High-Pressure Synthesis, Electron Energy-Loss Spectroscopy Investigations, and Single Crystal Structure Determination of a Spinel-Type Gallium Oxonitride Ga-2.79 square(0.21)(O3.05N0.76 square(0.19)),* Chem. Mater., 2009, **21**, 2101-2107.

9 C. E. Zvoriste, L. Dubrovinsky, S. A. Hering, H. Huppertz, R. Riedel and I. Kinski, *Diamond anvil cell syntheses and compressibility studies of the spinel-structured gallium oxonitride,* High Pressure Res, 2009, **29**, 389-395.

10 C. C. Tang, Y. Bando, Y. Huang, C. Y. Zhi, D. Golberg, X. W. Xu, J. L. Zhao and Y. X. Li, *Synthesis of nanoporous spheres of cubic gallium oxynitride and their lithium ion intercalation properties,* Nanotechnology, 2010, **21**, 115705.

11 A. Oberlander, I. Kinski, W. L. Zhu, G. Pezzotti and A. Michaelis, *Structure and optical properties of cubic gallium oxynitride synthesized by solvothermal route,* J. Solid State Chem., 2013, **200**, 221-226.

12 I. Kinski, F. Scheiba and R. Riedel, *Advances in gallium oxonitride ceramics: A new class of materials in the system Ga-O-N,* Adv. Eng. Mater., 2005, **7**, 921-927.

13 W. S. Jung, *Preparation of gallium nitride powders and nanowires from a gallium(III) nitrate salt in flowing ammonia,* Bull. Korean Chem. Soc., 2004, **25**, 51-54.

14 A. C. Malingowski, P. W. Stephens, A. Huq, Q. Z. Huang, S. Khalid and P. G. Khalifah, *Substitutional Mechanism of Ni into the Wide-Band-Gap Semiconductor InTaO4 and Its Implications for Water Splitting Activity in the Wolframite Structure Type,* Inorg. Chem., 2012, **51**, 6096-6103.

15 C. C. Hu and H. S. Teng, *Gallium Oxynitride Photocatalysts Synthesized from Ga(OH)(3) for Water Splitting under Visible Light Irradiation,* J. Phys. Chem. C., 2010, **114**, 20100-20106.

16 V. B. R. Boppana, D. J. Doren and R. F. Lobo, *A Spinel Oxynitride with Visible-Light Photocatalytic Activity,* Chemsuschem, 2010, **3**, 814-817.

17 W. H. Lin, C. Cheng, C. C. Hu and H. S. Teng, *NaTaO3 photocatalysts of different crystalline structures for water splitting into H-2 and O-2,* Appl. Phys. Lett., 2006, **89**, 211904.

18 T. Luttrell, S. Halpegamage, J. G. Tao, A. Kramer, E. Sutter and M. Batzill, *Why is anatase a better photocatalyst than rutile? - Model studies on epitaxial TiO2 films,* Scientific Reports, 2014, **4**, 4043.

19 A. Kudo and Y. Miseki, *Heterogeneous photocatalyst materials for water splitting,* Chem. Soc. Rev., 2009, **38**, 253-278.

20 K. Ikarashi, J. Sato, H. Kobayashi, N. Saito, H. Nishiyama and Y. Inoue, *Photocatalysis for water decomposition by RuO2-dispersed ZnGa2O4 with d(10) configuration,* J. Phys. Chem. B, 2002, **106**, 9048-9053.

21 A. Kudo and I. Mikami, *Photocatalytic activities and photophysical properties of Ga2-xInxO3 solid solution,* Journal of the Chemical Society-Faraday Transactions, 1998, **94**, 2929-2932.

22 M. Higashi, K. Domen and R. Abe, *Fabrication of efficient TaON and Ta3N5 photoanodes for water splitting under visible light irradiation,* Energ Environ Sci, 2011, **4**, 4138-4147.

23 A. Kasahara, K. Nukumizu, T. Takata, J. N. Kondo, M. Hara, H. Kobayashi and K. Domen, *LaTiO2N as a visible-light (<= 600 nm)-driven photocatalyst (2),* J. Phys. Chem. B, 2003, **107**, 791-797.

24 A. Kasahara, K. Nukumizu, G. Hitoki, T. Takata, J. N. Kondo, M. Hara, H. Kobayashi and K. Domen, *Photoreactions on LaTiO2N under visible light irradiation,* J. Phys. Chem. A, 2002, **106**, 6750-6753.

25 S. Hu, M. R. Shaner, J. A. Beardslee, M. Lichterman, B. S. Brunschwig and N. S. Lewis, *Amorphous TiO2 coatings stabilize Si, GaAs, and GaP photoanodes for efficient water oxidation,* Science, 2014, **344**, 1005-1009.

26 K. Maeda, K. Teramura and K. Domen, *Effect of post-calcination on photocatalytic activity of (Ga1-xZnx)(N1-xOx) solid solution for overall water splitting under visible light,* J. Catal., 2008, **254**, 198-204.

27 J. W. Liu, G. Chen, Z. H. Li and Z. G. Zhang, *Hydrothermal synthesis and photocatalytic properties of ATaO(3) and ANbO(3) (A = Na and K),* Int. J. Hydrogen Energy, 2007, **32**, 2269-2272.

28 K. Maeda, H. Terashima, K. Kase, M. Higashi, M. Tabata and K. Domen, *Surface modification of TaON with monoclinic ZrO2 to produce a composite photocatalyst with enhanced hydrogen evolution activity under visible light,* Bull. Chem. Soc. Jpn., 2008, **81**, 927-937.

Chapter 4

1 K. Maeda, T. Takata, M. Hara, N. Saito, Y. Inoue, H. Kobayashi and K. Domen, *GaN : ZnO solid solution as a photocatalyst for visible-light-driven overall water splitting,* J. Am. Chem. Soc., 2005, **127**, 8286-8287.

2 K. Maeda, K. Teramura and K. Domen, *Effect of post-calcination on photocatalytic activity of (Ga1-xZnx)(N1-xOx) solid solution for overall water splitting under visible light,* J. Catal., 2008, **254**, 198-204.

3 K. Maeda, K. Teramura, D. L. Lu, T. Takata, N. Saito, Y. Inoue and K. Domen, *Photocatalyst releasing hydrogen from water - Enhancing catalytic performance holds promise for hydrogen production by water splitting in sunlight.,* Nature, 2006, **440**, 295-295.

4 T. Hirai, K. Maeda, M. Yoshida, J. Kubota, S. Ikeda, M. Matsumura and K. Domen, *Origin of visible light absorption in GaN-Rich (Ga1-xZnx)(N1-xOx) photocatalysts,* J. Phys. Chem. C., 2007, **111**, 18853-18855.

5 K. Maeda, K. Teramura, D. L. Lu, N. Saito, Y. Inoue and K. Domen, *Roles of Rh/Cr2O3 (core/shell) nanoparticles photodeposited on visible-light-responsive (Ga1-xZnx)(N1-xOx) solid solutions in photocatalytic overall water splitting,* J. Phys. Chem. C., 2007, **111**, 7554-7560.

6 L. L. Jensen, J. T. Muckerman and M. D. Newton, *First-principles studies of the structural and electronic properties of the (Ga1-xZnx)(N1-xOx) solid solution photocatalyst,* J. Phys. Chem. C., 2008, **112**, 3439-3446.

7 H. Y. Chen, L. P. Wang, J. M. Bai, J. C. Hanson, J. B. Warren, J. T. Muckerman, E. Fujita and J. A. Rodriguez, *In Situ XRD Studies of ZnO/GaN Mixtures at High Pressure and High Temperature: Synthesis of Zn-Rich (Ga1-xZnx)(N1-xOx) Photocatalysts,* J. Phys. Chem. C., 2010, **114**, 1809-1814.

8 A. A. Reinert, C. Payne, L. M. Wang, J. Ciston, Y. M. Zhu and P. G. Khalifah, *Synthesis and Characterization of Visible Light Absorbing (GaN)(1-x)(ZnO)(x) Semiconductor Nanorods,* Inorg. Chem., 2013, **52**, 8389-8398.

9 K. Lee, B. M. Tienes, M. B. Wilker, K. J. Schnitzenbaumer and G. Dukovic, *(Ga1-xZnx)(N1-xOx) Nanocrystals: Visible Absorbers with Tunable Composition and Absorption Spectra,* Nano Lett., 2012, **12**, 3268-3272.

10 S. Z. Wang and L. W. Wang, *Atomic and Electronic Structures of GaN/ZnO Alloys,* Phys. Rev. Lett., 2010, **104**.

11 L. Li, J. T. Muckerman, M. S. Hybertsen and P. B. Allen, *Phase diagram, structure, and electronic properties of (Ga1-xZnx)(N1-xOx) solid solutions from DFT-based simulations,* Physical Review B, 2011, **83**.

12 K. Maeda and K. Domen, *Solid Solution of GaN and ZnO as a Stable Photocatalyst for Overall Water Splitting under Visible Light,* Chem. Mater., 2010, **22**, 612-623.

13 L. Vegard, *The constitution of the mixed crystals and the filling of space of the atoms,* Z. Phys., 1921, **5**, 17-26.

14 J. Liu, M. V. Fernandez-Serra and P. B. Allen, *Special quasiordered structures: Role of short-range order in the semiconductor alloy (GaN)(1-x)(ZnO)(x),* Physical Review B, 2016, **93**.

15 V. B. R. Boppana, D. J. Doren and R. F. Lobo, *A Spinel Oxynitride with Visible-Light Photocatalytic Activity,* Chemsuschem, 2010, **3**, 814-817.

16 R. C. Rai, *Analysis of the Urbach tails in absorption spectra of undoped ZnO thin films,* J. Appl. Phys., 2013, **113**.

17 M. Feygenson, J. C. Neuefeind, T. A. Tyson, N. Schieber and W. Q. Han, *Average and Local Crystal Structures of (GaZn)(NO) Solid Solution Nanoparticles,* Inorg. Chem., 2015, DOI: 10.1021/acs.inorgchem.5b01605.

18 J. P. Wang, B. B. Huang, Z. Y. Wang, P. Wang, H. F. Cheng, Z. K. Zheng, X. Y. Qin, X. Y. Zhang, Y. Dai and M. H. Whangbo, *Facile synthesis of Zn-rich (GaN)(1-x)(ZnO)(x) solid solutions using layered double hydroxides as precursors,* J. Mater. Chem., 2011, **21**, 4562-4567.

19 T. Ohno, L. Bai, T. Hisatomi, K. Maeda and K. Domen, *Photocatalytic Water Splitting Using Modified GaN:ZnO Solid Solution under Visible Light: Long-Time Operation and Regeneration of Activity,* J. Am. Chem. Soc., 2012, **134**, 8254-8259.

20 K. Maeda, K. Teramura, H. Masuda, T. Takata, N. Saito, Y. Inoue and K. Domen, *Efficient overall water splitting under visible-light irradiation on (Ga1-xZnx)(N1-xOx) dispersed with Rh-Cr mixed-oxide nanoparticles: Effect of reaction conditions on photocatalytic activity*, J. Phys. Chem. B, 2006, **110**, 13107-13112.

21 K. Maeda and K. Domen, *Oxynitride materials for solar water splitting*, MRS Bull., 2011, **36**, 25-31.